Modeling and Analysis of User Association and Wireless Backhauling in Small Cell Networks

by

Uzma Siddique

A Thesis submitted to The Faculty of Graduate Studies of

The University of Manitoba

in partial fulfillment of the requirements for the degree of

Doctor of Philosophy

Department of Electrical and Computer Engineering

University of Manitoba

Winnipeg

December 2016

Abstract

Dense deployment of small cells underlaying the traditional macrocells is considered as a key enabling technique for the emerging fifth generation (5G) cellular networks. However, the diverse transmit powers of the base stations (BSs) in such a network lead to uneven distribution of the traffic loads among different BSs when received signal power (RSP)-based user association is used. Moreover, provisioning of efficient and economical backhauling for these small cells is a crucial challenge. To combat this, wireless backhauling is been considered as a viable and cost-effective approach that allows operators to obtain end-to-end control of their network rather than leasing third party wired backhaul connections. But the scarcity of radio frequency (RF) spectrum in the licensed bands is still a major constraint which necessitates efficient spectrum planning for backhaul/access links of small cells. Emerging communications techniques such as full-duplexing, which allows transmission and reception in the same spectrum band, can be used to tackle the problem of spectrum scarcity. In the above contexts, the objective of the research work presented in this thesis is to develop efficient user association and wireless backhauling schemes for small cell networks and analyze their performances. In particular, i) A channel-access aware user association scheme is proposed to tackle the problem of uneven distribution of traffic load among different BSs, ii) Performance analysis of full-duplex (FD) wireless backhauling of small cells is carried out when compared to half-duplex (HD) wireless backhauling), iii) A method for downlink spectrum allocation for in-band and out-of-band wireless backhauling of full-duplex small cells is presented to optimally allocate spectrum for access and backhaul links, iv) A method for optimal channel and power allocation

is presented for downlink access and backhaul links for half-duplex small cells. The proposed methods and performance analysis models will be useful for optimizing the design and deployment of small cell networks.

Table of Contents

List of Figures **v**

List of Tables **viii**

List of Abbreviations **ix**

Publications **xii**

1 Introduction **1**
1.1 Small Cell Networks 1
1.2 5G Small Cell Networks 2
1.3 Key Challenges for the Deployment of Small Cells 5
1.4 Motivations and Objectives of the Thesis 7
1.4.1 Motivations 7
1.4.2 Objectives 9
1.5 Contributions and Scope of the Thesis 11
1.6 Mathematical Preliminaries 13
1.6.1 Small Cell Network Model 13
1.6.2 Signal-to-Interference-Plus-Noise Ratio (SINR) Model and Spectral Efficiency 15
1.6.3 Order Statistics 16
1.6.4 Moment Generating Function (MGF)-Based Approach 17
1.7 Organization of the Thesis 17

2 Channel Access-Aware User Association in Small Cell Networks **19**
2.1 Introduction 20
2.1.1 Overview 20
2.1.2 Contribution 21
2.2 Related Work 22
2.3 System Model and Assumptions 25
2.3.1 Network Model 25
2.3.2 Channel Model 28
2.3.3 Channel Access-Aware (CAA) User Association 29

2.3.4 Analytical Approach: Evaluation of Spectral Efficiency 31
2.4 Association Probabilities 33
2.4.1 Distribution of Q and Distance Between the NU and the SBSs 33
2.4.2 Association Probabilities When the MBSs are in the NABS Mode 36
2.4.3 Association Probabilities When the MBSs are in the ABS Mode 38
2.4.4 Association Probability of a Given NU 39
2.5 Statistics of Signal and Interference Powers 40
2.5.1 Statistics of Received Signal Powers 40
2.5.2 Statistics of Received Interference 41
2.6 Spectral Efficiency of Downlink Transmission to the NU 44
2.6.1 Spectral Efficiency in the NABS Mode 45
2.6.2 Spectral Efficiency in the ABS Mode 45
2.6.3 Spectral Efficiency of a Given NU 46
2.7 Network-Wide Spectral Efficiency of Downlink Transmission 46
2.7.1 Spectral Efficiency of Transmission to a Given MU 46
2.7.2 Spectral Efficiency for a Given SU Served by an SBS Located Within Radius T 47
2.7.3 SE for a Given SU Served by an SBS Located Outside Radius T 48
2.7.4 Network-Wide SE of Downlink Transmission 49
2.8 Numerical Results and Discussion 50
2.8.1 Results: No Interference Coordination 52
2.8.2 Results: Interference Coordination 53
2.9 Chapter Summary 59

3 Wireless Backhauling in 5G Small Cell Networks 61
3.1 Introduction 62
3.1.1 Overview 62
3.1.2 Contributions 65
3.2 Related Work 66
3.3 Existing Wireless Backhaul Solutions and Related Challenges 68
3.4 Design Guidelines to Overcome the Limitations of RF-Backhauled Small Cells 78
3.5 System Model and Assumptions 83
3.5.1 SBS Operating Modes 84
3.5.2 Backhaul and Access Link Capacities 85
3.6 Downlink Analysis of a Full/Half-Duplex SBS 87
3.6.1 Backhaul Link Capacity for Full-Duplex SBS 87
3.6.2 Access Link Capacity of a Full-Duplex SBS 89
3.6.3 Transmission Capacity of a Downlink User 91
3.7 Uplink Analysis of a Full/Half-Duplex SBS 92
3.8 Numerical Results and Discussion 93
3.8.1 Results: Downlink Transmission 93

3.8.2 Results: Downlink and Uplink Transmissions 97
3.9 Chapter Summary 98

4 Downlink Spectrum Allocation for Wireless Backhauling in Full-Duplex Small Cells 99
4.1 Introduction 100
4.1.1 Overview 100
4.1.2 Contribution 102
4.2 Related Work 104
4.3 System Model and Assumptions 106
4.3.1 Modes of Backhauling at SBSs 107
4.3.2 Spectrum Allocation for Different Transmission Modes 108
4.3.3 Performance Metric: Rate Calculations 110
4.4 Centralized Access/Backhaul Spectrum Allocation 114
4.5 Distributed Backhaul/Access Spectrum Allocation Schemes 123
4.5.1 Distance-based Ranking of SBSs 125
4.5.2 Probability of Backhaul Channel Allocation 125
4.5.3 Number of Allocated Backhaul/Access Channels 128
4.6 Rate Coverage Analysis for IBFD/OBFD Backhauling With Distributed Spectrum Allocation 129
4.6.1 OBFD Backhauling 129
4.6.2 IBFD Backhauling 132
4.7 Numerical Results and Discussion 135
4.7.1 Optimized Spectrum Allocation - Centralized Solution 136
4.7.2 Optimum Achievable Downlink Rate - Centralized Solution . . 139
4.7.3 Spectrum Allocation - Distributed Solution 142
4.7.4 Rate Coverage Probability - Distributed Solution 143
4.7.5 Extensions to Spectrum Sharing Scenarios 144
4.8 Chapter Summary 146

5 Downlink Resource Allocation for Wireless Backhauling in Full-Duplex Small Cells 149
5.1 Introduction 150
5.1.1 Overview 150
5.1.2 Contribution 150
5.2 Related Work 151
5.3 System Model and Assumptions 152
5.4 Maximization of Common Achievable Rate per SBS: Centralized Approach 154
5.5 Distributed Backhaul Channel Scheduling: Target Rate Coverage Analysis 158
5.5.1 Distance-Based Ranking of SBSs 159

5.5.2 Probability of Backhaul Channel Allocation 160
5.5.3 Analysis of Rate Coverage 162
5.6 Numerical Results and Discussion 164
5.7 Chapter Summary 169

6 Conclusion and Future Research Directions **170**
6.1 Conclusion 170
6.2 Future Research Directions 175
References 177

A Appendix A **189**
A.1 PDF and CDF of h_m 189
A.2 PDF and CDF of h_s 190
A.3 Proof of (2.28) 192

List of Figures

1.1 Graphical illustration of a heterogeneous cellular network where macrocell is overlaid with femtocells, picocells, and microcells. The solid and dotted lines indicate the coverage area of macrocell and small cell, respectively. The red dotted line indicates the wireless backhaul connectivity between MBS and small cells. 4

1.2 Graphical illustration of a two-tier cellular network with a macro-tier (black squares) which is overlaid with lower power and denser small cells (red squares). Solid blue lines represent the coverage area of each cell. Solid black circles represent the macro users and Solid green circles represents the small cell users, respectively, for $M = 7, S = 3$. 14

2.1 (a) Graphical illustration of a two-tier small cell network. In this part of the figure, the distances are demonstrated graphically. (b) Enlarged view of the reference macrocell is provided when the MBS is in ABS and in NABS mode. Moreover, the working mechanisms of RSP, BRSP, and CAA-based association schemes are illustrated. 26

2.2 Comparison between the approximated distribution of the number of SBSs within T given in (2.14) and the exact distribution obtained from Monte-Carlo simulations (for $R_m = 300$ m, $\beta = 2, T = 100$ m, $D_l = 600$ m). 34

2.3 Association probabilities of the NU with the reference MBS and S SBSs without interference coordination (for $R_m = 300$ m, $T = 100$ m, $\rho_m = 0$ (no interference coordination)). BS indices $[2, \cdots, 4]$ represent the S SBSs within distance T. 38

2.4 Association probabilities of the NU with a reference MBS and S SBSs within distance T with interference coordination (for $R_m = 300$ m, $T = 100$ m, $S' = 200$, $\lambda_m = 15$, $\lambda_s = 3$). BS indices $[2, \cdots, 4]$ represent the S SBSs within distance T. 39

2.5 Comparison of the CDF of the cumulative interference from S and S' SBSs considering (i) the exact location of the NU; (ii) NU is located at origin (assumption) (for $T = 100$, $P_m = 10W, P_s = 0.1W, \beta = 2.0$). 42

2.6 Traffic load balancing after arrival of 250 NUs in the two-tier small cell network considering different association schemes (for $\lambda_m = 15$, $\lambda_s = 3$, $\rho_m = 0$). 51
2.7 SE of downlink transmission to the NU with increase in small cell user intensity (λ_s) for different user association schemes (for $\rho_m = 0$). . . . 52
2.8 SE of downlink transmission to the NU as a function of S' considering different user association schemes (for $\lambda_m = 15, \lambda_s = 3$). 53
2.9 SE of downlink transmission to the MU / SU as a function of S' considering CAA scheme. 54
2.10 SE of downlink transmission to the NU as a function of λ_m considering RSP and CAA user association schemes (for (i) $\lambda_s = 3$ for (a) $\rho_m = 0.2$, (b) $\rho_m = 0.8$, (ii) $\lambda_s = 5$ for (a) $\rho_m = 0.2$, (b) $\rho_m = 0.8$). 55
2.11 Impact of the bias value on the downlink SE of transmission to NU for different user association schemes (for $\lambda_s = 3$). 57
2.12 Downlink SE of transmission to NU as a function of ρ_m for different λ_m values and association schemes. 58
2.13 Downlink SE of transmission to MU /SU as a function of ρ_m for different λ_m values. 58

3.1 Graphical illustration of backhaul evolution of 5G small cell networks with wireless backhauls and cloud-RAN architecture [1]. 63
3.2 Graphical illustration of the backhaul-limited regions and user capacity as a function of D (for R_m = 500m, R_s = 40m, $\beta_i = 2$, $\beta_o = 3$, P_m = 5W, P_s = 2W, $\sigma^2 = 1 \times 10^{-12}$W/Hz), d=30 m. 81
3.3 Downlink user capacity as a function of distance between MBS and SBS considering symmetric deployment of A-BSs (for R_m = 500m, R_s = 40m, $\beta_i = 2$, $\beta_o = 3$, P_m = 5W, P_s = 2W, P_a = 2W, $\sigma^2 = 1 \times 10^{-12}$W/Hz), d=30 m. 82
3.4 Graphical illustration of the downlink operation of FD self-backhauled small-cell and HD self-backhauled small cell. Operating mechanism of FD, HD, and adaptive FD self-backhauling. 84
3.5 Backhaul link and user capacity in the downlink as a function of distance between MBS and SBS for both the HD SBS and FD SBS (for $\theta = 0^o$, $d = 50$ m). 95
3.6 User capacity in the downlink as a function of distance between user and SBS for both the HD SBS and FD SBS (for $\theta = 0^o$). 95
3.7 Capacity of SBS in the downlink when operating in FD or adaptive FD mode considering both the throughput and fairness maximization scheduling criteria (for $\theta = 0^o$). 97
3.8 Uplink and downlink user capacity as a function of self-interference cancellation value (C_{SI}) (for $\theta = 0^o$). 97

4.1 Graphical illustration of the downlink backhaul and access transmission in small cells considering in-band full-duplex (IBFD) backhauling and out-of-band full-duplex (OBFD) backhauling. 106
4.2 Spectrum partitioning for backhaul and access transmissions considering out-of-band full-duplex (OBFD), in-band full-duplex (IBFD), and hybrid IBFD/OBFD backhauling. 108
4.3 Access and backhaul spectrum allocation to SBSs ranked according to their distance from the WBH. 137
4.4 Spectrum allocation to the cell-center SBS (1^{st} ranked) and cell-edge SBS (6^{th} ranked) as a function of C_{SI} considering OBFD backhauling, IBFD backhauling, and hybrid OBFD/IBFD backhauling. The portion of spectrum for hybrid backhaul (hybrid access) is obtained by summing up the portions of spectrum for IBFD and OBFD backhaul (IBFD and OBFD access). 138
4.5 Optimized achievable downlink rate (R_{th}) in a small cell as a function of the self-interference cancellation value C_{SI} in OBFD, IBFD, and hybrid OBFD/IBFD backhauling. 140
4.6 Optimized achievable downlink rate (R_{th}) of a small cell user as a function of the transmit power of SBS per channel P_s in OBFD, IBFD, and hybrid OBFD/IBFD backhauling by setting (a) $C_{\text{SI}} = 125$ dB, and (b) $C_{\text{SI}} = 130$ dB. 141
4.7 Portion of spectrum for OBFD and IBFD backhauling with max-RSP and min-RSP schemes by setting $N_b = 14$ channels 142
4.8 Rate coverage probability of ranked SBSs considering OBFD backhauling and IBFD backhauling for max-RSP and min-RSP schemes ($N_b =$ 14 channels). 143
4.9 Average minimum rate per ranked SBS as a function of fraction of backhaul spectrum considering both OBFD backhauling and IBFD backhauling for max-RSP and min-RSP schemes, respectively, by setting: R^*_{th} for OBFD backhauling = 42, R^*_{th} for IBFD backhauling = 46 taken from Fig. 5. 144

5.1 (a)-(b) Number of backhaul channels allocated to ranked SBSs with max-RSP and min-RSP schemes, (c) Rate coverage probability of ranked SBSs with max-RSP and min-RSP schemes (for $\alpha = 0.8$, R^*_{th} = 5.4). 165
5.2 Rate of the ranked SBSs for (a) $R^*_{\text{th}} = 5.4$, (b) $R_{\text{th}} = 16$ (for $\alpha = 0.8$, $N = 20$). 166
5.3 Network rate as a function of access/backhaul spectrum partition α (for $N = 20$). 167
5.4 Network rate as a function of the number of SBSs for R_{th} =16, $\alpha = 0.8$. 168

List of Tables

2.1 Chapter 2: Summary of the main variables and their definitions . . . 25

4.1 Chapter 4:Summary of the main variables and their definitions 113

List of Abbreviations

ABS	Almost blank subframe
A-BSs	Anchor-base stations
ACLR	Adjacent channel leakage ratio
BRSP	Biased received signal power
BSs	Base stations
CAA	Channel access-aware
CDF	Cumulative distribution function
CF	Collaborative filtering
CN	Connector node
CRE	Cell range expansion
DL	Downlink
DTV	Digital TV
eICIC	Enhanced inter-cell interference coordination
FD	Full-duplex
FM	Fairness maximization
FTTC	Fiber-to-the-cell
HD	Half-duplex
IBFD	In-band full-duplex
LOS	Line of sight

max-RSP	Maximum received signal power
MBSs	Macro base stations
MGF	Moment generating function
min-RSP	Minimum received signal power
MU	Macro user
NABS	Non-ABS
NLOS	Non line of sight
NU	New user
OBFD	Out-of-band full-duplex
O & M	Operation and maintenance
P2MP	Point-to-multipoint
PDF	Probability density function
QoS	Quality of service
RAN	Radio access networks
RF	Radio frequency
RSP	Received signal power
RVs	Random variables
SBSs	Small base stations
SE	Spectral efficiency
SFR	Soft frequency reuse
SI	Self-interference
SINR	Signal-to-interference-plus-noise ratio
SU	Small cell user
TDD	Time-division duplex
TM	Throughput maximization

TNFD	Three node full-duplex
TVWS	TV white spaces
UL	Uplink
WBH	Wireless backhaul hub
WSR	Weighted sum-rate

Publications

- Journal Publications:

  1. **Uzma Siddique**, Hina Tabassum, and Ekram Hossain, "Downlink spectrum allocation for in-band/out-band wireless self-backhauling in full-duplex small cells" submitted to the *IEEE Transactions on Communications*.
  2. **Uzma Siddique**, Hina Tabassum, and Ekram Hossain, "Wireless bck-hauling of 5G small cells: Challenges and solution approaches," *IEEE Wireless Communications*, vol. 22, no. 5, pp. 22–31, Oct. 2015.
  3. **Uzma Siddique**, Hina Tabassum, and Ekram Hossain, "Channel access-aware user association with interference coordination in two-tier downlink cellular networks," *IEEE Transactions on Vehicular Technology*, vol. 65, no. 7, pp. 5579–5594, July. 2016.
  4. Hina Tabassum, **Uzma Siddique**, and Ekram Hossain, "Downlink performance of cellular systems with base station sleeping, user association, and scheduling," *IEEE Wireless Communications*, vol. 13, no. 10, pp. 5752–5767, Oct. 2014.

- Conference Publications:

1. **Uzma Siddique**, Hina Tabassum, and Ekram Hossain, "Spectrum allocation for wireless backhauling of 5G small cells," in Proc. of *IEEE International Conference on Communications (ICC'16)*, pp. 122–127, May 2016.

2. **Uzma Siddique**, Hina Tabassum, and Ekram Hossain, "Adaptive in-band self-backhauling for full-duplex small cells," in Proc. of *IEEE International Conference on Communications (ICC'15)*, pp. 44–49, June 2015.

3. **Uzma Siddique**, Hina Tabassum, and Ekram Hossain, "Channel access-aware user association in two-tier cellular networks," in *IEEE International Conference on Communications (ICC'15)*, pp. 2463–2468, June 2015.

Chapter 1

Introduction

1.1 Small Cell Networks

A basic communication system is comprised of a transmitter, a receiver, and a communication channel, i.e., a medium through which the message travels from the transmitter to the receiver. In wireless communications, a medium is wireless channel that uses electromagnetic radio spectrum (waves) to carry signals from transmitter to receiver. Wireless communications is not new, but it has been continuously evolving since the first wireless communication system was demonstrated by Marconi. Nevertheless, the capacity of early wireless systems were severely limited due to the inefficient use of the radio spectrum. Latterly, the development of cellular concept by AT&T Bell lab significantly helped to enhance the system capacity [2]. Cellular system concept is based on the fact that the strength of a transmitted signal exponentially decreases with increase in distance between the transmitter and the receiver. Hence, the same spectrum can be reused at spatially separate locations without having significant interference.

Generally, a cellular network is comprised of a set of cells. Each cell has a fixed

location transceiver known as base station and can serve a number of users. As cells can be of hexagonal, square, circular or some other regular shapes but hexagonal cells are conventional and well known. Generally, base stations have omnidirectional antennas and cover a circular region, hence, in reality a network may not be comprised of hexagonal shaped cells. Since the characteristics such as transmit power, coverage area etc. of all base stations are nearly the same; therefore, this type of a conventional cellular network is also known as a homogenous network. Depending on the coverage area, a cell can be categorized as macrocell (2-30 km), microcell (less than 2 kilometers), picocell (less than 200 meters), and femtocell (around 10-20 meters). Usually, microcells, picocells, and femtocells are known as small cells due to their smaller coverage area.

1.2 5G Small Cell Networks

The cellular wireless networks are evolving through generations namely from 1G (first generation) to 4G (fourth generation). From the early analog generation (1G) to the last implemented fourth generation (4G), the standards have changed. The new generations do not pretend to improve the voice communication experience yet an effort to give the user access to a new global communication reality. The main objective of the fifth generation is to provide communication ubiquity (every time, everywhere), and users with a new set of services.

The evolving fifth generation (5G) cellular wireless networks are envisioned to overcome the fundamental challenges of existing cellular networks, for example, higher data rates, efficient spectral reuse, excellent end-to-end performance, and user-coverage in hot-spots and crowded areas with lower latency, energy consumption, and cost per information transfer [3]. Base station (BS) densification is emerging as one

of the effective and potential solutions to meet the requirements of 5G wireless networks. However, deploying more macro BSs in a homogeneous network to achieve densification is infeasible due to a high cost and infrastructure complexity. Alternatively, small cells in addition to macrocell (also known as heterogeneous network) have recently attracted significant attention to densify cellular networks as well as to meet the ever-growing users' demand. The key drivers for deploying small cells are summarized as follows:

- Improved quality-of-services and provisioning of high data rate to users,
- Extended coverage for the users at cell edges (area of a cell where users receive the weakest signal),
- Improved energy efficiency of communication and hence extended battery life of mobile phones,
- Efficient spectral reuse,
- Low latency in communication, and
- Offloading users from macro to small cells so that more resources are available for macrocell (e.g., outdoor and mobile) users.

Fig. 1.1 illustrates a heterogeneous network where a macrocell is overlaid with different types of small cells. It may be noted that the coverage area differs from one BS to another due to the difference in transmission powers. The SBSs are connected to the core network through a connector node (CN) that provides wireless backhaul to the small cell. The CN is typically situated at a fiber point-of-presence or where high-capacity line-of-sight (LOS) microwave link is available. An existing MBS can be an

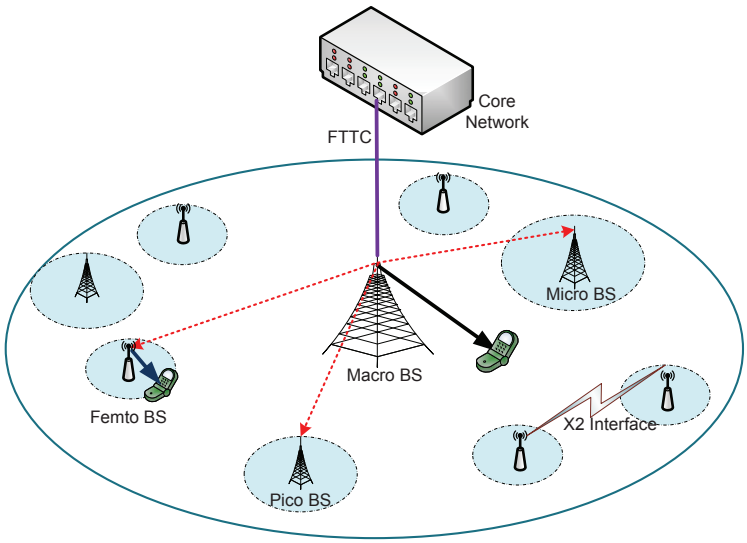

Figure 1.1: Graphical illustration of a heterogeneous cellular network where macrocell is overlaid with femtocells, picocells, and microcells. The solid and dotted lines indicate the coverage area of macrocell and small cell, respectively. The red dotted line indicates the wireless backhaul connectivity between MBS and small cells.

example of such a CN as MBSs are connected to the core network by fiber-to-the-cell (FTTC) links.

Small cells can be deployed by the end user or an operator at different locations such as user residences, small offices, enterprise buildings, public places, light posts, cable junction boxes at street corners, etc. Small cells can operate in closed access, open access, and hybrid access modes. In closed access, a small cell serves only a limited number of users who belong to the closed subscriber group (CSG). A closed access small cell acts as interferer for non-CSG users. Small cells with open access serve all users belonging to an operator. On the other hand, hybrid access is a combination of closed and open access, where a number of users can be given higher priority/preference in terms of offered services and their quality. Small cells can either share spectrum with the macrocells or can be deployed in their own dedicated spectrum.

1.3 Key Challenges for the Deployment of Small Cells

The massive deployment of small cell BSs (SBSs) is a key feature in the emerging 5G cellular networks [4] to satisfy gigabit-level data traffic in an economical and ecological fashion. However, there are following technical challenges that need to be taken into account when considering planning and deployment of small cells:

- **Load balancing:** The diverse transmit powers of BSs may lead to uneven distribution of traffic loads among different BSs when received signal power (RSP)-based user association is used. This causes under-utilization of the resources at SBSs. Efficient user association schemes need to be investigated that can enhance the spectral efficiency (SE) gains and simultaneously perform traffic load balancing among different BSs in the network.

- **Interference coordination:** The different tiers in a multi-tier cellular network can use dedicated spectrum (i.e., orthogonal or non-overlapping spectrum allocation). Even though this option for small cell deployment can eliminate interference among the different network tiers but this results in an inefficient radio spectrum utilization. On the other hand, a co-channel deployment (i.e., overlapping spectrum allocation), where different network tiers share the same spectrum, enables efficient spectral reuse but at the cost of interference. Intelligent interference coordination techniques are required in this case. Almost Blank Subframe (ABS)-based interference coordination, also referred as enhanced intercell interference coordination (eICIC), can be used at MBS to protect small cell users from strong macro-tier interference and at SBSs. eICIC not only protects macro users from small cell-tier interference but also minimizes co-tier interference at small cell users.

- **Backhauling:** Forwarding the backhaul traffic from the dense small cell networks efficiently is a crucial challenge. Typically, the backhaul of small cells exploits either wired connectivity (e.g., optical fiber) or wireless connectivity (e.g., microwave links). However, the high cost of wired connectivity and the line-of-sight (LOS) requirement of the microwave links make them less attractive backhaul solutions. Moreover, in half-duplex small cells, where backhaul link transmission and access link transmission takes place at different frequencies, the access link capacity is usually constrained by backhaul link capacity. Consequently, it decreases the overall network spectral efficiency.

- **Backhaul channel allocation:** The allocation of backhaul channels to SBSs is an important but an unexplored issue. The backhaul channel allocation has an immense impact on the network spectral efficiency and the outage probability. There is a need to explore efficient backhaul channel allocation schemes that can overcome the backhaul limitation of user spectral efficiency and enhance the network spectral efficiency.

- **In-band full-duplex transmission:** In-band full-duplex (FD) communication at low-power wireless devices (such as SBSs) has recently been considered as a viable technique for capacity enhancement of 5G networks. In-band FD communication implies simultaneous transmission and reception of information in the same frequency band. However, the gains of in-band FD communication are limited by the overwhelming nature of self-interference (SI), which is generated by the transmitter to its own collocated receiver [5]. Fortunately, with the recently developed antenna and digital baseband technologies, SI can be reduced close to the level of the noise floor in low-power devices [6]. The interference from MBS to small cell user in downlink and interference from small

cell users to MBS in the uplink are needed to be mitigated in order to achieve the full-duplex gains.

- **Electric power issues:** The location of small cells is very different compared to MBSs. Often, small cells are placed on the side of buildings, on lamp posts and utility poles, in shopping malls and stadiums, at transport hubs, or on outdoor street furniture. The diversity of the environment and the increased number of cell sites impose diverse challenges, and access to electrical power becomes a far greater problem compared to the traditional tower and rooftop sites.

- **Site acquisition and maintenance:** Unlike macro site acquisition and installation/ commissioning, small cell deployments need to be managed an order-of-magnitude increase in number of cell sites. Dense small cells deployment creates new challenges in handover configurations, and operation/maintenance processes. Self-organizing capabilities such as self-configuration, self-optimization, and self-healing empower small cells to overcome this issue.

1.4 Motivations and Objectives of the Thesis

1.4.1 Motivations

The main motivations of the works presented in this thesis are to tackle some of the fundamental challenges in the deployment and operation of small cell networks as discussed below.

- The massive deployment of low-power small cells such as femtocells and picocells over existing macrocell networks is considered as a potential solution to

boost the spectral efficiency performance (in bits/sec/Hz) of 5G cellular networks [3,7]. These kind of cellular networks are commonly referred as heterogeneous or multi-tier networks. The heterogeneity among different base stations (BSs) is due to their varying coverage areas, diverse traffic loads, transmission power limits, capital, and operational expenditures [8] etc. The diversity among different BSs introduces several new challenges that may significantly impact the SE performance. For instance, due to diverse transmit powers of different BSs, mostly users prefer to associate with the high power BSs with the conventional received signal power (RSP)-based association scheme. This results in the uneven distribution of traffic load among different BSs and in turn under utilization of the resources at low power BSs [9]. *An association that can balance traffic load among different BSs and simultaneously improves the SE gains of the network is required.*

- An efficient forwarding of the backhaul traffic from the dense small cell networks will, therefore, become a key challenge. Typically, the backhaul of small cells exploits either wired connectivity (e.g., optical fiber) or wireless connectivity (e.g., microwave links). However, the high cost of wired connectivity and the line-of-sight (LOS) requirement of the microwave links make them less attractive backhaul solutions for small cells. Generally, the access link capacity depends on the backhaul link capacity which is highly dependent on the distance between MBS and SBS. As the distance between MBS and SBS increases, the backhaul link capacity decreases which in turn limits the access link capacity. *There is a need to characterize the cellular region in which the downlink transmission capacity of a given half-duplex (HD) small cell becomes limited by the backhaul capacity and to propose some solution techniques to overcome this issue.*

- In practice, small cells operate in half-duplex (HD) mode, i.e., each SBS either transmits information to small cell user in access link or receives information from MBS in backhaul link in a given time slot. This mode is also known as out-of-band full-duplex (OBFD) mode. OBFD and HD terms are used interchangeably through out the thesis. *HD mode leads to inefficient spectrum reuse due to utilizing different frequency channel for access link transmission and backhaul link transmission. As spectrum is scarce resource, it needs to be used efficiently.*

- Recent advancements in the self-interference (SI) cancellation capability of low-power wireless devices pave the way of implementing full-duplex (FD) self-backhauling in small cell, i.e., using both the access link and the backhaul link at the same time in each time slot (also known as in-band full-duplex (IBFD)). IBFD and FD terms are used interchangeably through out the thesis. To this end, leveraging the use of the spectrum utilized by the radio access network (RAN) simultaneously for both the access and backhaul links (referred as in-band or self-backhauling) has emerged as a potential solution for wireless backhauling. *However, the feasibility of IBFD over traditional OBFD backhauling needs to be investigated. Since the IBFD backhauling may not always be beneficial due to additional interference such as self-interference (SI) and backhaul interference. Hence, backhaul resources (spectrum and/or power) need to be allocated in an efficient manner.*

1.4.2 Objectives

The main objective of this work is to develop accurate yet tractable frameworks to model small cell networks underlying macro cellular networks. Specifically, I study

several system models of small cell networks considering different characteristics as well as objectives.Throughout this work, I use the geometric probability theory for statistical modeling of two-tier (macro-tier and small cell tier) cellular networks. I aim at using the developed system models to analyze the network performance and optimize the network design parameters.

In particular, in this work, I address the following challenges/scenarios of small cell networks with different objectives as noted below.

1. To combat an uneven distribution of traffic load among different BSs, a channel-access aware user association scheme is proposed. This scheme can adopt per-BS bias value, enhance the SE performance in the system by exploiting traffic load information in the different BSs (in different tiers as well as different BSs in a specific tier) in addition to the link quality information.

2. The cellular region in which the downlink transmission capacity of a user served by a half-duplex (HD) small cell becomes limited by the backhaul link capacity is characterized. The achievable capacity gains of downlink (uplink) transmission from (to) the macrocell base station (MBS) to (from) a user associated to an FD self-backhauled small cell over its HD counter part are characterized.

3. Downlink spectrum allocation for in-band/out-of-band wireless self-backhauling in full-duplex small cells to allocate spectrum for access link and backhaul link transmissions optimally.

4. Downlink access/ backhaul resource allocation for out-of-band small cells to allocate channel and power optimally.

Chapter 2, 3, 4, and 5 of this thesis present each of the aforementioned scenarios. The explicit features of system models and considered problems as well as proposed

solutions will be explained in each chapter.

1.5 Contributions and Scope of the Thesis

In this thesis, I develop different models for the performance analysis of 5G small cell networks. In the following, a short discussion on the contributions of this thesis is presented.

1. Performance modeling and analysis of channel access-aware user association in small cell networks:

    - A channel access-aware (CAA) user association scheme that can simultaneously enhance the SE of downlink transmission and achieve traffic load balancing among different BSs is proposed.
    - A geometric probability theory and order statistics are used to develop a tractable mathematical model to derive the SE of the network and SE of downlink transmission to a user who associates with a BS using the proposed CAA scheme considering almost blank subframe (ABS)-based interference coordination at macro BS.
    - The framework can model and analyze the individual traffic load distributions of different BSs.

2. Performance modeling and analysis of full-duplex wireless backhauling in small cell networks:

    - I mathematically characterize the cellular region in which the downlink transmission capacity of half-duplex (HD) small cell base station (SBS) becomes limited by its backhaul capacity.

- To overcome this limitation, I propose enabling full-duplex (FD) mode of operation and mathematically analyze the interference scenarios in which the FD mode of operation is a potential solution.
- The achievable capacity gains of downlink transmission from the macrocell base station (MBS) to a user associated to an FD self-backhauled small cell over its HD counter part are characterized. The results are further extended for the uplink transmission scenarios.
- The performance of adaptive FD scheme is then numerically analyzed for two different user selection schemes at the small cell that maximizes throughput and fairness, respectively.

3. Downlink spectrum allocation for in-band and out-band wireless backhauling in full-duplex small cells:

   - A problem of optimal access/backhaul spectrum allocation for SBSs considering both the IBFD backhauling and out-of-band FD (OBFD) backhauling (in which the access and backhaul transmissions take place on different spectrum) is formulated.
   - The spectrum allocation for hybrid IBFD/OBFD backhauling in which each SBS can optimally exploit both the IBFD and OBFD backhauling is presented.
   - The solution of the centralized problem, which serves as a benchmark for any sub-optimal solution, is provided.
   - The closed-form optimal solutions for the access/backhaul spectrum allocation of OBFD backhauling as well as IBFD backhauling are provided.
   - Two distributed low-complexity backhaul spectrum allocation schemes,

namely, maximum received signal power (max-RSP) and minimum received signal power (min-RSP) are proposed and comparatively analyzed.

4. Downlink resource allocation for out-of-band wireless backhauling in full-duplex small cells:

   - The problem of downlink access/backhaul resource allocation for multiple small cells is considered.
   - A common rate maximization problem is formulated for the access and backhaul links of small cells.
   - The relaxed version of the original problem is formulated and used as a benchmark.
   - Two simple and distributed backhaul channel allocation criteria are proposed and comparatively analyzed.

A more detailed discussion on the contribution will be provided in latter chapters of the thesis.

1.6 Mathematical Preliminaries

1.6.1 Small Cell Network Model

The locations and number of MBSs in the network are assumed to be planned. On the other hand, the locations of SBSs are assumed to be independent and uniformly distributed in the coverage of each macrocell with given spatial density. The individual traffic load distributions per SBS as well as MBS is modeled. In this work, the Poisson traffic load distribution per SBS and MBS is considered. The Poisson traffic load distribution per BS can be characterized by two properties:

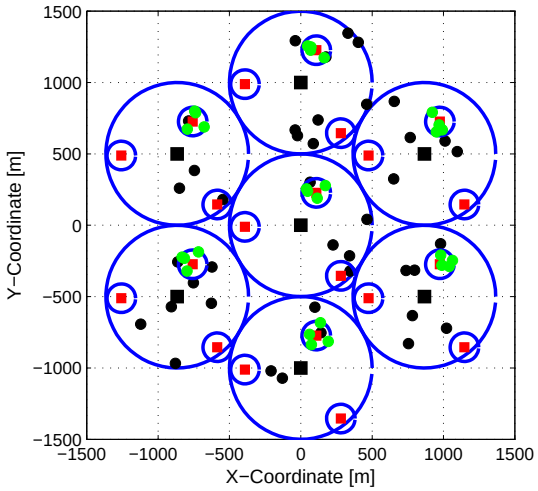

Figure 1.2: Graphical illustration of a two-tier cellular network with a macro-tier (black squares) which is overlaid with lower power and denser small cells (red squares). Solid blue lines represent the coverage area of each cell. Solid black circles represent the macro users and Solid green circles represents the small cell users, respectively, for $M = 7, S = 3$.

- For any two disjoint areas, the numbers of users falling within the two regions are independent random variables.

- The expected number of users falling within region with area A is distributed according to a Poisson random variable, i.e.,

$$\mathbb{P}(U = u) = \frac{(\lambda)^u}{u!} e^{-\lambda}, \tag{1.1}$$

where λ is the spatial density of Poisson process and measured in number of users in a unit area.

Without loss of generality, Fig. 1.2 demonstrates a realization of a two-tier cellular network where M macrocells represent macro-tier. Each macrocell is overlaid with S low power small cells. In Fig 1.2, the locations of MBSs are planned, whereas, SBSs are uniformly distributed in the coverage area of a macrocell. It is assumed that the

BSs belonging to the macro-tier have transmit power P_m and the BSs belonging to the small cell-tier have transmit power P_s.

1.6.2 Signal-to-Interference-Plus-Noise Ratio (SINR) Model and Spectral Efficiency

The received signal power at a typical user on a given transmission channel from its serving BS can be expressed as follows:

$$\gamma_{(\cdot)} = P_{(\cdot)} r_{(\cdot)}^{-\beta} \chi_{(\cdot)}, \tag{1.2}$$

where $(\cdot)$ can be m for MBS and s for SBS, $r_{(\cdot)}$ represents the distance between a typical user and its serving BS, β represents the path loss exponent, and $\chi_{(\cdot)}$ represents the composite shadowing and fading channel.

When both tiers share the same spectrum, the received interference at a typical user can be expressed as:

$$I_{(\cdot)} = I_{(\cdot)}^{\text{co}} + I_{(\cdot)}^{\text{cr}}, \tag{1.3}$$

where $I_{(\cdot)}^{\text{co}}$ represents the cumulative co-tier interference and $I_{(\cdot)}^{\text{cr}}$ represents the cumulative cross-tier interference received at a user. For a macro user, co-tier interference is the interference received from all neighboring $M-1$ MBSs and cross-tier interference is the interference received from S SBSs. Similarly, for a small cell user, co-tier interference is the interference received from all neighboring $S-1$ SBSs and cross-tier interference is the interference received from M MBSs.

For a communication link, the signal-to-interference-plus-noise ratio (SINR) at

the receiver is then given by

$$\text{SINR} = \frac{\gamma}{I + \sigma^2}, \tag{1.4}$$

where σ^2 denotes the noise power. Accordingly, using Shannon's formula, the spectral efficiency of transmission in that link is given by

$$\text{SE} = \log_2 (1 + \text{SINR}), \tag{1.5}$$

where it is assumed that the interference has the same statistical characteristics as noise.

1.6.3 Order Statistics

Order statistics is useful when relative magnitude of observations is of importance. I use order statistics to derive the distribution of the ranked distance between a user and SBSs within a specific region. For a given number of SBSs (N) in a given region, the distances between a user and N SBSs can be reordered such that $r_{(1)} < r_{(2)} < \cdots < r_{(N)}$, where $r_{(1)}$ and $r_{(N)}$ represent the SBS at the minimum distance and the SBS at the maximum distance from a user, respectively. If r_n has PDF $f_{r_n}(r_n)$ and distribution function $F_{r_n}(r_n)$, then the probability function of $f_{r_{(n)}}(r_{(n)})$ is given by

$$f_{r_{(n)}}(r_{(n)}) = \frac{N!}{(r-1)!(N-r)!} \left(F_{r_n}(r_n)\right)^{r-1} \left(1 - F_{r_n}(r_n)\right)^{N-r} f_{r_n}(r_n), \quad \forall n = 1, \cdots, N, \tag{1.6}$$

where $f_{r_n}(r_n)$ and $F_{r_n}(r_n)$ represent the PDF and CDF of the distance of a user from its serving SBS.

1.6.4 Moment Generating Function (MGF)-Based Approach

The moment generating function (MGF)-based approach is used to evaluate the spectral efficiency (SE) of transmission to a user. The reason is to derive the distribution of the cumulative interference received at a user requires convolution of the probability density function (PDF) of many random variables (RVs). For instance, to derive the distribution of cumulative co-tier interference and cross-tier interference received at a macro user requires convolution of PDF of $M-1$ RVs and S RVs, respectively, which is a tedious task for many practical scenarios. To avoid the convolutions, I utilize an MGF - based approach. Given a random variable X with PDF $f_X(x)$, if there exists an $h>0$ such that $\mathcal{M}_X(t) := \mathbb{E}\left[e^{tx}\right]$ for $|t|<h$, then $\mathcal{M}_X(t)$ is called the MGF of RV X. For a continuous distribution, $\mathcal{M}_X(t) := \int_{-\infty}^{\infty} e^{tx} f_X(x)dx$.

The SE of transmission to a user can be calculated by using the following lemma [10]:

$$\begin{aligned}\mathcal{C}_{(\cdot)} &= \frac{1}{\ln(2)}\mathbb{E}\left[\ln\left(1+\frac{\gamma_{(\cdot)}}{I_{(\cdot)}+\sigma^2}\right)\right] \\ &= \int_0^{\infty} \frac{\mathcal{M}_{I_{(\cdot)}}(t)(1-\mathcal{M}_{\gamma_{(\cdot)}}(t))}{t\,\ln(2)} e^{-t\sigma^2} dt,\end{aligned} \tag{1.7}$$

where $\mathcal{M}_{\gamma_{(\cdot)}}(t)$ represents the moment generating function (MGF) of the received signal power at a user $\gamma_{(\cdot)}$ and $\mathcal{M}_{I_{(\cdot)}}(t)$ represents the MGF of the received interference at a user $I_{(\cdot)}$, σ^2 represents the thermal noise power of the receiver. The factor ln2 is due to the conversion of natural log with base 10 to natural log with base 2.

1.7 Organization of the Thesis

Chapter 2, Chapter 3, Chapter 4, and Chapter 5 present the core contributions of this thesis. Specifically, Chapter 2 presents a channel access-aware user association

with interference coordination in two-tier downlink cellular networks and its impact on the network-wide performance. Chapter 3 explains in detail wireless backhauling for small cells and characterizes the achievable capacity gains of downlink as well as uplink transmissions between the macrocell base station (MBS) and a user associated to a FD self-backhauled small cell. Chapter 4 provides downlink spectrum allocation scheme for in-band/out-band wireless self-backhauling in full-duplex small cells. Chapter 5 furnishes downlink resource (channel and power) allocation for out-band wireless self-backhauling in full-duplex small cells. Chapter 6 summarizes and concludes the research presented in this thesis and explore some directions for future research. Symbols and notations used throughout the chapters are provided in the corresponding chapters.

Chapter 2

Channel Access-Aware User Association in Small Cell Networks

The diverse transmit powers of the base stations (BSs) in a multi-tier cellular network, on the one hand, lead to uneven distribution of the traffic loads among different BSs when received signal power (RSP)-based user association is used. This causes under-utilization of the resources at low-power BSs. On the other hand, strong interference from high-power BSs affects the downlink transmissions to the users associated with low-power BSs. In this context, this chapter proposes a channel access-aware (CAA) user association scheme that can simultaneously enhance the spectral efficiency (SE) of downlink transmission and achieve traffic load balancing among different BSs. The CAA scheme is a network-assisted user association scheme that requires traffic load information from different BSs in addition to the channel quality indicators. I develop a tractable mathematical model to derive the SE of the network and SE of downlink transmission to a user who associates with a BS using the proposed CAA scheme considering almost blank subframe (ABS)-based interference coordination at macro BS. The framework can model and analyze the individual traffic load distributions

of different BSs in a two-tier network. The derived expressions provide approximate solutions compared to the results obtained from Monte-Carlo simulations. Numerical results comparatively analyze the gains of CAA scheme over conventional received signal power (RSP)-based association and biased RSP-based association. Based on this, important insights are extracted related to the selection of the proportion of ABS in various traffic load scenarios.

2.1 Introduction

2.1.1 Overview

In this chapter, I proposed channel access-aware (CAA) user association scheme and presented a brief mathematical model to analyze its usefulness in Rayleigh fading environment. In CAA-based association, a user estimates its channel access probability (i.e., the probability that a channel will be available for this user) from different BSs and associates to a BS that maximizes the product of channel access probability and received signal power from the BS. The CAA scheme exhibits the following features:

- The channel access probability serves as a dynamic bias towards a given BS regardless of which tier it belongs to. This is different from the conventional BRSP in which a higher bias is given to low-power BSs.
- Since the channel access probability reduces with increasing traffic load of a BS, a user may not select a congested BS despite its high received signal power.
- For a large number of incoming users, the CAA scheme balances the traffic load among different BSs.
- The CAA scheme reduces to RSP-based association if channel access probabili-

ties from all BSs are same and it reduces to traffic load-based association if the received signal powers from different BSs are alike.

Nonetheless, the performance of CAA-based association is vulnerable to interference as a user can associate to a distant BS with high channel access probability.

2.1.2 Contribution

In this chapter, I introduce a comprehensive mathematical framework to analyze the performance of CAA scheme with Almost Blank Subframe (ABS)-based interference coordination at MBSs. The main contributions of this chapter can be summarized as follows:

- I characterize the SE of downlink transmission to a user with CAA-based user association with and without interference coordination at the MBS.
- I characterize the network-wide SE of downlink transmission.
- I consider a more general channel fading model, namely, the generalized-$\mathcal{K}$ composite fading which is approximated with Gamma fading channels for tractable analysis.
- I model the individual traffic load distributions per SBS as well as MBS. In this chapter, I consider Poisson traffic load distribution per SBS and MBS. Note that this set-up corresponds to clustered Poisson Point Processes which are difficult to analyze with the stochastic geometry-based approaches.

Numerical results are presented to compare the performance of user friendly schemes such as RSP and BRSP, with CAA-based user association schemes and analyze their feasibility in different scenarios. The performance gains of BRSP compared

to RSP are highly dependent on the bias values and selection of optimal bias is extremely important in order to achieve useful gains. Nevertheless, even with the optimal bias selection, CAA scheme is shown to outperform BRSP scheme. This fact highlights the importance of adopting per-BS biasing rather than per-tier biasing as well as per-tier and per-BS traffic load modeling. Finally, insights are extracted related to selecting the proportion of ABS as a function of traffic load intensities at MBS and SBSs.

2.2 Related Work

A number of research works investigate the problem of joint user association, interference coordination, and/or traffic load balancing [11–14]. CRE with fixed bias is considered in [11,14] for traffic load balancing. An optimal proportion of ABS frames is derived by solving a network-wide utility maximization problem [11] and a sum-rate utility maximization problem considering full buffer and non full buffer traffic types [14]. Another interesting work to achieve traffic load balancing is [12] where centralized and distributed user association schemes are proposed. The centralized algorithms execute repetitively in order to adapt to the network variations. To cope with this issue, low-complexity signal-to-interference-plus-noise ratio (SINR) bias and rate bias-based association criteria are recommended. The SINR bias is obtained by a brute force search and the best rate bias is the optimal BS price determined by the BS load. *Both best SINR bias and rate bias are evaluated to be same for all BSs in a specific tier which may not be true in practice.* In [13], the framework of [12] is extended to consider interference coordination. The long-term network-wide utility is maximized to find the optimal user association and proportion of blank resources. The scheme is centralized and maximizes the utility of all BSs and all users in the

network.

Other research works focus on developing tractable stochastic geometry models to characterize the performance of CRE with fixed arbitrary bias either without interference coordination [15, 16] or with interference coordination [17–22]. In [15, 16], the performance of CRE is analyzed by deriving outage probability expressions for users. The SE performance for the offloaded users is analyzed in [17] considering ABS at MBS assuming that the distances between different users and their nearest BSs are independent. This assumption is relaxed in [18]. The outage probability and SE performances for the tagged link are analyzed in [19] considering CRE, ABS at MBS, and distributed antenna system. In [20], the success probability of a victim user (macro-user in macro/femto scenario and pico-user in macro/pico scenario) is derived. Then, the number of ABS frames is optimized to maximize the average throughput of the victim user under minimum throughput constraint. In [22], the SE performance of a given user is analyzed by taking into consideration both CRE and ABS at the MBS.

Most of the aforementioned optimized cell-association schemes exploit significant knowledge of network information and thus are non-scalable. On the other hand, the analytical studies mainly characterize the network performance in an average sense and focus on biased RSP (BRSP)-based association that selects a static arbitrary bias for all BSs of a specific tier. Although BRSP-based association is simple, an optimal bias needs to be calculated for different network scenarios. Note that the "optimum" bias is typically obtained per-tier and is not unique for each BS of a given tier [12]. This bias can actually be quite sensitive to the spatio-temporal distribution of users in the network [23], i.e., the traffic load may significantly differ among various BSs of a specific tier. This traffic load imbalance, if not taken into account, can deteriorate

the SE performance of an offloaded user (e.g., due to channel unavailability as well as strong interference from high-power or nearby BSs and poor link quality) as is also highlighted in [23]. Thus, there is a need to develop low-complexity user association schemes that can adopt per-BS bias value, enhance the SE performance in the system by exploiting traffic load information in the different BSs (in different tiers as well as different BSs in a specific tier) in addition to the link quality information. Also, the performances of such schemes need to be characterized in the presence of interference coordination schemes.

Notation: Gamma$(\kappa_{(\cdot)}, \Theta_{(\cdot)})$ represents a Gamma distribution with shape parameter κ, scale parameter Θ and $(\cdot)$ displays the name of the random variable (RV). $\mathcal{K}_G(m_{c_{(\cdot)}}, m_{s_{(\cdot)}}, \Omega_{(\cdot)})$ represents the generalized-$\mathcal{K}$ distribution with fading parameter m_c, shadowing parameter m_s and average power Ω. $\Gamma(a) = \int_0^\infty x^{a-1}e^{-x}dx$ represents the Gamma function, $\Gamma_u(a;b) = \int_b^\infty x^{a-1}e^{-x}dx$ denotes the upper incomplete Gamma function, $\Gamma_l(a;b) = \int_0^b x^{a-1}e^{-x}dx$ denotes the lower incomplete Gamma function and $\Gamma(a;b_1;b_2) = \Gamma_u(a;b_1) - \Gamma_u(a;b_2) = \int_{b_1}^{b_2} x^{a-1}e^{-x}dx$ denotes the generalized Gamma function [24]. ${}_2F_1[\cdot,\cdot,\cdot,\cdot]$ denotes the Gauss's hyper geometric function. $\Pr(A)$ denotes the probability of event A. $f(\cdot)$, $F(\cdot)$, and $\mathcal{M}(\cdot)$ denote the probability density function (PDF), cumulative distribution function (CDF), and moment generating function (MGF), respectively. $\mathbb{E}[\cdot]$ denotes the expectation operator. A list of the main notations and their definitions is given in Table 2.1.

Table 2.1: Chapter 2: Summary of the main variables and their definitions

Variable	Definition
γ_m	Received signal power at the NU from MBS m
γ_s	Received signal power at the NU from SBS s
$\gamma_{(s)}$	Received signal power at the NU from $(s)^{\text{th}}$ ranked SBS
D_l	Distance between the reference MBS wherein the NU is located and the neighboring MBS l
S	Average number of SBSs within distance T of the NU
h_m	Hybrid association metric for MBS m
$h_{(s)}$	Hybrid association metric for the $(s)^{\text{th}}$ ranked SBS within distance T
p_m^{nabs}	Association probability of the NU with MBS m in NABS mode
$p_{(s)}^{(\cdot)}$	Association probability of the NU with $(s)^{\text{th}}$ ranked SBS within distance T; $(\cdot)$ denotes NABS mode or ABS mode
$r_{z,w}$	Distance between the NU located on polar coordinate (r_z, θ_w) in the reference MBS m and the neighboring MBS l, $r_z \in \{r_1, r_2, \cdots, r_{\mathcal{Z}}\}$, $\theta_w \in \{\theta_1, \theta_2, \cdots, \theta_{\mathcal{W}}\}$
I_m^{nabs}	Cumulative interference at the NU when associated with MBS m in NABS mode
$I_{(s)}^{(\cdot)}$	Cumulative interference at the NU when associated with $(s)^{\text{th}}$ ranked SBS within distance T; $(\cdot)$ denotes NABS mode or ABS mode
ρ_m	Proportion of macrocell ABS
$\mathcal{C}_{\text{nu}}$	Average SE of a newly arriving user
$\mathcal{C}_{\text{mu}}$	Average SE of a given macro user
$\mathcal{C}_{\text{su}_\text{i}}$	Average SE of a given user served by the SBS that lies within radius of the user T
$\mathcal{C}_{\text{su}_\text{o}}$	Average SE of a given user served by the SBS that lies outside radius T
$\mathcal{C}_{\text{net}}$	Average network-wide SE of downlink transmission

2.3 System Model and Assumptions

2.3.1 Network Model

I consider a downlink network of M circular macrocells. Each macrocell m has a coverage radius of R_m and number of users U_m. The macrocells are overlaid with S' randomly deployed small cells. A given small cell s has radius R_s and number of users U_s. The Poisson distribution is a commonly used distribution to model the traffic load (arrival of number of users) or calls per unit time at a given BS of the cellular network [25–28]. It has been empirically found that the stochastic user

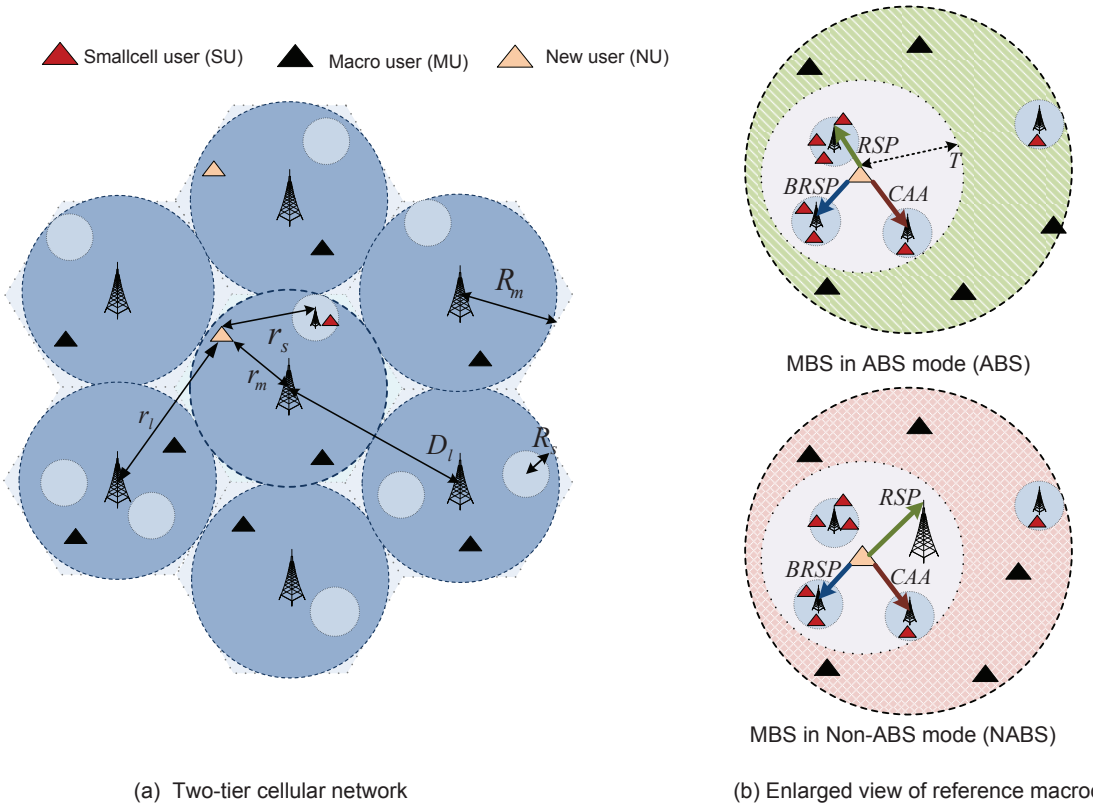

Figure 2.1: (a) Graphical illustration of a two-tier small cell network. In this part of the figure, the distances are demonstrated graphically. (b) Enlarged view of the reference macrocell is provided when the MBS is in ABS and in NABS mode. Moreover, the working mechanisms of RSP, BRSP, and CAA-based association schemes are illustrated.

arrival processes can be well approximated by a Poisson process and the length of each transmission/call can be modeled as an exponential distribution. For an event that occurs at a time interval with an exponential distribution, the rate of occurrence of the event is Poisson distributed. Hence, the numbers of users U_m in a macrocell and U_s in a small cell are considered as Poisson distributed RVs with intensities λ_m and λ_s, respectively. The distribution of U_m and U_s, respectively, can, therefore, be given as:

$$P(U_m = u_m) = \frac{\lambda_m^{u_m}}{u_m!} e^{-\lambda_m}, \tag{2.1}$$

$$P(U_s = u_s) = \frac{\lambda_s^{u_s}}{u_s!} e^{-\lambda_s}. \tag{2.2}$$

Each MBS or SBS selects a user on a given transmission channel considering round-robin scheduling scheme. The small cells are assumed to operate in the open access mode. Both MBSs and SBSs possess an initial traffic load, i.e., U_m and U_s users are already associated with MBS m and SBS s, respectively. Once a new user (NU) arrives within the macrocell region, it associates to either an SBS within a given circular region[1] of radius T around it or its nearest MBS depending on the association criterion. The number of SBSs Q which fall within distance T is random and follows a Binomial distribution which I will derive in Section III. Nevertheless, for analytical tractability, I approximate the number of SBSs within distance T by its average, i.e., $\mathbb{E}[Q] = S$. Note that this approximation is not a limitation and the framework can be extended to consider the exact distribution of Q in a straight-forward manner.

I consider that both the macro-tier and small cell-tier use the same radio spectrum; however, the interference coordination at MBSs is exercised to control macro-tier interference. All MBSs mute their transmissions in a synchronous manner for a given proportion ρ_m of time instants, i.e., each MBS operates in either ABS or non-ABS mode. In the ABS mode, all MBSs mute their transmissions so that the NU can only associate with S SBSs. The associated MUs will remain in the coverage hole (outage) and are not assumed to change their associations in the ABS mode. In the non-ABS (NABS) mode, all MBSs operate normally. Note that it is only the incoming new user that decides whether to associate with the MBS or SBS depending on the association criterion.

[1]The region of radius T around the NU is considered to restrict the association distance of NU from being very large and practically infeasible.

2.3.2 Channel Model

The received signal power at NU on a given transmission channel from the MBS is defined as follows:

$$\gamma_m = P_m r_m^{-\beta} \chi_m, \qquad \forall m = 1, 2, \cdots, M, \tag{2.3}$$

where β is the path-loss exponent, r_m is the distance of the NU from the MBS m, P_m denotes the transmit power of m^{th} MBS per channel, and χ_m represents the composite shadowing and fading channel and $\chi_m = \xi_m \, \varsigma_m$. ξ_m represents the shadowing part and ς_m represents the fading part of the composite shadowing and fading channel. The received signal power at the NU from any neighboring MBS is given as:

$$X_l = P_l r_l^{-\beta} \chi_l, \qquad \forall l \neq m, \tag{2.4}$$

where r_l denotes the distance of the NU in the reference MBS from the neighboring MBS l located at distance D_l from the reference MBS, P_l denotes the transmit power of l^{th} MBS per transmission channel, and χ_l represents the composite shadowing and fading channel power gain and $\chi_l = \xi_l \, \varsigma_l$. ξ_l represents the shadowing part and ς_l represents the fading part of the composite shadowing and fading channel.

Similarly, the received signal power at the NU from SBS s is given as follows:

$$\gamma_s = P_s \bar{r}_s^{-\beta} \zeta_s, \quad \forall s = 1, 2, \cdots, S', \tag{2.5}$$

where P_s represents the transmit power of SBS s, $\bar{r}_s$ denotes the distance between the NU and the SBS s, and ζ_s represents the composite shadowing and fading channel and $\zeta_s = \xi_s \, \varsigma_s$. ξ_s represents the shadowing part and ς_s represents the fading part of

the composite shadowing and fading channel.

Generally, composite fading distributions can be used to jointly model the shadowing and fading channels. Nakagami-m is a generic fading distribution that involves Rayleigh distribution for $m = 1$ (typically used for non line of sight (NLOS) conditions) and can well approximate the Ricean fading distribution for $1 \leq m \leq \infty$ (typically used for strong LOS conditions). Shadowing is modeled by the lognormal distribution; nevertheless, due to the lack of closed-form expressions, lognormal-based composite fading models complicates the analysis. Recently, the generalized-$\mathcal{K}$ distribution has been proposed wherein Gamma distribution [29, 30] is used to model the shadowing, as well as fading channels. Since the PDF, CDF, and MGF of the Generalized-$\mathcal{K}$ distribution involves computation-intensive special functions; thus the distribution is approximated with a more tractable Gamma distribution using the moment matching method, i.e., $\mathcal{K}_G(m_c, m_s, \Omega) \approx \text{Gamma}(\kappa, \Theta)$ [30]. By matching the first and second moments of the two distributions, the corresponding values of κ and Θ can be given as [30]:

$$\kappa = \frac{m_c m_s}{m_c + m_s + 1 - m_c m_s \epsilon}, \Theta = \frac{\Omega}{\kappa}, \tag{2.6}$$

where ϵ is an adjustment parameter. Thus, ζ and χ will be considered as Gamma RVs in this chapter.

2.3.3 Channel Access-Aware (CAA) User Association

The CAA user association is a generalized scheme that considers both the channel access probability (i.e., the probability of obtaining a channel for transmission from a BS) as well as the received signal power from different BSs as the association metric.

A given BS can schedule its user using any scheduling criteria such as greedy

scheduling, and round-robin scheduling schemes. With greedy scheduling scheme, a BS selects a user whose received signal power is greater than the received signal power of all other users. That is a user with strong received signal power will have high channel access probability. Whereas with round-robin scheduling, a BS selects a user randomly which results in equal channel access probability for all users.

Given that the round-robin scheduling is used at each BS, the channel access probability of the NU with MBS m is $p_m^{\text{access}} = \frac{1}{U_m+1}$ and with SBS s is $p_s^{\text{access}} = \frac{1}{U_s+1}$.

Remark: Similarly, the channel access probability of the NU with MBS m considering greedy scheduling scheme is $p_{m,g}^{\text{access}} = \Pr\{\gamma_m > \underset{i=1,\cdots,U_m}{\gamma_i}\} = \int_0^\infty \prod_{i=1}^{U_m} \Pr\{\gamma_i \leq \gamma_m\} f_{\gamma_m}(x)dx = \int_0^\infty \prod_{i=1}^{U_m} F_{\gamma_i}(x) f_{\gamma_m}(x)dx$ and with SBS s is $p_{s,g}^{\text{access}} = \Pr\{\gamma_s > \underset{j=1,\cdots,U_s}{\gamma_j}\} = \int_0^\infty \prod_{j=1}^{U_s} \Pr\{\gamma_j \leq \gamma_s\} f_{\gamma_s}(y)dy = \int_0^\infty \prod_{j=1}^{U_s} F_{\gamma_j}(y) f_{\gamma_s}(y)dy$.

The association criterion can then be written as follows:

$$k_{\text{CAA}}^* = \arg\max\{h_m, h_s\}, \qquad \forall\, s = 1, 2, ..., S, \tag{2.7}$$

where hybrid association metric for a given MBS (h_m) and SBS (h_s) is defined, respectively, as follows:

$$h_m = \frac{P_m r_m^{-\beta} \xi_m}{U_m + 1}, h_s = \frac{P_s \bar{r}_s^{-\beta} \xi_s}{U_s + 1}, \tag{2.8}$$

where ξ_m and ξ_s represent the shadowing[2] parts of the composite fading channel gains χ_m and ζ_s, respectively. For comparison purposes, I consider the following user association schemes:

a) **Conventional RSP-based association:** In this case, the NU utilizes the received signal powers from all SBSs within distance T as well as its nearest

[2]To avoid the ping-pong effect, the association decisions do not consider the effect of short-term fast fading.

MBS to select the best BS, i.e.,

$$k^*_{\text{RSP}} = \arg\max \left\{ P_m r_m^{-\beta} \xi_m, P_s \bar{r}_s^{-\beta} \xi_s \right\}, \ \forall s = 1, 2, ..., S. \tag{2.9}$$

b) **Conventional BRSP-based association:** In this case, an arbitrary bias value b is assigned to all SBSs. The NU utilizes the biased received signal powers from all SBSs within distance T and the received power from the nearest MBS to select the best BS, i.e.,

$$k^*_{\text{BRSP}} = \arg\max \left\{ P_m r_m^{-\beta} \xi_m, b P_s \bar{r}_s^{-\beta} \xi_s \right\}, \ \forall s = 1, 2, ..., S. \tag{2.10}$$

For clear exposition, consider a scenario where the NU is near to the MBS, the NU association decision will vary for different association schemes as follows:

- **RSP:** The new user will likely associate to MBS due to high transmit power.
- **BRSP:** For reasonably high values of bias, the new user will select the SBSs.
- **CAA:** Depending on the existing load at MBS, the new user can choose to associate between MBS and SBSs.

2.3.4 Analytical Approach: Evaluation of Spectral Efficiency

I outline the methodology to evaluate the SE of downlink transmission to the NU, a given MU, a given SU and the network SE in the following.

- Derive the average number of SBSs within distance T, i.e., S.

- Derive the association probability of the NU with reference MBS (p_m^{nabs}) and S SBSs ($p_{(s)}^{\text{nabs}}$) in NABS mode and with S SBSs ($p_{(s)}^{\text{abs}}$) in ABS mode.

- Derive the MGF of the received signal power and cumulative interference at the NU in both modes.

- Derive the SE of transmission to the NU in ABS mode ($\mathcal{C}_{\text{nu}}^{\text{abs}}$) and NABS mode ($\mathcal{C}_{\text{nu}}^{\text{nabs}}$). The average SE of downlink transmission to the NU can thus be given as:

$$\mathcal{C}_{\text{nu}} = \rho_m \, \mathcal{C}_{\text{nu}}^{\text{abs}} + (1 - \rho_m) \, \mathcal{C}_{\text{nu}}^{\text{nabs}}, \tag{2.11}$$

where $\mathcal{C}_{\text{nu}}^{\text{abs}}$ represents the SE of the NU in ABS mode and $\mathcal{C}_{\text{nu}}^{\text{nabs}}$ represents the SE of the NU in NABS mode. Following a similar method, the average SE of downlink transmission to a given MU and SU can be calculated, respectively, as follows:

$$\begin{aligned} \mathcal{C}_{\text{mu}} =& (1 - \rho_m)\mathcal{C}_{\text{mu}}^{\text{nabs}}, \\ \mathcal{C}_{\text{su}} =& \rho_m \mathcal{C}_{\text{su}}^{\text{abs}} + (1 - \rho_m)\mathcal{C}_{\text{su}}^{\text{nabs}}, \end{aligned} \tag{2.12}$$

where $\mathcal{C}_{\text{mu}}^{\text{nabs}}$ and $\mathcal{C}_{\text{su}}^{\text{nabs}}$ represent the SE of a MU and a SU, respectively, in NABS mode, and $\mathcal{C}_{\text{su}}^{\text{abs}}$ represents the SE of a SU in ABS mode. Note that the SE of transmission to an MU will be zero for ρ_m proportion of time when the MBSs are in the ABS mode. Finally, the network-wide SE of downlink transmission can be computed as:

$$\mathcal{C}_{\text{net}} = \rho_m \mathcal{C}_{\text{net}}^{\text{abs}} + (1 - \rho_m)\mathcal{C}_{\text{net}}^{\text{nabs}}, \tag{2.13}$$

where $\mathcal{C}_{\text{net}}^{\text{abs}}$ and $\mathcal{C}_{\text{net}}^{\text{nabs}}$ represent the network-wide SE when MBSs are in ABS mode and NABS mode, respectively.

2.4 Association Probabilities

In this section, first I derive the distribution of Q (the number of SBSs within the circular region of radius T around the NU). Then, using the theory of order statistics I derive the distribution of the ranked distance between the NU and the SBSs within radius T. Subsequently, I evaluate the association probabilities of the NU with MBS (p_m^{nabs}) and with SBSs ($p_{(s)}^{\text{nabs}}$) in NABS mode and with SBSs ($p_{(s)}^{\text{abs}}$) in ABS mode, respectively.

2.4.1 Distribution of Q and Distance Between the NU and the SBSs

a) **Distribution of Q:** Since Q is a discrete random variable, the distribution of Q can be given by the Binomial distribution as:

$$p_Q(q) = \binom{S'}{q} p^q (1-p)^{S'-q}, \ \forall \ q = 0, 1, \cdots, S', \tag{2.14}$$

where p is the probability that an SBS falls within distance T around the NU. To compute p, the distribution of the distance between an arbitrary SBS and NU is required. Note that the NU can be located anywhere within R_m and an arbitrary SBS can be located anywhere within $R_m + D_l$ from the reference MBS, where $D_l = 2R_m$. The exact distribution of distance between the NU and an SBS that are distributed in different radii is unknown[3]. To make the framework analytically tractable, I use the following assumption which simplifies the distribution of the distance between an arbitrary SBS and the NU.

[3]However, the distribution of distance between two random points uniformly distributed in the same radius can be obtained by using random line picking theory [31].

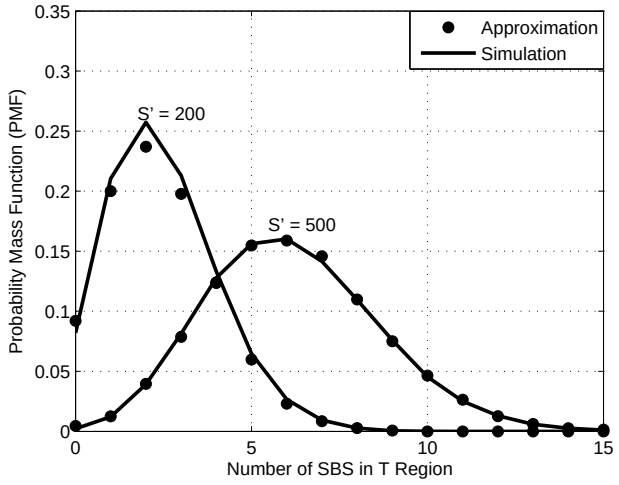

Figure 2.2: Comparison between the approximated distribution of the number of SBSs within T given in (2.14) and the exact distribution obtained from Monte-Carlo simulations (for $R_m = 300$ m, $\beta = 2, T = 100$ m, $D_l = 600$ m).

Assumption: Since the NU considers SBSs only within circular region of radius T around her, the impact of the location of NU within $R_m + D_l$ is not significant (specifically in the calculations that relate to the distance between the NU and S SBSs within distance T). This is verified through Monte-Carlo simulations in Fig. 2.1. As such, for calculations related to the distance between NU and S SBSs, I assume that the NU is located at the origin. Thus, the exact distance distribution between an NU and an arbitrary SBS ($f_{\bar{r}_s}(\bar{r}_s)$) is approximated as $f_{\bar{r}_s}(\bar{r}_s) \approx f_{r_s}(r_s) = \frac{2r_s}{(R_m+D_l)^2}$, where $0 \leq r_s \leq R_m + D_l$.

Based on this assumption, I derive the value of $p = F_{r_s}(T) = P(r_s \leq T)$, as follows:

$$F_{r_s}(T) = \int_0^T f_{r_s}(r_s) dr_s = \frac{T^2}{(R_m + D_l)^2}. \tag{2.15}$$

The average number of SBSs within distance T can then be given as $S = \mathbb{E}[Q] = S'p = S'F_{r_s}(T)$. To validate the accuracy of the considered approximation, Fig. 2.2 compares the approximated distribution of Q in (2.14) with the exact

distribution obtained from the Monte-Carlo simulations (in which the NU can be located anywhere within R_m). The analytical approximation corroborates with the simulation results.

b) **Distribution of distance between the NU and the SBSs:** I now derive the ranked distribution of the distance between the NU and S SBSs within distance T from the NU. By utilizing the assumption stated above and the theory of ordered statistics, I have $r_{(1)} < \cdots < r_{(S)}$, where $r_{(1)}$ and $r_{(S)}$ represent the SBS at the minimum distance and the SBS at the maximum distance from the NU, respectively. The PDF of $r_{(s)}$ can be defined as:

$$f_{r_{(s)}}(r_{(s)}) = \frac{S!\left(F_{r_s}(r_s)\right)^{s-1}\left(1-F_{r_s}(r_s)\right)^{S-s} f_{r_s}(r_s)}{(s-1)!(S-s)!}. \tag{2.16}$$

Substituting $f_{r_s}(r_s)$, and $F_{r_s}(r_s)$, (2.16) can be rewritten as:

$$f_{r_{(s)}}(r_{(s)}) = \frac{S!\left(\frac{r_{(s)}^2}{(R_m+D_l)^2}\right)^{s-1}\left(1-\frac{r_{(s)}^2}{(R_m+D_l)^2}\right)^{S-s} 2r_{(s)}}{(R_m+D_l)^2(s-1)!\,(S-s)!}. \tag{2.17}$$

Using Binomial expansion, (2.17) can be simplified as:

$$f_{r_{(s)}}(r_{(s)}) = \sum_{n=0}^{S-s} \frac{2\ S!\ (-1)^{S-s-n}\left(\frac{r_{(s)}}{R_m+D_l}\right)^{2S-2n-1}}{(s-1)!\ (S-s-n)!\ n!\ (R_m+D_l)^2}. \tag{2.18}$$

Since $0 \leq r_{(s)} \leq R_m + D_l$, I truncate this distribution to a maximum distance of T. The truncated distribution[4] of $r_{(s)}$ can be described as:

$$\tilde{f}_{r_{(s)}}(r_{(s)}) = \frac{f_{r_{(s)}}(r_{(s)})}{\int_0^T f_{r_{(s)}}(r_{(s)})dr_{(s)}}. \tag{2.19}$$

[4]The truncated distribution is a conditional distribution that results from restricting the domain of $f_{r_{(s)}}(r_{(s)})$.

Now h_s corresponding to ranked SBS s is defined as follows:

$$h_{(s)} = \frac{P_s \; r_{(s)}^{-\beta} \zeta_s}{U_s + 1}, \quad \forall s = 1, \cdots, S. \tag{2.20}$$

Note that after multiplying $r_{(s)}$ with a random variable ζ_s, $h_{(s)}$ is no longer a ranked random variable.

2.4.2 Association Probabilities When the MBSs are in the NABS Mode

In the NABS mode, the MBSs operate normally and serve their associated users. In this case, the NU has opportunity to associate with either an MBS or an SBS depending on the association probability.

a) **Association with the reference MBS:** Conditioned on h_m in (2.8), the association probability of the NU with the nearest (i.e., reference) MBS can be derived as:

$$p_{m|h_m}^{\text{nabs}} = \Pr(\underset{s=1,2,\ldots,S}{h_{(s)}} \leq h_m) = \prod_{s=1}^{S} F_{h_{(s)}}(h_m), \tag{2.21}$$

where $F_{h_{(s)}}(h_{(s)})$ represents the CDF of the $h_{(s)}$ and can be derived as given in Appendix A.2. The unconditional p_m^{nabs} can then be derived by averaging over the distribution of h_m as follows:

$$p_m^{\text{nabs}} = \int_0^{\infty} \prod_{s=1}^{S} F_{h_{(s)}}(h_m) f_{h_m}(h_m) dh_m, \tag{2.22}$$

where $f_{h_m}(h_m)$ represents the PDF of h_m and can be derived as given in Appendix A.1. Substituting $F_{h_{(s)}}(h_{(s)})$ and $f_{h_m}(h_m)$, (2.22) can be solved using standard mathematical software packages.

b) **Association with an SBS:** Similarly, when the MBSs are in the NABS mode, the association probability of the NU with the s ranked SBS can be derived by conditioning on $h_{(s)}$ as follows:

$$\begin{aligned} p^{\text{nabs}}_{(s)|h_{(s)}} &= \Pr(\underset{\substack{n=1,2,\ldots,S \\ n\neq s}}{h_{(n)}}, h_m \leq h_{(s)}) \\ &= \prod_{\substack{n=1 \\ n\neq s}}^{S} F_{h_{(n)}}(h_{(s)}) F_{h_m}(h_{(s)}). \end{aligned} \tag{2.23}$$

The unconditional $p^{\text{nabs}}_{(s)}$ can be derived by averaging over the distribution of $h_{(s)}$ as follows:

$$p^{\text{nabs}}_{(s)} = \int_0^\infty \prod_{\substack{n=1 \\ n\neq s}}^{S} F_{h_{(n)}}(h_{(s)}) F_{h_m}(h_{(s)}) f_{h_{(s)}}(h_{(s)}) dh_{(s)}, \tag{2.24}$$

where PDF and CDF of $h_{(s)}$, i.e., $f_{h_{(s)}}(h_{(s)})$ and $F_{h_{(s)}}(h_{(s)})$ can be derived as given in Appendix A.2 and CDF of h_m, i.e., $F_{h_m}(h_m)$ can be derived as given in Appendix A.1. Substituting $F_{h_{(s)}}(h_{(s)})$, $F_{h_m}(h_m)$, and $f_{h_{(s)}}(h_{(s)})$, I can solve (2.24) using standard mathematical softwares.

Fig. 2.3 compares the analytical and simulation results for the association probabilities of the NU considering no interference coordination (or 100% NABS mode) and two traffic load scenarios, i.e., (i) $\lambda_m = \lambda_s, S' = 500$, (ii) $\lambda_m \geq \lambda_s$ for (a) $S' = 200$ (b) $S' = 500$. Analytical results corroborate with the simulation results. In (i) the association probability of the NU is higher for MBS than the nearest SBS. This is due to the fact that with same traffic load intensities in both tiers, the CAA scheme follows the RSP scheme. Thus, the NU is highly likely to associate with a high power MBS. On the other hand, when $\lambda_m \geq \lambda_s$

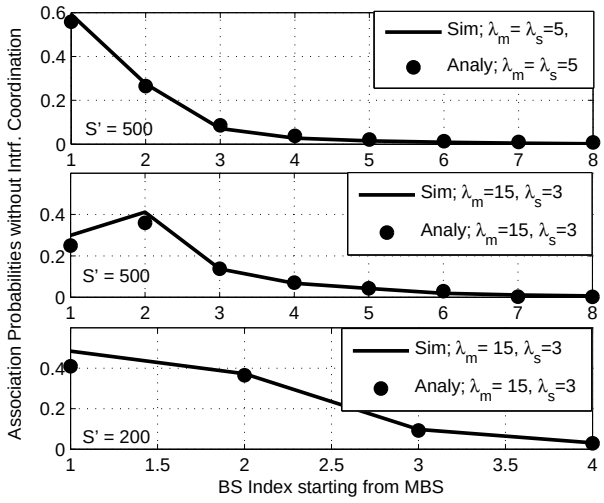

Figure 2.3: Association probabilities of the NU with the reference MBS and S SBSs without interference coordination (for $R_m = 300$ m, $T = 100$ m, $\rho_m = 0$ (no interference coordination)). BS indices $[2, \cdots, 4]$ represent the S SBSs within distance T.

and $S' = 500$, the association probability of the NU with the nearest SBS turns out to be greater than the MBS. Clearly, in this case, the NU has a higher association probability with SBSs within distance T due to high traffic load in the MBS. It is, however, important to note that, the association probability of the NU with an MBS turns out to be higher again if S' reduces to 200. This occurs due to the small number of SBSs that are relatively far apart from the NU compared to the case when $S' = 500$.

2.4.3 Association Probabilities When the MBSs are in the ABS Mode

In this case, the NU has only option to associate with one of the SBSs. Thus, the association probability of the NU with the s ranked SBS can be derived by conditioning on $h_{(s)}$ as $p^{\text{abs}}_{(s)|h_{(s)}} = \prod_{\substack{n=1 \\ n \neq s}}^{S} F_{h_{(n)}}(h_{(s)})$. The unconditional $p^{\text{abs}}_{(s)}$ can then be

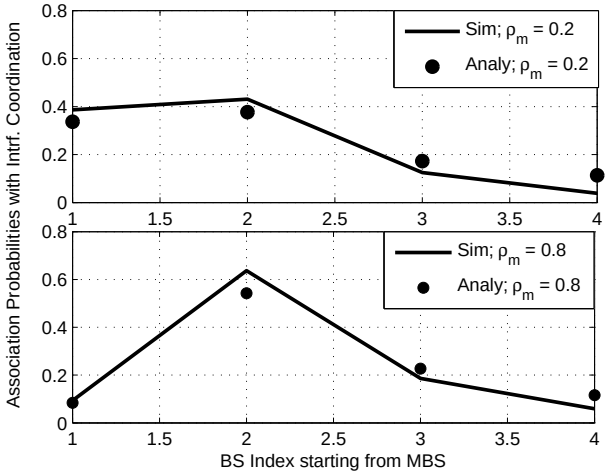

Figure 2.4: Association probabilities of the NU with a reference MBS and S SBSs within distance T with interference coordination (for $R_m = 300$ m, $T = 100$ m, $S' = 200$, $\lambda_m = 15$, $\lambda_s = 3$). BS indices $[2, \cdots, 4]$ represent the S SBSs within distance T.

derived by averaging over the distribution of $h_{(s)}$ as follows:

$$p_{(s)}^{\text{abs}} = \int_0^\infty \prod_{\substack{n=1 \\ n \neq s}}^{S} F_{h_{(n)}}(h_{(s)}) f_{h_{(s)}}(h_{(s)}) dh_{(s)}. \tag{2.25}$$

Substituting $F_{h_{(s)}}(h_{(s)})$, and $f_{h_{(s)}}(h_{(s)})$, (2.25) can be solved.

2.4.4 Association Probability of a Given NU

The association probability of a given NU with the SBS at rank s and the nearest MBS can then be calculated as $\rho_m p_{(s)}^{\text{abs}} + (1-\rho_m) p_{(s)}^{\text{nabs}}$ and $(1-\rho_m) p_{(m)}^{\text{nabs}}$, respectively.

Fig. 2.4 compares the analytical and simulation results for the association probabilities of the NU with a reference MBS and S SBSs in an interference coordinated system considering (i) $\rho_m = 0.2$ (ii) $\rho_m = 0.8$. For $\rho_m = 0.2$, the association probability of the NU with the nearest SBS is slightly higher than the MBS which is different from the case of no interference coordination in Fig. 2.3. For $\rho_m = 0.8$, the

association probability with the MBS further decreases. This is because, in the ABS mode, the NU has only the option to select one of SBSs. Therefore, the higher ρ_m, the higher would be the chance to associate with an SBS.

2.5 Statistics of Signal and Interference Powers

In this section, I derive the statistics of the received signal and interference powers at the NU when it is associated with the reference MBS or an SBS (when the MBSs are in NABS mode) or with an SBS (when the MBSs are in ABS mode).

2.5.1 Statistics of Received Signal Powers

a) **Association with reference MBS:**

Since the NU can associate with the reference MBS when the MBSs are in the NABS mode, the received signal power at the NU from the reference MBS, γ_m is defined in (3.2). The MGF of γ_m can be derived as [32]:

$$\mathcal{M}_{\gamma_m}(t) = {}_2F_1\left[\kappa_\chi, -\frac{2}{\beta}, 1-\frac{2}{\beta}, \frac{-P_m t\Theta_\chi}{R_m^\beta}\right] - \frac{\Gamma\left(\kappa\chi+\frac{2}{\beta}\right)\Gamma\left(1-\frac{2}{\beta}\right)}{R_m^2\Gamma\left(\kappa_\chi\right)\left(P_m t\Theta_\chi\right)^{\frac{2}{\beta}}}. \quad (2.26)$$

b) **Association with an SBS:**

In both NABS and ABS modes, the NU can associate with the s^{th} ranked SBS within distance T. In both cases, when the NU associates with the s ranked SBS, the received signal power at the NU is defined as:

$$\gamma_{(s)} = P_s r_{(s)}^{-\beta}\zeta_s, \qquad \forall\ s = 1, ..., S, \quad (2.27)$$

where $r_{(s)}$ represents the distance between the NU and the s ranked SBS. The

MGF of $\gamma_{(s)}$ can then be derived as follows:

$$\mathcal{M}_{\gamma_{(s)}}(t) = \sum_{n=0}^{S-s} \frac{K_n \, {}_2F_1[1, \kappa_\zeta, \frac{\beta\kappa_\zeta - 2n + 2S + \beta}{\beta}, \frac{T^\beta}{T^\beta + P_s \Theta_\zeta \ t}]}{(\beta\kappa_\zeta - 2n + 2S)(T^\beta + P_s\Theta_\zeta t)^{\kappa_\zeta} T^{\beta\kappa_\zeta - 2n + 2S}}. \tag{2.28}$$

Proof. See Appendix A.3. □

2.5.2 Statistics of Received Interference

a) **Association with the reference MBS:** When the NU associates with the reference (i.e., nearest) MBS, the cumulative interference at the NU is given by:

$$I_m^{\text{nabs}} = I_m^{\text{co}} + I_m^{\text{cr}}, \tag{2.29}$$

where I_m^{co} and I_m^{cr} are independent random variables and denote the co-tier and cross-tier interferences at the NU when it is associated with the reference MBS (in NABS mode). The MGF of I_m^{nabs} can thus be given by:

$$\mathcal{M}_{I_m^{\text{nabs}}}(t) = \mathcal{M}_{I_m^{\text{co}}}(t) \, \mathcal{M}_{I_m^{\text{cr}}}(t). \tag{2.30}$$

The co-tier interference from the neighboring MBSs is defined as:

$$I_m^{\text{co}} = \sum_{l=1, l\neq m}^{M} X_l, \tag{2.31}$$

where X_l is defined in (2.4). The distribution of the distance r_l is given in [32, Eq. 5]. Note that, $X_l \ \forall l$ are correlated random variables. To avoid the complexity of correlation due to the locations of interfering MBSs, I use the approximate approach presented in [32]. I approximate r_l with $r_{w,z}$ such that $r_l \approx r_{z,w} = \sqrt{r_z^2 + D_l^2 - 2r_z \ D_l \cos(\theta_l - \theta_w)}$, where (r_z, θ_w) represents the polar

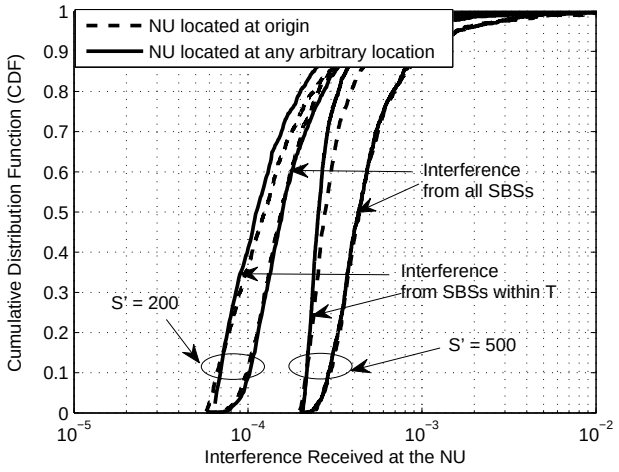

Figure 2.5: Comparison of the CDF of the cumulative interference from S and S' SBSs considering (i) the exact location of the NU; (ii) NU is located at origin (assumption) (for $T = 100$, $P_m = 10W, P_s = 0.1W, \beta = 2.0$).

coordinate of the NU's location from reference MBS. The detailed approximation procedure can be found in [32].

Conditioned on $r_{z,w}$, the MGF of X_l can then be written as $\mathcal{M}_{X_l|r_{z,w}}(t) = 1 + \frac{t\ P_l}{r_{z,w}^{\beta}\lambda}$, where $\mathcal{Z}$ represents the number of circular zones of equal width and $\mathcal{W}$ represents the equal angular intervals. Consequently, the MGF of I_m^{co} can then be derived as follows:

$$\mathcal{M}_{I_m^{\text{co}}}(t) = \sum_{z=1}^{\mathcal{Z}} \sum_{w=1}^{\mathcal{W}} \frac{1}{\mathcal{Z}\mathcal{W}} \prod_{l=1, l\neq m}^{M} \mathcal{M}_{X_l|r_{z,w}}(t). \tag{2.32}$$

Since the NU is affected more by the interference caused by nearby SBSs, I approximate the cumulative interference of all SBSs with the cumulative interference of all SBSs that are located within distance T. The effect of SBSs outside radius T is nearly negligible because of low transmission powers of the SBSs as illustrated in Fig. 2.5. A comparison of the CDF of cumulative cross-

tier interference I_m^{cr} from S and S' SBSs considering (i) the exact location of the NU; (ii) NU is located at origin (assumption), is demonstrated in Fig. 2.5. It is observed that the approximation turns out to be quite accurate for small values of S' because SBSs are highly likely to be located far apart and thus the effect of interference received from SBSs beyond T is negligible. On the other hand, with increasing S', the impact of interference received from $S' - S$ SBSs becomes slightly more dominant. However, this approximation reduces the computational complexity significantly without affecting the SE of transmission, as will be shown later. The MGF of I_m^{cr} from S SBSs within distance T can then be derived as follows:

$$\mathcal{M}_{I_m^{\text{cr}}}(t) = \prod_{s=1}^{S} \mathcal{M}_{\gamma_{(s)}}(t), \tag{2.33}$$

where $\mathcal{M}_{\gamma_{(s)}}(t)$ is given in (2.28).

b) **Association with an SBS:** The NU can associate with an SBS when the MBSs are in either NABS mode or ABS mode. Therefore, I derive the MGF of cumulatively received interference at the NU in both modes.

In the NABS mode, when the NU associates with the s^{th} ranked SBS out of S SBSs, the cumulative interference can be defined as $I_{(s)}^{\text{nabs}} = I_{(s)}^{\text{co}} + I_{(s)}^{\text{cr}}$. The MGF of $I_{(s)}^{\text{nabs}}$ can, therefore, be given as follows:

$$\mathcal{M}_{I_{(s)}^{\text{nabs}}}(t) = \mathcal{M}_{I_{(s)}^{\text{co}}}(t)\, \mathcal{M}_{I_{(s)}^{\text{cr}}}(t). \tag{2.34}$$

The MGF of $I^{\text{co}}_{(s)}(t)$ can be derived as:

$$\mathcal{M}_{I^{\text{co}}_{(s)}}(t) = \prod_{n=1, n\neq s}^{S} \mathcal{M}_{\gamma_{(n)}}(t), \tag{2.35}$$

where $\mathcal{M}_{\gamma_{(s)}}(t)$ is given in (2.28). Also, the MGF of the cross-tier interference can be given as:

$$\mathcal{M}_{I^{\text{cr}}_{(s)}}(t) = \mathcal{M}_{I^{\text{co}}_{m}}(t)\mathcal{M}_{\gamma_m}(t), \tag{2.36}$$

where $\mathcal{M}_{I^{\text{co}}_{m}}$ and $\mathcal{M}_{\gamma_m}$ are given in (2.32) and (2.26), respectively.

In the ABS mode of operation of the MBSs, when the NU associates with the s^{th} ranked SBS out of S SBSs within distance T, the MGF of cumulative received interference at NU can be defined as:

$$\mathcal{M}_{I^{\text{abs}}_{(s)}} = \mathcal{M}_{I^{\text{co}}_{(s)}}, \tag{2.37}$$

where $\mathcal{M}_{I^{\text{co}}_{(s)}}$ is given in (2.35).

2.6 Spectral Efficiency of Downlink Transmission to the NU

In this section, I derive the SE of downlink transmission to the NU considering the NABS mode, ($\mathcal{C}^{\text{nabs}}_{\text{nu}}$) and the ABS mode, ($\mathcal{C}^{\text{abs}}_{\text{nu}}$). Finally, I compute the overall SE of transmission to the NU ($\mathcal{C}_{\text{nu}}$).

The SE of transmission to the NU in both the NABS and ABS modes can be calculated by using the following lemma proposed in [10]:

$$\hat{\mathcal{C}}^{(\cdot)}_{\text{nu},(\cdot)} = \frac{1}{\ln(2)}\mathbb{E}\left[\ln\left(1+\frac{\gamma_{(\cdot)}}{I^{(\cdot)}_{(\cdot)}+\sigma^2}\right)\right] = \int_0^{\infty} \frac{\mathcal{M}_{I^{(\cdot)}_{(\cdot)}}(t)(1-\mathcal{M}_{\gamma_{(\cdot)}}(t))}{t\,\ln(2)} e^{-t\sigma^2} dt, \tag{2.38}$$

where σ^2 is the thermal noise power of the receiver, $(\cdot)$ in the subscript can be m for association with the reference MBS or (s) for association with the s ranked SBS. $(\cdot)$ in the superscript can be NABS (i.e., when the MBSs are in the NABS mode) or ABS (i.e., when the MBSs are in the ABS mode).

2.6.1 Spectral Efficiency in the NABS Mode

If the NU associates with the MBS, it accesses the transmission channel with probability $\frac{1}{U_m+1}$. Thus, the SE ($\hat{\mathcal{C}}^{\text{nabs}}_{\text{nu},m}$) of transmission to the NU, conditioned on U_m, can be calculated by substituting $\mathcal{M}_{\gamma_m}(t)$ from (2.26) and $\mathcal{M}_{I^{\text{nabs}}_m}(t)$ from (2.30) in (2.38).

Similarly, in the NABS mode, if the NU associates with the s^{th} ranked SBS, it accesses the transmission channel with probability $\frac{1}{U_s+1}$. The SE of transmission to the NU ($\hat{\mathcal{C}}^{\text{nabs}}_{\text{nu},(s)}$) conditioned on U_s can then be calculated by substituting $\mathcal{M}_{\gamma_{(s)}}(t)$ from (2.28) and $\mathcal{M}_{I^{\text{nabs}}_{(s)}}(t)$ from (2.34) in (2.38).

The overall SE in the NABS mode can be then derived as:

$$\mathcal{C}^{\text{nabs}}_{\text{nu}} = \mathbb{E}_{U_m}\left[p^{\text{nabs}}_m \frac{\hat{\mathcal{C}}^{\text{nabs}}_{\text{nu},m}}{U_m+1}\right] + \mathbb{E}_{U_s}\left[\sum_{s=1}^{S} p^{\text{nabs}}_{(s)} \frac{\hat{\mathcal{C}}^{\text{nabs}}_{\text{nu},(s)}}{U_s+1}\right]. \tag{2.39}$$

2.6.2 Spectral Efficiency in the ABS Mode

Conditioned on U_s, the SE ($\hat{\mathcal{C}}^{\text{abs}}_{\text{nu},(s)}$) of the NU when associated with the s^{th} ranked SBS, when MBS is in the ABS mode, can be computed by substituting $\mathcal{M}_{\gamma_{(s)}}(t)$ and $\mathcal{M}^{\text{abs}}_{I_{(s)}}(t)$ in (2.38). The average SE in ABS mode can, therefore, be given as:

$$\mathcal{C}^{\text{abs}}_{\text{nu}} = \mathbb{E}_{U_s}\left[\sum_{s=1}^{S} p^{\text{abs}}_{(s)} \frac{\hat{\mathcal{C}}^{\text{abs}}_{\text{nu},(s)}}{U_s+1}\right]. \tag{2.40}$$

2.6.3 Spectral Efficiency of a Given NU

The average SE of transmission to a given NU can be computed in an interference coordinated system as follows:

$$\mathcal{C}_{\text{nu}} = \rho_m \, \mathcal{C}_{\text{nu}}^{\text{abs}} + (1 - \rho_m) \, \mathcal{C}_{\text{nu}}^{\text{nabs}}. \tag{2.41}$$

2.7 Network-Wide Spectral Efficiency of Downlink Transmission

The association of the NU with MBS/SBS degrades the channel access probability of existing MUs/SUs, respectively. As such, in this section, I evaluate the SE of a given MU and SU considering NU association. Recall that S SBSs are located within radius T of the NU and $(S' - S)$ SBSs are located outside radius T. Thus, I separately evaluate (i) the SE of a given SU of ranked s SBS located inside radius T which may be affected by the association of the NU; (ii) the SE of a given SU of any arbitrary SBS outside T which is unaffected by the NU association process. Finally, I derive the overall SE of downlink transmission.

2.7.1 Spectral Efficiency of Transmission to a Given MU

The received signal power at a given MU from its serving MBS m can be defined as given in (3.2). When the MBSs are in the ABS mode, a given MU would be in the coverage hole. As such, the SE of transmission to a given MU exists only when the MBSs are in the NABS mode.

If the NU associates with the reference MBS, the channel access probability of a given MU reduces from $\frac{1}{U_m}$ to $\frac{1}{U_m+1}$. Accordingly, conditioned on U_m, the SE

of transmission to a given MU can be calculated as $\hat{\mathcal{C}}^{\text{nabs}}_{\text{nu},m}/(U_m+1)$. On the other hand, in the NABS mode of operation of the MBSs, if the NU selects an SBS for association, the channel access probability of a given MU remains $\frac{1}{U_m}$. As defined in (2.38), the SE of transmission to a given MU ($\hat{\mathcal{C}}^{\text{nabs}}_{\text{mu}}$) conditioned on U_m can be calculated by substituting $\mathcal{M}_{\gamma_m}(t)$ from (2.26) and $\mathcal{M}_{I^{\text{nabs}}_m}(t)$ from (2.30) in (2.38). In the NABS mode, the average unconditional SE of transmission to a given MU can then be derived as follows:

$$\mathcal{C}^{\text{nabs}}_{\text{mu}} = \mathbb{E}_{U_m}\left[\left(1-p^{\text{nabs}}_m\right)\frac{\hat{\mathcal{C}}^{\text{nabs}}_{\text{mu}}}{U_m} + p^{\text{nabs}}_m\frac{\hat{\mathcal{C}}^{\text{nabs}}_{\text{nu},m}}{U_m+1}\right]. \tag{2.42}$$

The average SE of transmission to a given MU can thus be computed as:

$$\mathcal{C}_{\text{mu}} = (1-\rho_m)\times\mathcal{C}^{\text{nabs}}_{\text{mu}}. \tag{2.43}$$

2.7.2 Spectral Efficiency for a Given SU Served by an SBS Located Within Radius T

The received signal power of an SU in ranked s SBS can be given as in (2.27). When the NU does not associate with an SBS at rank s, the channel access probability of a given SU in s ranked SBS remains $\frac{1}{U_s}$. The SE of transmission to a given SU ($\hat{\mathcal{C}}^{\text{nabs}}_{\text{su}_i,(s)}$) conditioned on U_s can be calculated by substituting $\mathcal{M}_{\gamma_{(s)}}$ from (2.28) and $\mathcal{M}_{I^{\text{nabs}}_{(s)}}$ from (2.34) in (2.38). On the other hand, in the NABS mode, if the NU associates with ranked s SBS, the channel access probability of a given SU reduces to $\frac{1}{U_s+1}$. The SE for a given SU conditioned on U_s can then be given as $\hat{\mathcal{C}}^{\text{nabs}}_{\text{nu},(s)}/(U_s+1)$. In the NABS mode, the average unconditional SE for a given SU served by ranked (s) SBS

can thus be calculated as:

$$\mathcal{C}_{\mathrm{su_i}}^{\mathrm{nabs}} = \mathbb{E}_{U_s}\Big[p_{(s)}^{\mathrm{nabs}} \frac{\hat{\mathcal{C}}_{\mathrm{nu},(s)}^{\mathrm{nabs}}}{U_s+1} + \Big(1-p_{(s)}^{\mathrm{nabs}}\Big)\frac{\hat{\mathcal{C}}_{\mathrm{su_i},(s)}^{\mathrm{nabs}}}{U_s}\Big], \quad \forall s = 1, \cdots, S. \tag{2.44}$$

Similarly, in ABS mode, if the NU associates with the s ranked SBS, the channel access probability of a given SU reduces to $\frac{1}{U_s+1}$. The SE for a given SU conditioned on U_s can then be given as $\hat{\mathcal{C}}_{\mathrm{nu},(s)}^{\mathrm{abs}}/(U_s+1)$. On the other hand, in the ABS mode, if the NU does not associate with the s ranked SBS, the channel access probability of a given SU remains $\frac{1}{U_s}$. Conditioned on U_s, the SE ($\mathcal{C}_{\mathrm{su_i},(s)}^{abs}$) can the be calculated by substituting $\mathcal{M}_{\gamma_s(t)}$ from (2.28) and $\mathcal{M}_{I_{(s)}^{abs}(t)}$ from (2.37) in (2.38). In the ABS mode, the average unconditional SE for the SU can then be given as:

$$\mathcal{C}_{\mathrm{su_i}}^{\mathrm{abs}} = \mathbb{E}_{U_s}\Big[p_{(s)}^{\mathrm{abs}} \frac{\hat{\mathcal{C}}_{\mathrm{nu},(s)}^{\mathrm{abs}}}{U_s+1} + \Big(1-p_{(s)}^{\mathrm{abs}}\Big)\frac{\hat{\mathcal{C}}_{\mathrm{su_i},(s)}^{\mathrm{abs}}}{U_s}\Big], \quad \forall s = 1, \cdots, S. \tag{2.45}$$

The overall SE for a given SU served by the SBS s located within radius T of the NU in an interference coordinated system can thus be computed as follows:

$$\mathcal{C}_{\mathrm{su_i}} = \rho_m \times \mathcal{C}_{\mathrm{su_i}}^{\mathrm{abs}} + (1-\rho_m) \times \mathcal{C}_{\mathrm{su_i}}^{\mathrm{nabs}}. \tag{2.46}$$

2.7.3 SE for a Given SU Served by an SBS Located Outside Radius T

The received signal power at a given SU from its serving SBS s can be defined as given in (2.5). When the NU associates to MBS or ranked s SBS, the channel access probability of a given SU of an SBS outside T remains $\frac{1}{U_s}$. The MGF of γ_s, i.e., $\mathcal{M}_{\gamma_s}(t)$ can be derived as given in (2.26) by replacing R_m and P_m with R_s and P_s. The MGF of interference received at a given SU in NABS mode and ABS mode can be derived in similar manner as for a given NU.

Conditioned on U_s, the SE of a given SU ($\hat{\mathcal{C}}^{\text{nabs}}_{\text{su}_\text{o},s}$) in NABS mode can be derived by substituting $\mathcal{M}_{\gamma_s}(t)$ and $\mathcal{M}_{I^{nabs}_{(s)}}(t)$ in (2.38). The average unconditional SE of SU in NABS mode can then be given as:

$$\mathcal{C}^{\text{nabs}}_{\text{su}_\text{o}} = \mathbb{E}_{U_s}\left[\frac{\hat{\mathcal{C}}^{\text{nabs}}_{\text{su}_\text{o},s}}{U_s}\right], \quad \forall s = 1, \cdots, S' - S. \tag{2.47}$$

Similarly, conditioned on U_s, the SE of a given SU ($\hat{\mathcal{C}}^{\text{abs}}_{\text{su}_\text{o},s}$) can be calculated by substituting $\mathcal{M}_{\gamma_s}(t)$ and $\mathcal{M}_{I^{\text{abs}}_{(s)}}(t)$ in (2.38). The average unconditional SE of SU in ABS mode can then be given as:

$$\mathcal{C}^{\text{abs}}_{\text{su}_\text{o}} = \mathbb{E}_{U_s}\left[\frac{\hat{\mathcal{C}}^{\text{abs}}_{\text{su}_\text{o},s}}{U_s}\right], \quad \forall s = 1, \cdots, S' - S. \tag{2.48}$$

The overall SE for a given SU served by SBS s outside radius T can be determined as follows:

$$\mathcal{C}_{\text{su}_\text{o}} = \rho_m \, \mathcal{C}^{\text{abs}}_{\text{su}_\text{o}} + (1 - \rho_m) \, \mathcal{C}^{\text{nabs}}_{\text{su}_\text{o}}. \tag{2.49}$$

2.7.4 Network-Wide SE of Downlink Transmission

Conditioning on U_m and U_s, in the NABS mode, the network-wide SE can be evaluated as:

$$\mathcal{C}^{\text{nabs}}_{\text{net}} = \mathcal{C}^{\text{nabs}}_{\text{mu}} \times \; M \times U_m + \left(S \times \mathcal{C}^{\text{nabs}}_{\text{su}_\text{i}} + (S' - S) \times \mathcal{C}^{\text{nabs}}_{\text{su}_\text{o}}\right) \times U_s. \tag{2.50}$$

Substituting $\mathcal{C}_{\text{mu}}^{\text{nabs}}$, $\mathcal{C}_{\text{su}_\text{i}}^{\text{nabs}}$, and $\mathcal{C}_{\text{su}_\text{o}}^{\text{nabs}}$, the average unconditional SE of network ($\mathcal{C}_{net}^{\text{nabs}}$) can be written as:

$$\begin{aligned}\mathcal{C}_{\text{net}}^{\text{nabs}} = M \times \mathbb{E}_{U_m}\left[\left(1-p_m^{\text{nabs}}\right)\hat{\mathcal{C}}_{\text{mu}}^{\text{nabs}} + \frac{p_m^{\text{nabs}}\hat{\mathcal{C}}_{\text{nu},m}^{\text{nabs}}}{1+1/U_m}\right] \\ + \mathbb{E}_{U_s}\left[S\left(p_{(s)}^{\text{nabs}}\frac{\hat{\mathcal{C}}_{\text{nu},(s)}^{\text{nabs}}}{1+1/U_s} + \left(1-p_{(s)}^{\text{nabs}}\right)\hat{\mathcal{C}}_{\text{su}_\text{i},(s)}^{\text{nabs}}\right)\right] \\ + \mathbb{E}_{U_s}\left[(S'-S)\hat{\mathcal{C}}_{\text{su}_\text{o},s}^{\text{nabs}}\right].\end{aligned}$$

Similarly, conditioned on U_m and U_s, the network SE in ABS mode can be evaluated as:

$$\mathcal{C}_{\text{net}}^{\text{abs}} = \left(S \times \mathcal{C}_{\text{su}_\text{i}}^{\text{abs}} + (S'-S) \times \mathcal{C}_{\text{su}_\text{o}}^{\text{abs}}\right) \times U_s. \tag{2.51}$$

Substituting $\mathcal{C}_{\text{su}_\text{i}}^{\text{abs}}$, and $\mathcal{C}_{\text{su}_\text{o},s}^{\text{abs}}$, the average unconditional network-wide SE of downlink transmission can be written as:

$$\begin{aligned}\mathcal{C}_{\text{net}}^{\text{abs}} = \mathbb{E}_{U_s}\left[S\left(p_{(s)}^{\text{abs}}\frac{\hat{\mathcal{C}}_{\text{nu},(s)}^{\text{abs}}}{1/U_s+1} + (1-p_{(s)}^{\text{abs}})\frac{\hat{\mathcal{C}}_{\text{nu},(s)}^{\text{abs}}}{U_s}\right)\right] \\ + \mathbb{E}_{U_s}\left[(S'-S)\hat{\mathcal{C}}_{\text{su}_\text{o},s}^{\text{abs}}\right].\end{aligned}$$

The average network-wide SE of downlink transmission can then be computed as:

$$\mathcal{C}_{\text{net}} = \rho_m\, \mathcal{C}_{\text{net}}^{\text{abs}} + (1-\rho_m)\, \mathcal{C}_{\text{net}}^{\text{nabs}}. \tag{2.52}$$

2.8 Numerical Results and Discussion

This section presents numerical results on the SE for NU, MU, and SU considering different user association schemes in the absence and presence of interference coordination. I start with no interference coordination scenarios and gradually move on to

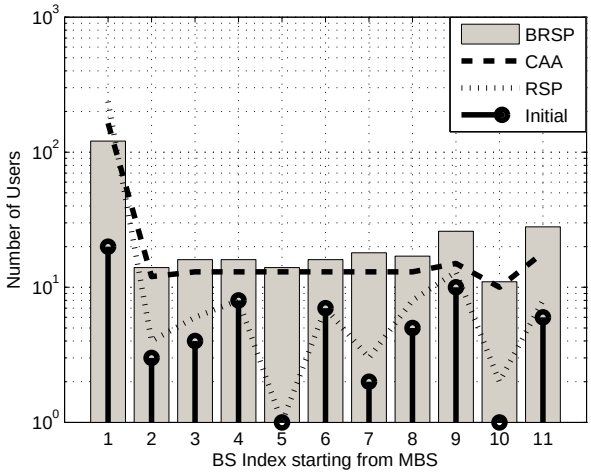

Figure 2.6: Traffic load balancing after arrival of 250 NUs in the two-tier small cell network considering different association schemes (for $\lambda_m = 15$, $\lambda_s = 3$, $\rho_m = 0$).

analyze the impact of adopting interference coordination on the SE performance for the NU, MU, and SU as a function of network design parameters.

In Monte-Carlo simulations, I consider 7 circular macrocells, i.e., $M = 7$ and $S' = 200$ small cells arbitrarily deployed in $R_m + D_l$ region. I consider generalized-$\mathcal{K}$ composite shadowing and fading, i.e., $f_\chi(\chi) \approx \mathcal{K}_{\mathrm{G}}(4, 3/4, 2) \approx \mathrm{Gamma}(0.5, 3.8)$, i.e., $\mathcal{K}_{\mathrm{G}}(4, 3/4, 2)$ is a product of fading $\eta_m \sim \mathrm{Gamma}(3/4, 4/3)$ and shadowing $\xi_m \sim \mathrm{Gamma}(4, 0.5)$. Similarly, $f_\zeta(\zeta) \approx \mathcal{K}_{\mathrm{G}}(1, 2, 2) \approx \mathrm{Gamma}(2, 1)$, i.e., $\mathcal{K}_{\mathrm{G}}(1, 2, 2)$ is a product of fading $\eta_s \sim \mathrm{Gamma}(2, 1/2)$ and shadowing $\xi_s \sim \mathrm{Gamma}(1, 2)$. The coverage radii of an MBS and an SBS are $R_m = 300$ m and $R_s = 50$ m, respectively. I set $T = 100$ m, path-loss exponent $\beta = 2.0$, the thermal noise power density $\sigma^2 = 1 \times 10^{-10}$ W/Hz, the transmission powers of an MBS and an SBS as $P_m = 10$ W and $P_s = 0.1$ W, respectively, and bias $b = 5$ dBW [23].

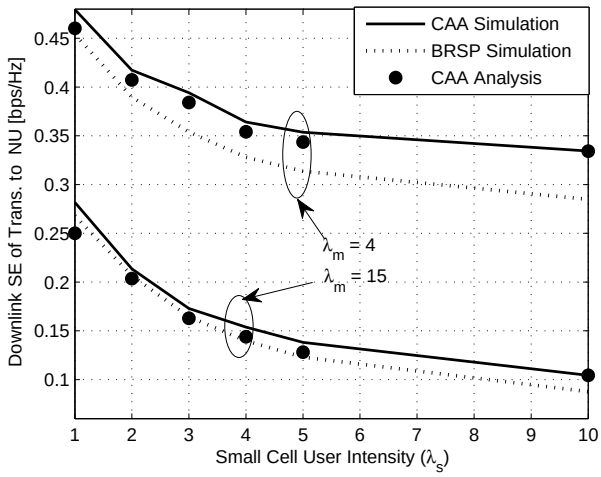

Figure 2.7: SE of downlink transmission to the NU with increase in small cell user intensity (λ_s) for different user association schemes (for $\rho_m = 0$).

2.8.1 Results: No Interference Coordination

Traffic load balancing: Fig. 2.6 considers a two-tier cellular network that comprises of ten small cells. First, the initial traffic loads of different BSs are generated. A large number of NUs (250 NUs) are then assumed to be entering into the system who become associated to different BSs depending on the user association schemes (i.e., CAA, RSP, and BRSP). The impact of different user association schemes on the network traffic load is then analyzed by characterizing the final traffic load of each BS. It can be observed that RSP-based association allows more users to associate with the reference MBS due to its high transmission power. On the other hand, the BRSP-based association tends to balance the traffic loads of the SBSs and the MBS. Finally, the traffic load balancing accomplished by the CAA scheme between the MBS and the SBSs is observed to be in between the two extremes of traditional BRSP and RSP-based association schemes.

SE as a function of λ_m and λ_s: Fig. 2.7 demonstrates the degradation in SE with increasing in λ_s and λ_m. This degradation is due to decrease in channel access

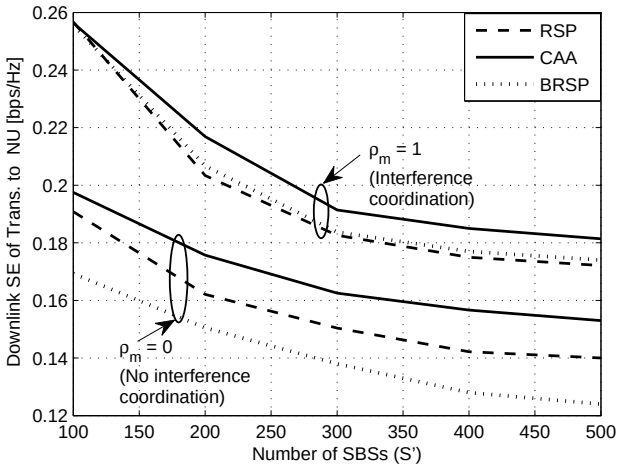

Figure 2.8: SE of downlink transmission to the NU as a function of S' considering different user association schemes (for $\lambda_m = 15, \lambda_s = 3$).

probability with MBS and SBSs. The derived expressions closely follow the Monte-Carlo simulations and the impact of the approximation is also observed to be minimal. For small values of λ_m, the gains with CAA association are significantly higher than those with BRSP-based association because the NU can select the nearest MBS due to its high signal power and channel access probability. With BRSP-based association, the NU is forcefully pushed to low-power SBSs and the presence of strong macro interference further deteriorates the SE performance. For high λ_m, the performance gains with CAA over BRSP are still evident. This is due to the fact that CAA allows the NU to associate with an SBS having high channel access probability as well as high signal power. On the other hand, BRSP-based association does not distinguish different small cells based on their traffic loads.

2.8.2 Results: Interference Coordination

Impact of ρ_m ***on SE:*** Fig. 2.8 illustrates the impact of increasing the number of SBSs (S') on the SE of transmission to the NU. With increasing S', the co-tier

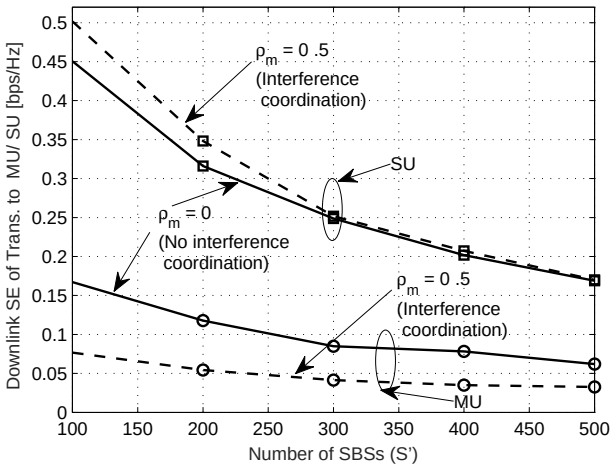

Figure 2.9: SE of downlink transmission to the MU / SU as a function of S' considering CAA scheme.

interference increases which degrades the SE for the NU. Fig. 2.8 comparatively analyzes the CAA, RSP, and BRSP-based user association schemes considering $\rho_m = 1$ and $\rho_m = 0$. For both cases, the performance gains of CAA over RSP and BRSP are significant. However, when $\rho_m = 0$, the RSP scheme tends to select the MBS due to high transmit power and the BRSP scheme selects SBSs without considering their traffic load conditions. Thus, the performance loss of RSP relative to BRSP-based association is intuitive due to high traffic load intensity of MBS. On the other hand, with $\rho_m = 1$, RSP-based association performs similarly to BRSP-based association. This is due to the fact that both schemes allow association with the SBSs irrespective of their traffic loads.

Fig. 2.9 demonstrates the impact of number of SBSs on the downlink SE of transmission to the MU and SU. With increasing S', the interference from smallcell tier increases which decreases the SE performance of the MU and SU. The SE of SU is high compared to the MU. This is due to the low traffic load of SBSs which in turn provide high channel access probability to the SUs. On the other hand side, the

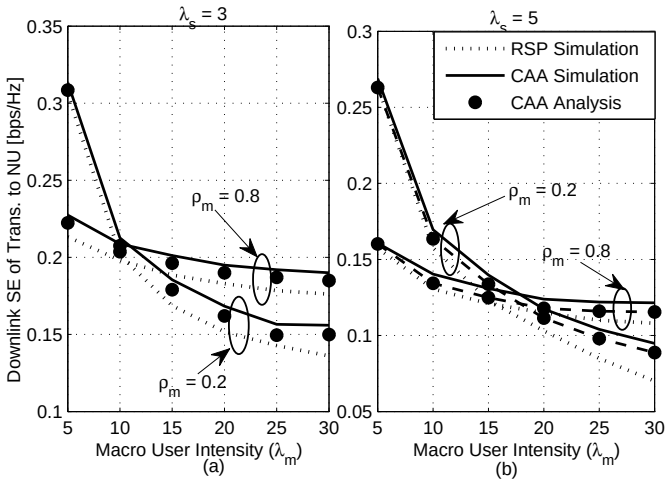

Figure 2.10: SE of downlink transmission to the NU as a function of λ_m considering RSP and CAA user association schemes (for (i) $\lambda_s = 3$ for (a) $\rho_m = 0.2$, (b) $\rho_m = 0.8$, (ii) $\lambda_s = 5$ for (a) $\rho_m = 0.2$, (b) $\rho_m = 0.8$).

high traffic load of MBS and small tier interference lower down the SE of MU. With interference coordination, the SE improvements of the SU can be observed up to a certain point. It happens due to the reduction in cross-tier interference. After the certain point the benefit obtained with interference coordination at MBS is nullified with the co-tier interference and the SE of SU with as well as without interference coordination becomes similar.

Selecting ρ_m as a function of traffic load intensities: Fig. 2.10(a)-(b) depict the effect of increasing λ_m on the SE for the NU. The SE decreases as λ_m increases due to reduced channel access probability with the MBS. This reduction is, however, less for high values of ρ_m in which case the NU associates with an SBS with high probability.

For small values of λ_m, the higher SE gains can be obtained with small values of ρ_m. This is due to the fact that the benefit achieved by the NU from the reference MBS (i.e., high channel access probability) in CAA-based association outweighs the

need for interference mitigation. On the other hand, for large values of λ_m, high SE gains can be achieved by selecting large values of ρ_m. It happens because the NU is highly likely to associate with an SBS due to high channel access probability and thus the need for reduced cross-tier interference becomes crucial. Finally, it can be observed that setting low values of ABS at MBS become more beneficial for the NU as the traffic load intensity λ_s of the SBSs increases. This is due to the fact that, in this case, the NU will prefer to associate with the reference MBS again due to high transmit power and can benefit more from low ABS durations. As such, the fraction of ABS ρ_m needs to be designed carefully according to the traffic load intensities λ_m and λ_s of different tiers.

Fig. 2.11(a)-(b) demonstrate the impact of bias values on the SE for NU with CAA, RSP, and BRSP-based association schemes. It is intuitive that the SE performance for the NU with RSP and CAA is independent of the bias. Moreover, with the bias value of one, the performance of NU with BRSP is the same as RSP which is self-explanatory. The performance of NU with BRSP over RSP-based association increases with increasing bias value up to a certain point due to increasing opportunity of selecting an SBS with high channel access probability. A further increase in the bias value degrades the SE performance of the NU due to the high probability of excluding the reference MBS from the association process. Also, with no interference coordination ($\rho_m = 0$), significant gains of BRSP over RSP can be achieved at optimal bias values. However, as ρ_m increases the performance of RSP and BRSP-based association schemes tend to become same. Finally, it can be observed that for high traffic load of MBS, the performance gains of BRSP-based association remain always higher over RSP-based association regardless of the selected bias value. This is due to the minimal benefits from associating with a highly congested MBS with RSP-based

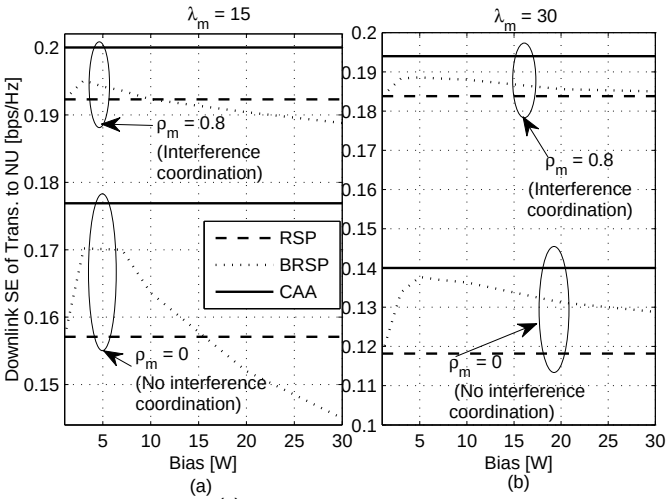

Figure 2.11: Impact of the bias value on the downlink SE of transmission to NU for different user association schemes (for $\lambda_s = 3$).

association scheme.

It can be concluded that the performance gains of BRSP compared to RSP are highly dependent on the bias values and selection of the optimal bias value is extremely important in order to achieve useful gains. Nevertheless even with the optimal bias selection, the CAA scheme outperforms the BRSP scheme. *This fact highlights the importance of adopting per BS biasing rather than per tier biasing as well as per-tier and per-BS traffic load modeling.*

Fig. 2.12 illustrates the effect of introducing ABS on the downlink SE of transmission to the NU. It is interesting to note that introducing ABS is beneficial for the NU when the reference MBS is highly congested. In this case, the NU can get better SE from SBSs with interference coordination. On the other hand, if the traffic load intensity is low at the reference MBS it is not beneficial to perform interference coordination from the perspective of newly arriving users. The same conclusion can also be derived from Fig. 2.10. Note that the reverse is true from the perspective of already associated MUs. Therefore, the interference coordination factor ρ_m can

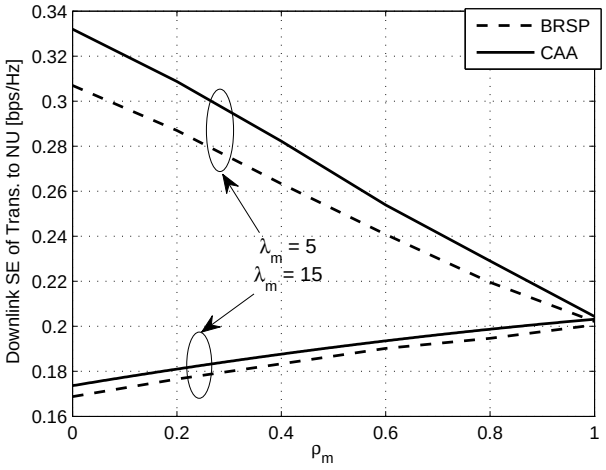

Figure 2.12: Downlink SE of transmission to NU as a function of ρ_m for different λ_m values and association schemes.

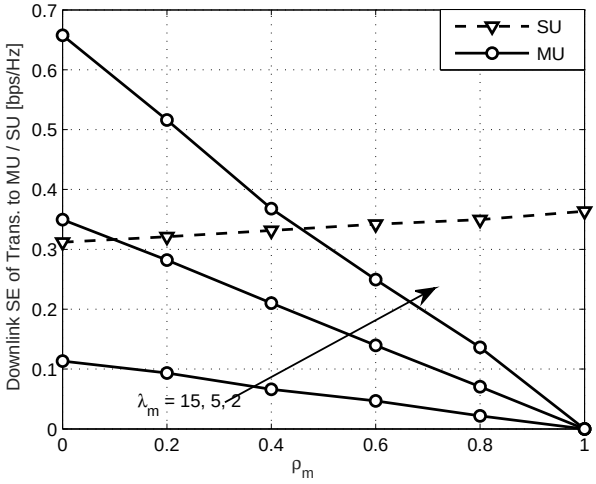

Figure 2.13: Downlink SE of transmission to MU /SU as a function of ρ_m for different λ_m values.

be selected depending on the number of newly arriving users NUs and the already associated MUs.

Finally, Fig. 2.13 analyzes the impact of interference coordination on the SE of downlink transmission to the MU and SU. The SE of a given SU increases with increasing ρ_m due to the reduction in co-channel cross-tier interference. Whereas, the

SE of a given MU decreases by increasing ρ_m due to prolong coverage hole durations. The fairness between MU and SU can be provided by carefully selecting value of ρ_m which is 0.5 for $\lambda_m = 2$ and 0.1 for $\lambda_m = 5$. At very high values of λ_m, there is no value at which fairness can be provided. Nevertheless, since the density of SBSs is generally much higher compared to that of MBSs, interference coordination at MBSs can protect a large number of SUs from severe cross-tier interference which in turn enhance the overall network-wide SE of downlink transmission.

2.9 Chapter Summary

I have developed a tractable mathematical framework to characterize the SE of downlink transmission to a user who associates with a BS using the proposed CAA scheme. The framework characterizes the impact of ABS-based interference coordination in macrocell-tier on the performance of the proposed CAA scheme as well as BRSP and RSP schemes. It has been shown that the performance gains of BRSP compared to RSP are highly dependent on the bias values and selection of optimal bias is extremely important in order to achieve useful gains. Nevertheless, even with the optimal bias selection, the CAA scheme outperforms the BRSP scheme. This fact highlights the importance of adopting per-BS biasing rather than per-tier biasing. Numerical results highlight that the fraction of ABS (ρ_m) needs to be designed carefully according to the traffic load intensities λ_m and λ_s of the two network tiers.

From the perspective of newly arriving users, small values of ρ_m are feasible when $\lambda_m < \lambda_s$. On the other hand, the reverse is true when $\lambda_m \geq \lambda_s$. Conversely, from the perspective of macrocell users, more coverage holes are expected with the increase in ρ_m which is not feasible at high values of λ_m. Therefore, depending on the number of newly arriving users and the already associated macrocell users interference coordi-

nation factor ρ_m can be selected. Finally, since the density of SBSs is generally much higher compared to MBS, high values of ρ_m can protect a large number of small cell users from severe cross-tier interference which in turn enhance the overall network SE significantly. The fairness between macro users and small cell users can also be provided by carefully selecting value of ρ_m.

Chapter 3

Wireless Backhauling in 5G Small Cell Networks

Dense deployment of small cells over traditional macrocells is considered as a key enabling technique for the emerging 5G cellular networks. A fundamental challenge is however to provide economical and ubiquitous backhaul connectivity to these small cells. There is a wide range of backhaul solutions that together can address the backhaul challenges of 5G networks. In this context, I provide an overview of the different backhaul solutions and highlight the perceived challenges in backhauling small cells. A qualitative overview of the existing research studies and their critical assumptions are then discussed. Next, for backhauling downlink traffic of a small cell user, I characterize the cellular region in which the downlink transmission capacity for a user served by a given half-duplex (HD) small cell becomes limited by the backhaul link capacity. I then illustrate solution techniques such as full-duplex backhauling to improve the performance of wireless backhauling for small cells.

Recent advancements in the self-interference (SI) cancellation capability of low-power wireless devices pave the way of implementing full-duplex (FD) self-backhauling

in 5G small-cell networks. FD self-backhauling allows exploiting the radio spectrum used by the radio access network (RAN) for backhaul links as well as access links concurrently. I characterize the performance of FD self-backhauling for both downlink and uplink transmissions in a two-tier macrocell-small cell network and compares it against half-duplex (HD) self-backhauling. The performance of small cell base stations (SBSs) with adaptive FD scheme that switches between HD and FD modes depending on the network parameters such as the distance of backhaul link (i.e., link between the macrocell base station and SBS), SI cancellation value at the SBS, and the distance of the served user from the SBS is then numerically analyzed for two different user selection schemes used by the SBS. Numerical results show the usefulness of adaptive FD self-backhauling over FD self-backhauling, especially in fairness-constrained scheduling schemes.

3.1 Introduction

3.1.1 Overview

To enable efficient spectral reuse, massive deployment of small cells will be a key technique for 5G cellular networks [4]. However, provisioning of efficient and economical backhauling solutions for these small cells is a challenging problem. The reason is it is difficult to reach street levels using inexpensive LOS links as deploying backhauling at street levels also requires backhaul equipment which has to be compact and secure to avoid accidental damages and tampering as well as to ease the deployment. By definition, the small cell backhaul connections are used to (i) forward/receive the end-user (small cell user) data to/from the core network and (ii) exchange mutual information among different small cells over X2 interface. The backhaul evolution for 5G small

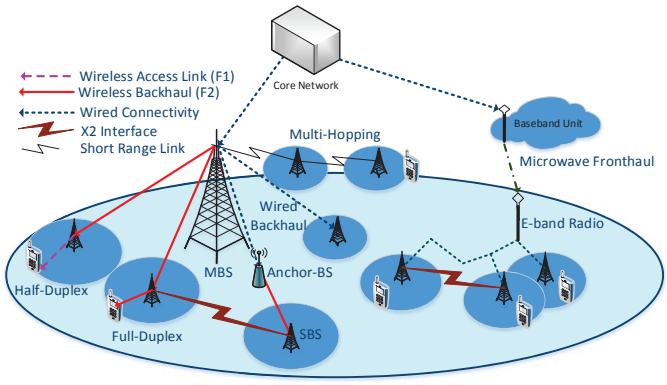

Figure 3.1: Graphical illustration of backhaul evolution of 5G small cell networks with wireless backhauls and cloud-RAN architecture [1].

cells will include wired and wireless backhauling to and from core network aggregators (e.g., macro base stations (MBSs)), cooperation through anchor-base stations (A-BSs)[1], multi-hopping at short range links, and cloud-based architecture as illustrated in Fig. 3.1. Since the backhaul requirements can significantly vary depending on the location of small cells, the cost of implementing backhaul connections, traffic load intensity of small cells, latency and target quality of service requirement of the small-cell users, there is not a single optimal approach for the backhauling of small cells.

Although wired backhaul solutions ensure reliability with high data rates, the cost of wired connections is highly dependent on the offered capacity as well as the distance. Moreover, highly reliable wired backhaul connectivity may not be necessary for the small cells that are typically serving a relatively reduced traffic load compared to a macrocell. Nevertheless, the five-nines reliability[2] and capacity of wired backhauling can not be completely overlooked. As such, the backhaul transmission of 5G small cell networks will certainly leverage on the combination of wired and wireless

[1]These refer to the BSs with wired connectivity to MBSs and forward backhaul data from MBSs to small cells wirelessly in downlink.

[2]It means that the backhaul link remains reliable for 99.999% of the time.

backauling solutions. However, since the reliability, challenges, and performance of wired backhaul solutions have been quite well-investigated and the associated cost-complexity trade-offs are well-known, this chapter focuses mainly on the investigation and performance analysis of the wireless backhaul networks.

Wireless backhauling has been recently considered as a viable and cost-effective approach that allows operators to obtain end-to-end control of their network rather than leasing third party wired backhaul connections. The key wireless backhaul solutions leverage on exploiting the millimeter wave (mm-wave) spectrum in 60 GHz and 70-80 GHz band, microwave spectrum between 6 GHz and 60 GHz bands, sub 6 GHz band, TV white spaces, and satellite technologies. However, an optimal selection of the wireless backhaul solution depends on the propagation environment as well as a number of system parameters such as locations and deployment density of small cells, desired backhaul capacity, interference conditions, cost, coverage, hardware requirements, and the spectrum availability.

On the other side, in-band full-duplex (FD) communication at low-power wireless devices (such as SBSs) has also been recently considered as a viable technique for capacity enhancement of 5G networks. In-band FD communication implies simultaneous transmission and reception of information in the same frequency band. However, the gains of in-band FD communication are limited by the overwhelming nature of self-interference (SI), which is generated by the transmitter to its own collocated receiver [5]. Fortunately, with the recently developed antenna and digital baseband technologies, SI can be reduced close to noise floor level (i.e., background noise level) in low-power devices [6]. Since FD transmission requires the in-band operation of transmitting and receiving RF chains, the conventional duplexers cannot separate the two RF transmissions. FD transmission can, however, be realized through the

shared antenna configuration where a single antenna can be used for simultaneous the in-band transmission and reception through a three-port circulator. The circulator prevents the leakage of signals from the transmit to the receive RF chain ideally. However, in practice, the transmit signals causes SI to the signals received.

3.1.2 Contributions

The contributions of this chapter can be summarized as follows.

- I provide a comprehensive overview of the existing wireless backhaul solutions and their fundamental implementation challenges.
- Next, I focus on the wireless backhaul solutions and mathematically characterize the cellular region in which the downlink transmission capacity of half-duplex (HD) small cell base station (SBS) becomes limited by its backhaul capacity. To overcome this limitation, I propose enabling full-duplex (FD) mode of operation and mathematically analyze the interference scenarios in which the FD mode of operation is a potential solution. I further investigate the performance enhancements offered by deploying anchor-BSs in the presence of either HD or FD SBS.
- The performance gains of the aforementioned solution techniques are quantitatively analyzed through simulations and insights are extracted related to the scenarios in which the FD mode and deployment of A-BS are advantageous. In the HD mode, an SBS operates on the access link (link between SBS and its user) and the backhaul link (link between SBS and MBS) in different time slots, while in the FD mode, an SBS operates (i.e., receives and transmits) on both the access and backhauls link simultaneously.

- Then, I characterize the achievable capacity gains of downlink transmission from the macrocell base station (MBS) to a user associated to an FD self-backhauled small cell over its HD counter part. The results are further extended for the uplink transmission scenarios.

- The performance of adaptive FD scheme is then numerically analyzed for two different user selection schemes at the small cell that maximizes throughput and fairness, respectively. Numerical results exhibit the usefulness of adaptive FD backhauling over pure FD self-backhauling, especially in fairness-constrained scheduling schemes.

3.2 Related Work

Wireless backhauling has been recently considered as a viable and cost-effective approach that allows operators to obtain end-to-end control of their network rather then leasing third party wired backhaul connections. Particularly, the key wireless backhaul solutions leverage on exploiting the millimeter wave (mm-wave) spectrum in 60 GHz and 70-80 GHz band, microwave spectrum between 6 GHz and 60 GHz bands, sub 6 GHz band, TV white spaces, and satellite technologies. However, an optimal selection of the wireless backhaul solution depends on the propagation environment as well as a number of system parameters such as locations and deployment density of small cells, desired backhaul capacity, interference conditions, cost, coverage, hardware requirements, and the spectrum availability.

The major deployment techniques that are recently considered to ensure reliable RF backhauling include the deployment of aggregator nodes [33], wireless backhaul hubs with multiple antennas [34], deployment of Type-A relay systems [35], etc. Several recent studies focus on developing efficient backhaul interference management

and delay minimization solutions or the performance characterization of integrated backhaul systems where wired and wireless backhauls for SBSs can coexist.

In [33], a two-tier network is considered where MBSs are connected to the core network and small cells can access the MBSs wirelessly. Small cells that can not access the MBSs using single-hop wireless links utilize *aggregator nodes (ANs)* to ensure backhaul connectivity. The joint cost function of placing the aggregator nodes, power control, channel scheduling and routing is formulated and minimized to optimize the location of the ANs. Another two-tier network underlaid with single-antenna small cells is considered in [34]. The small cells are connected to the core network via wireless backhaul links. A wireless backhaul hub (WBH) with multiple antennas is deployed to provide backhauling for the SBSs. To maximize the deployment benefits, it is desirable for the WBH to support as many SBSs as possible. As such, given the service constraints at the SBSs and power constraints at the WBH, the number of SBSs that can be admitted into the network is optimized. In [35], the deployment of Type-A relay is proposed where the MBS transports backhaul data wirelessly to SBSs. From a functional perspective, Type-A relay resembles a user powered with relaying capability. However, Type-A relay differ in terms of deployment (e.g., Type-A relays are operator-deployed), protocol stack, scheduling strategy, transmission power, etc. Type-A relay communicates simultaneously with two BSs by leveraging the downlink resources of MBS as well as the uplink resources of SBS to effectively increase the spectral efficiency while addressing the issue of DL/UL traffic asymmetry. The position of the Type-A relay is optimized to maximize the backhaul capacity.

The performance gains of FD SBSs are recently analyzed for concurrent uplink and downlink transmissions in various research studies considering a single antenna [36] and multi-antenna [37] transmissions. In [36], the feasibility conditions of FD

operation are investigated followed by developing an uplink/downlink user scheduling scheme that maximizes the overall utility of all users. In [38] the spectral efficiency of FD small cell system is maximized under the sum transmit power constraint in the downlink channel and per-user power constraints in the uplink. In [39], analytical expressions are derived for the achievable rates in uplink and downlink for single-cell processing and cloud-RAN operation considering both half-duplex (HD) or FD base stations. In [40], closed-form expressions for the outage probability are derived to assess the performance of FD implementation.

Although the feasibility of the in-band backhauling has been investigated recently in [41, 42], there have not been any comprehensive study on the performance, feasibility, and benefits of FD self-backhauling in small cell networks. Combining the benefits of FD transmission at SBSs with the in-band wireless backhauling leads to efficient reuse of RAN spectrum, alleviates the need to procure dedicated spectrum for backhauling, and facilitates hardware implementation by enabling the use of same hardware for access links and backhaul links. Nonetheless, the usefulness of FD transmission remains strongly limited by a variety of interference issues which necessitates the feasibility analysis of FD self-backhauling over conventional half-duplex (HD) self-backhauling.

3.3 Existing Wireless Backhaul Solutions and Related Challenges

This section discusses the existing wireless backhaul solutions and related challenges in implementing these solutions.

Overview of Wireless Backhaul Solutions

- **Sub 6 GHz spectrum:** Sub 6 GHz frequencies support non-line-of-sight

(NLOS) propagation and provide ubiquitous coverage through obstacles. Due to NLOS feature, point-to-multipoint (P2MP) backhaul connectivity is possible at the cost of interference. For licensed sub 6 GHz spectrum, the licensee is responsible to manage the interference within this spectrum. Moreover, no new hardware is required to manage the access and backhaul links. Nonetheless, the wireless backhaul solution using sub 6 GHz frequencies is highly vulnerable to the interference, traffic congestion, and it has a high licensing cost.

- **Microwave spectrum:** The microwave frequency range has been mentioned as 6-60 GHz [43]. The frequencies of microwave links are typically reported as 10.5, 13, 15, 18, 23, 26, and 32 GHz [44]. However, in a number of countries, these bands such as 13, 15 and 23 GHz are becoming congested. As a result, the exploitation of higher frequencies are currently under consideration. For instance, in the UK, an auction of spectrum in the 10, 28, 32 and 40 GHz bands was conducted in 2008 to meet the demand for microwave frequencies [44]. Due to shorter wavelengths, microwave spectrum is suitable for LOS scenarios with fixed antenna alignments on both transmitting and receiving ends. Since the signal attenuation is high in microwave frequencies, they are favorable for short-range communications, e.g., neighborhood backhauling in ultra-dense small cell deployment scenarios.

- **Millimeter wave (mm-wave) spectrum:** The propagation properties of mm wave (60 GHz and 70-80 GHz) are attractive for high capacity short-range links. This mm-wave spectrum is spacious and can potentially minimize interference with highly directive narrow beam-width antennas. Nevertheless, mm-waves are affected by the atmospheric attenuation to a greater degree compared to lower frequencies. The power attenuation at 60 GHz is basically due to the oxygen

or dry air, whereas 70-80 GHz is more similar to conventional microwave where attenuation is mainly caused by water molecules in the air. As a result, 60 GHz is more heavily attenuated. However, the license-exempt nature of 60 GHz makes it more cost-effective from the operators' perspective.

- **TV white spaces (TVWS):** The TV band is divided into two bands: VHF band (54-60 MHz, 76-88 MHz, 174-216 MHz) and UHF band (470-698 MHz) [45]. With the emerging digital TV (DTV) transmissions, large amount of TV spectrum has become vacant which is referred to as TV white spaces (TVWS). While TVWS are licensed for TV transmissions, they can be exploited for backhaul provisioning to small cells in a cognitive (unlicensed) manner. That is, the backhaul interference caused to primary TV transmissions should not exceed a prescribed threshold. The TVWS offers larger footprint due to their longer wavelengths and unlicensed nature help minimizing the cost. The channels in the TVWS offer much better propagation characteristics compared to low-frequency cellular bands. Nonetheless, the usefulness of TVWS for small cell backhauling would be strictly limited by the transmit power and location of primary TV transmitters.

- **Satellite frequency bands:** In a satellite backhaul link, the degree of attenuation due to weather or rain fade would depend on the frequency band selected. Lower frequency bands, i.e., 4-6 GHz (also known as C band) are practically unaffected by weather, while the Ku-band (10-12 GHz) is slightly more affected. However, the highest currently used band, i.e., Ka-band (20-30 GHz) could expect up to 24 dB of rain fade. The main benefit of satellite-based backhauling is, it becomes possible at any location from where a suitable satellite is visible and also in high mobility scenarios. By high mobility scenarios, I refer to those sce-

narios where the small cells are located on aeroplanes (business or large-bodied jets), ships (ranging from large yachts to commercial vessels and cruise ships) and land deployed "cells on wheels" to provide extra coverages. In such a case, the wireless backhaul solutions should be selected such that they are capable of providing continuous backhaul coverage to these mobile small cells. Typically, a satellite backhaul for a small cell requires to install a small parabolic dish and a remote satellite modem. For ships and airplanes, stabilized antenna systems can be used to point at the satellite and to switch between different satellites when moving from one coverage area to another.

Key Challenges

1. **Outdoor propagation impairments of mm-wave signals:** While the LOS nature of the mm-waves tend to limit the interference between small cells, the poor penetration (blocking) through obstacles is a critical problem [46]. For example, a 100 m mm-wave outdoor link requires an additional 32 dB or more gain to ensure reliable communication compared to an indoor mm-wave link. To overcome this, large-sized phased-array antennas can be used. However, the larger antenna arrays are more sensitive to wind induced misalignments. Further, due to short links and narrow beams, minor variations of propagation geometry could result in severe pointing errors that can degrade the backhaul performance.

2. **Multi-hoping in μwave and mm-wave bands:** For both microwave and mm-wave links, a physically clear and unobstructed radio path is required between the SBS and its backhaul gateway. This may require multiple hops to overcome obstacles in the propagation path. Multi-hop routing can significantly

increase the overall capital expenditure and the end-to-end delay. Further, the LOS requirements lead to more complex installation, precise alignment, and commissioning of the equipments compared to NLOS transmitters and receivers.

3. **Spectral mask requirements in TVWS:** While the TVWS can be a potential candidate for wireless backhauling, the radio design and interference threshold at primary user can be a performance limiting factor. For instance, the spectral mask requirements, i.e., adjacent channel leakage ratio (ACLR) and adjacent channel selectivity (ACS) may result in costly filter designs with increased power consumption [43]. ACLR requirements impact the dynamic range of the digital-to- analog converter. On the other hand, the ACS requirements impact receiver linearity, power consumption and analog-to-digital converter design. Thus the coexistence issue needs to be efficiently resolved to enable robust as well as reliable backhaul operation.

4. **Backhaul interference:** Wireless backhauling can be in-band or out-of-band. With the former, the same channel is used for access and backhaul links. With out-of-band backhauling, there is no interference between access and backhaul links due to the transmissions on different bands/spectrum or wired connectivity. With in-band wireless backhauling, network operators can upgrade their existing networks in a short time and at a low cost. However, this gives rise to additional sources of interference, which may severely degrade the benefits of resource reuse in both transmission and backhaul links. As such, intelligent cell association and resource allocation strategies are required that can potentially mitigate backhaul interference.

5. **Backhaul signaling overhead:** In dense small cell deployments, the infor-

mation exchange between small cells and macrocells, as well as between neighboring small cells would be much more frequent. This can be a direct consequence of frequent handovers [47], the execution of interference management, load balancing, and energy saving solutions, or other collaborative communications methods. Moreover, if the joint processing techniques like coordinated multi-point (CoMP) are applied, the user data needs to be shared among multiple BSs [48]. This data exchange can lead to a huge backhaul signaling overhead. Consequently, small cells should be able to dynamically manage and activate/deactivate different connections, and adapt according to favorable conditions such that backhaul signaling overhead can be minimized.

6. **Backhaul delay:** Transmission through a wireless medium incurs a delay when retransmissions are required due to transmission failures. This can happen, for example, due to interference from concurrent transmissions and due to channel fading. This delay, referred to as backhaul delay, can significantly degrade system reliability and the end-user performance. Therefore, characterizing the wireless backhaul delay will be crucial while analyzing the performance of different backhaul solutions [49].

7. **Jitter and time delays in satellite backhauling:** Satellite backhauling leads to large time delays due to: (a) signal propagation delay between the ground station to the satellite and that between the satellite and the ground station. This delay can range from 240-260 ms; (b) delays due to packetization and processing which can be in the range of 35-50ms, yielding a typical one-way trip time of 275-310 ms. Moreover, the expected variations in delay (jitter) in the uplink and downlink would be in the range of 5-25 ms and 10-50 ms, respectively [43].

8. **Non-uniform user traffic:** A direct consequence of small cell densification could be non-uniformity of user traffic. Due to reduced coverage, the number of users in a small cell would be typically not so large and the traffic load per small cell can be highly time varying (e.g., due to user mobility). Therefore, backhaul resource allocation solutions need to be developed that can adapt to the traffic load conditions in the small cells.

9. **Downlink (DL)/uplink (UL) traffic asymmetry:** The mobile traffic in the uplink and downlink can be highly asymmetric. The ratio of downlink to uplink traffic varies in the range from 4:1 to 8:1. The backhaul resource allocation solutions should be able to exploit this traffic asymmetry to utilize the backhaul resources efficiently.

Existing Approaches for Wireless Backhauling of Small Cells

The major deployment techniques that have been considered recently to ensure reliable wireless backhauling include the deployment of aggregator nodes [33], wireless backhaul hubs with multiple antennas [34], deployment of Type-A relay systems [35], etc. Several recent studies have focused on developing efficient backhaul interference management and delay minimization solutions or performance characterization of integrated backhaul systems where wired and wireless backhauls for SBSs can coexist.

- **Deployment-based backhauling solutions:** In [33], a two-tier network is considered where MBSs are connected to the core network and small cells can access the MBSs wirelessly. Small cells that are unable to access the MBSs using single-hop wireless links utilize *aggregator nodes (ANs)* to ensure backhaul connectivity. A joint cost function of placing the aggregator nodes, power control, channel scheduling and routing is formulated which is minimized to

optimize the locations of the ANs. Another two-tier network underlaid with single-antenna small cells is considered in [34]. The small cells are connected to the core network via wireless backhaul links. A wireless backhaul hub (WBH) with multiple antennas is deployed to provide backhauling for the SBSs. To maximize the deployment benefits, it is desirable for the WBH to support as many SBSs as possible. As such, given the service constraints at the SBSs and power constraints at the WBH, the number of SBSs that can be admitted into the network is optimized.

- **Flexible wireless backhaul (Challenges 8 and 9):** In [35], deployment of Type-A relay is proposed where the MBS transports backhaul data wirelessly to SBSs. From a functional perspective, a Type-A relay resembles a user equipment with relaying capability. However, Type-A relays differ in terms of deployment (e.g., Type-A relays are operator-deployed), protocol stack, scheduling strategy, transmission power, etc. A Type-A relay communicates simultaneously with two BSs by leveraging the downlink resources of MBS as well as the uplink resources of SBS to effectively increase the spectral efficiency while addressing the issue of DL/UL traffic asymmetry. The position of a Type-A relay is optimized to maximize the backhaul capacity.

- **Backhaul delay management solutions (Challenge 6):** In [49], a tractable analytical model is developed to characterize the average network backhaul delay and the delay experienced by a typical user in the downlink considering both wired and wireless backhaul scenarios. The network delay is further investigated for both the in-band and out-of-band wireless backhaul scenarios. It is shown that the total aggregate wired backhaul delay can be minimized for an optimal density of small cells. On the other hand, for wireless backhauling, it

is not cost-effective to increase the density of SBSs beyond a certain point. It is thus concluded that deploying dense small cell networks may not be as effective without comparable investment in the backhaul network.

The cooperation among small cells requires efficient exchange of channel state information (CSI). However, real-time CSI sharing is a crucial challenge since a user feedbacks CSI directly to its serving BS only, while any further inter-cell CSI exchange takes place over backhaul links. In practice, information exchange over the backhaul links introduces additional delays which further degrades the CSI reliability. Any CSI at transmitter pertaining to an interfering user is subject to a larger delay than that of the served user. In this context, [50] devise an efficient modified zero forcing beamforming technique to overcome the CSI discrepancy created by the backhaul delay.

- **Interference management (Challenge 4):** In [41], a large-scale MIMO is considered at the MBS to mitigate intra-cell and inter-cell interferences. On the other hand, the single-antenna small cell tier relies on large-scale MIMO links to the MBS for backhauling. A duplex and spectrum sharing scheme, which are based on co-channel reverse time-division duplex (TDD) and dynamic soft frequency reuse (SFR), are proposed for backhaul interference management. A joint optimization problem is formulated to optimize backhaul bandwidth allocation and user association such that the sum log-rate of the network is maximized.

  In [51], an interference management strategy is proposed for self-organized small cells considering the wired and wireless backhaul (termed as heterogeneous backhaul) constraints. The SBSs operate like decode-and-forward relays for the macrocell users and forward their uplink traffic to the MBS over heterogeneous

backhauls. Specifically, the users split their uplink traffic into two parts. The first part is the coarse message which can only be decoded at the MBS and second part is the fine message which can be decoded by neighboring SBSs as well as the MBS. The users select the best SBS and optimize their transmission strategy while accounting for the underlying backhaul conditions at the same time. The problem is formulated as a non-cooperative game and a reinforcement learning approach is used to find an equilibrium. Using the proposed approach, the users self-organize and implicitly coordinate their transmission strategies in a fully distributed manner while optimizing their utility function which captures the trade-off between throughput and delay.

- **Millimeter wave backhauling (Challenge 1):** Self-backhauled mm-wave small cell network is considered in [46] where a fraction of SBSs, referred as anchor BSs (A-BSs), have wired backhaul and the rest of SBSs backhaul wirelessly to A-BSs. The A-BSs serve the rest of the SBSs in the network resulting in two-hop links to the users associated with the SBSs. The uplink and downlink coverage and rate distribution are characterized. Mm-wave networks in dense urban scenarios employing high-gain narrow beam antennas have been shown to be noise-limited for practical BS densities. Consequently, densification of the network improves the signal-to-interference-plus-noise ratio (SINR) coverage. It is concluded that increasing the fraction of A-BSs improves the peak rates in the network, whereas increasing the density of BSs while keeping the density of A-BSs constant in the network, leads to saturation of user rate coverage.

- **Backhaul signaling overhead (Challenge 5):** When the joint processing technique is applied in the coordinated multi-point (CoMP) downlink transmissions, the data for each user needs to be shared among multiple BSs. This data

exchange can lead to a tremendous backhaul signaling overhead if the number of users is large. To address this backhaul signaling overhead, multi-cell CoMP network with multi-antenna BSs and single antenna users is assumed. The objective is to distribute the user data only to the minimum number of cooperating BSs, while satisfying the SINR constraint of each user. The problem of minimizing backhaul user data transfer is formulated, which jointly determines the optimal BS clustering and the transmit beamformers [48].

- **Use of TV white spaces (Challenge 3):** In [52] use of TV white spaces is proposed to provide a backhaul network for rural areas and areas with no pre-existing wired infrastructure. To quantify white space availability in the considered region, the area is divided into a grid of 5 mi $\times$ 5 mi square cells. Each cell has a radio tower in (or near) the middle. Each radio tower has 4 sector antennas covering all directions instead of one isotropic antenna. The distance between transmitter and receiver is 5 miles. This model allows more concentrated line-of-sight (LOS) transmission and less interference. Achievable capacity is derived using FCC power limits and widely accepted propagation models. Traffic demand per cell is derived using a Cisco data traffic survey.

3.4 Design Guidelines to Overcome the Limitations of RF-Backhauled Small Cells

In this section, considering traditional HD SBS, I first theoretically characterize the cellular region boundary beyond which the downlink transmission capacity of a user served by a given small cell becomes limited due to the backhaul link capacity. This region is referred to as "backhaul-limited" region in which the transmission link ca-

pacity cannot be improved any further. As the distance between MBS and SBS increases, the received signal power at SBS decreases due to path-loss which limits the backhaul link capacity and in turn the transmission capacity for a user in the downlink. For a clear exposition, I do not consider the shadowing and fading effects in the propagation model. Note that the distance between the MBS and the SBS is the root cause of this backhaul limitation. To tackle this problem, I demonstrate the usefulness of FD transmission in reducing the backhaul-limited areas under certain interference conditions. I then quantitatively analyze the benefits of FD transmission and deployment of anchor base-stations (A-BSs) to enhance the backhaul experience of a typical HD small cell. A-BSs are connected to a MBS through wired connection and provides wireless backhaul to the HD or FD SBSs. The transmission power of an A-BS is considered to be same as that of an SBS, i.e., $P_a = P_s$.

Backhaul-Limited Region for HD SBS Let us define, the HD *backhaul and access link capacities* as $\mathcal{C}_{h,b} = \alpha \log_2\left(1 + \frac{D^{-\beta_o} P_m}{\sigma^2}\right)$ and $\mathcal{C}_{h,a} = (1-\alpha)\log_2\left(1 + \frac{d^{-\beta_i} P_s}{\sigma^2}\right)$, respectively, where P_m represents the transmit power of MBS, β_o and β_i are path-loss exponents corresponding to macrocell and small cell propagation environments, respectively, D represents the distance between the MBS and the SBS, $\alpha = 0.5$ represents the fraction of time allocated for backhaul transmission, d is the distance between SBS and its user, P_s is the transmit power of SBS, and σ^2 is the noise power.

The *achieved downlink transmission capacity of a small cell user* can then be given as $\mathcal{C}_{h,u} = \min\{\mathcal{C}_{h,a}, \mathcal{C}_{h,b}\}$. Given the definitions of backhaul and access link capacities, the distance boundary R_1 at which $\mathcal{C}_{h,a} = \mathcal{C}_{h,b}$ can be derived as $R_1 = (d^{-\beta_i} P_s / P_m)^{-\frac{1}{\beta_o}}$. Beyond R_1, the user capacity becomes limited with the backhaul capacity.

Backhaul-Limited Region for FD SBS

Similarly, for FD SBS, the *backhaul and access link capacities* can be defined as

$\mathcal{C}_{f,b} = \log_2(1 + D^{-\beta_o} P_m/(R_{\text{SI}} + \sigma^2))$ and $C_{f,a} = \log_2\left(1 + \frac{d^{-\beta_i} P_s}{I_u + \sigma^2}\right)$, respectively, where $R_{\text{SI}} = P_s/C_{\text{SI}}$ [36], C_{SI} represents the self-interference cancellation value, and I_u is the backhaul interference received at a user from the MBS.

The *achieved capacity of a small cell user* can then be given as $\mathcal{C}_{f,u} = \min\{\mathcal{C}_{f,a}, \mathcal{C}_{f,b}\}$. Given the definitions of backhaul and access link capacities, the distance R_2 at which $\mathcal{C}_{f,a} = \mathcal{C}_{f,b}$ can be derived as $R_2 = \left(d^{-\beta_i} P_s A/P_m\right)^{-\frac{1}{\beta_o}}$ where $A = (R_{\text{SI}} + \sigma^2)/(I_u + \sigma^2)$. Beyond R_2, the user capacity becomes limited by the backhaul link capacity.

Remark: It can be observed that the boundary point R_2 depends on the value of A, i.e., if $A \leq 1$ (self-interference is less than the backhaul interference I_u, i.e., $R_{\text{SI}} \leq I_u$) then $R_2 > R_1$ otherwise $R_2 \leq R_1$.

Quantitative Analysis

HD vs. FD SBS: Fig. 3.2 demonstrates the backhaul-limited regions for HD and FD SBSs for a scenario when $A \leq 1$. As expected, due to increase in path-loss effects, the capacity of backhaul link decreases with the increasing distance D between the MBS and the SBS. This trend remains valid for both FD and HD SBS. However, the backhaul link capacity of HD SBS turns out to be relatively limited compared to FD SBS due to the orthogonal phases for backhauling and information transfer.

Conversely, in FD SBS, the attained user capacity is significantly reduced compared to backhaul capacity at small values of D. The reason is the curse of backhaul interference which does not allow a user to enjoy higher backhaul capacity at small values of D. Note that, in case of HD SBS, the attained user capacity is quite close to HD backhaul capacity and it monotonically decreases with increasing D which is the converse of FD SBS. The reason is the absence of backhaul interference and the dominating effect of path-loss. Interestingly, for small values of D, the user capacity

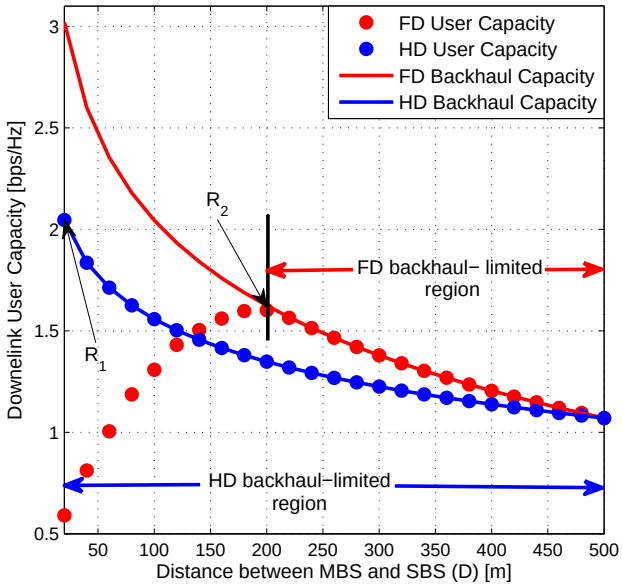

Figure 3.2: Graphical illustration of the backhaul-limited regions and user capacity as a function of D (for $R_m = 500$m, $R_s = 40$m, $\beta_i = 2$, $\beta_o = 3$, $P_m = 5$W, $P_s = 2$W, $\sigma^2 = 1 \times 10^{-12}$W/Hz), d=30 m.

in HD SBS turns out to be higher than that in FD SBS. However, as D increases the user capacity with FD SBS tends to increase due to reduced backhaul interference and becomes limited by the backhaul capacity at a certain point. This is the point beyond which an increase in the access link capacity will not bring any further benefits to user capacity.

Remark: These facts motivate the need of adaptive FD in RF-backhauled small cells that allow SBSs to decide their mode of operation in an opportunistic manner. Moreover, the need of other assisting deployments (e.g., anchor SBSs, relays) or backhaul interference management solutions (e.g., power control) becomes evident. As such, I now numerically investigate the performance gains in the backhaul limited regions by employing A-BSs.

Deployment of Anchor-Base Stations (A-BSs): The deployment of A-BSs

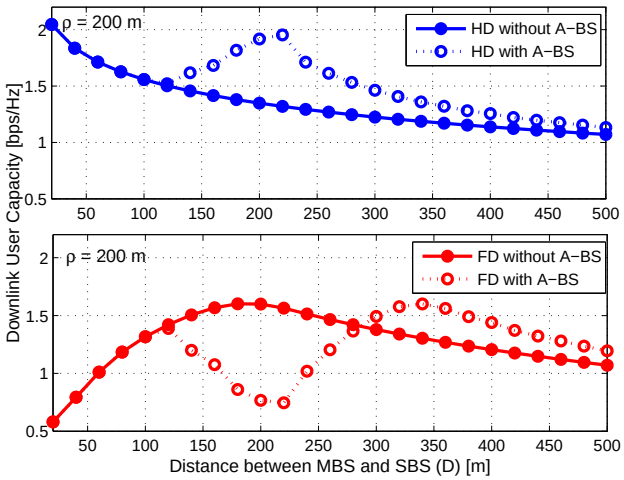

Figure 3.3: Downlink user capacity as a function of distance between MBS and SBS considering symmetric deployment of A-BSs (for $R_m = 500$m, $R_s = 40$m, $\beta_i = 2$, $\beta_o = 3$, $P_m = 5$W, $P_s = 2$W, $P_a = 2$W, $\sigma^2 = 1 \times 10^{-12}$W/Hz), d=30 m.

is another remedial solution that can potentially reduce the backhaul-limited regions.

Fig. 3.3 demonstrates the impact of deploying A-BSs on the user capacity considering A-BSs are placed around the MBS at a fixed distance ρ. A given SBS selects the nearest A-BS or MBS for backhauling. The gains of HD SBS with A-BSs in the backhaul limited region, especially in the vicinity of A-BSs, are observed to be significantly high compared to all other schemes. This is due to the strong received signal power at HD SBS from A-BS due to short distance and absence of backhaul interference due to orthogonal backhauling and transmission time slots. Hence, the optimal capacity can be achieved at the point ρ, i.e., the point where the A-BSs are deployed. However as the distance between HD SBS and A-BSs starts increasing, the user capacity degrades.

Conversely, the gains of FD SBS with A-BSs in the backhaul limited region, especially in the area far-away from A-BSs, are observed to be high compared to all other schemes. The worst case capacity can be achieved at ρ which is due to backhaul interference from the nearest A-BS. In this case, backhauling through MBS becomes

more feasible. However as the distance between FD SBS and A-BSs starts reducing, the user capacity tends to increase. This is due to reduction in backhaul interference and gain due to simultaneous backhaul and information transfer.

It has been observed that the optimal user capacity gains with HD SBS depend directly on the location of A-BSs. On the other hand, FD gains are mostly achieved at far-away locations from A-BSs. *It can thus be concluded that deploying A-BSs help improving the user capacity with HD SBS in the same region and enhances the user capacity with FD SBS in the far-away areas. Thus, I propose the use of HD-mode in the SBSs located nearby A-BSs and FD-mode for the SBSs located far-away from the A-BSs.*

Notation: Gamma$(\kappa_{(\cdot)}, \Theta_{(\cdot)})$ represents a Gamma distribution with shape parameter κ, scale parameter Θ and $(\cdot)$ is the name of the random variable (RV). $\mathcal{K}_G(m_{c_{(\cdot)}}, m_{s_{(\cdot)}}, \Omega_{(\cdot)})$ denotes the generalized-$\mathcal{K}$ distribution with fading parameter m_c, shadowing parameter m_s and average power Ω. $\Gamma(a) = \int_0^\infty x^{a-1}e^{-x}dx$ denotes the Gamma function, $\Gamma_u(a;b) = \int_b^\infty x^{a-1}e^{-x}dx$ denotes the upper incomplete Gamma function. ${}_1F_1[\cdot,\cdot,\cdot]$ denotes the confluent hypergeometric function. $f(\cdot)$ and $\mathcal{M}(\cdot)$ denote the probability density function (PDF) and moment generating function (MGF), respectively. $\mathbb{E}[\cdot]$ denotes the expectation operator.

3.5 System Model and Assumptions

In this section, I present the system model for adaptive in-band full-duplex small cells, SBS operating modes, and define the bakchaul and access link capacities.

I consider a circular macrocell of coverage radius R_m overlaid with a small cell of coverage radius R_s. The SBS is located at a distance D from the macrocell base station (MBS). The SBS is connected to the core network through a connector node

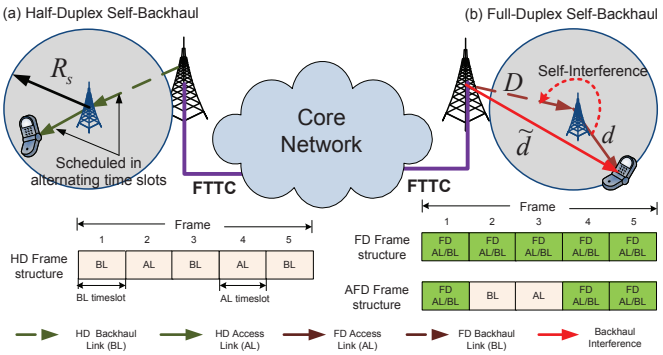

Figure 3.4: Graphical illustration of the downlink operation of FD self-backhauled small-cell and HD self-backhauled small cell. Operating mechanism of FD, HD, and adaptive FD self-backhauling.

(CN) that provides wireless backhaul to the small cell. The CN is typically situated at a fiber point-of-presence or where high-capacity LOS microwave link is available. An existing MBS can be an example of such a CN as MBSs are connected to the core network by fiber-to-the-cell (FTTC) links.

On a given channel, the SBS randomly selects a user for downlink transmission. Both MBS and the scheduled user operate in the HD mode for backhauling data and information reception, respectively. The SBS operates in the modes described below.

3.5.1 SBS Operating Modes

a) **Half-duplex mode:** The access link and the backhaul link are used by the SBS in different time slots, i.e., each SBS either transmits information (to small cell user/MBS in access link/backhaul link) or receive information (from MBS/small cell user in backhaul link/access link) in a given time slot.

b) **Full-duplex mode:** Both the access link and the backhaul link are used by the SBS in each time slot. The access link and backhaul link transmissions share the same frequency. In case of downlink transmission, since the data received by

the SBS from the MBS at backhaul link cannot be forwarded to the scheduled small cell user in the same time slot, the first time slot is always an HD time slot reserved for backhaul link data transmission. As such, during the first HD time slot, SBS receives data from the MBS and stores it for transmission in the next time slot.

c) **Adaptive full-duplex mode:** In this case, the SBS opportunistically decides whether to operate in HD mode or FD mode. Ideally, it would be desirable to configure every time slot as FD to achieve double spectral efficiency, but it may not be possible due to the presence of SI and *backhaul interference* as depicted in Fig.3.4.

When the SBS operates in the FD mode, in case of downlink transmission from the MBS, there are two types of interference issues: (i) self-interference (SI) at the SBS and (ii) the backhaul interference from the MBS to the downlink small cell user. On the other hand, the HD mode allows orthogonal operations of the access link and the backhaul link over time and these interferences do not exist. Consequently, depending on the network parameters, the use of FD operation may not be always suitable. To this end, in the subsequent sections, I characterize the capacity for a user (bits/s/Hz), in downlink and uplink, respectively, served by an HD and an FD self-backhauled small cell.

3.5.2 Backhaul and Access Link Capacities

The capacity of backhaul link for downlink transmission (i.e., from MBS) to an FD SBS is defined as:

$$\mathcal{C}_{\mathrm{F,BL}} = \mathcal{O} \times \log_2\Big(1 + \frac{P_m D^{-\beta_o} \zeta_B}{R_{\mathrm{SI}} + \sigma^2}\Big), \tag{3.1}$$

where β_o is the outdoor path-loss exponent, D represents the distance between MBS and SBS, P_m represents the transmission power of the MBS, ζ_B represents the composite shadowing and fading on the backhaul channel, and $\mathcal{O}$ represents the overhead due to the transmission protocols in the backhaul interface. Since the SBS receives the backhaul data from the MBS and transmits data to the scheduled user simultaneously, the residual SI experienced at a user is $R_{\mathrm{SI}} = \frac{P_s}{C_{\mathrm{SI}}}$, where C_{SI} represents the SI cancellation value [53].

The capacity of the access link for transmission from the FD SBS to the scheduled user in the small cell can be defined as follows:

$$\mathcal{C}_{\mathrm{F,AL}} = \mathcal{O} \times \log_2\Big(1 + \frac{P_s d^{-\beta_i} \zeta_A}{I_u + \sigma^2}\Big), \tag{3.2}$$

where β_i is the path-loss exponent in the small cell, d denotes the distance of the SBS from the user, ζ_A represents the composite shadowing and fading on the access channel, P_s denotes the transmission power of the SBS, and I_u is the backhaul interference from the MBS to the user.

Similarly, in the HD mode, the backhaul and access link capacities can be defined by removing R_{SI} and I_u from (3.1) and (3.2), respectively, as follows:

$$\mathcal{C}_{\mathrm{H,BL}} = \frac{1}{2} \times \mathcal{O} \times \log_2\Big(1 + \frac{P_m D^{-\beta_o} \zeta_B}{\sigma^2}\Big), \tag{3.3}$$

$$\mathcal{C}_{\mathrm{H,AL}} = \frac{1}{2} \times \mathcal{O} \times \log_2\Big(1 + \frac{P_s d^{-\beta_i} \zeta_A}{\sigma^2}\Big). \tag{3.4}$$

The downlink transmission capacity for a user served by an SBS in the FD and HD mode can be defined, respectively, as:

$$\mathcal{C}_{\mathrm{F,u}} = \min\left\{\mathcal{C}_{\mathrm{F,AL}}, \mathcal{C}_{\mathrm{F,BL}}\right\}, \tag{3.5}$$

$$\mathcal{C}_{\mathrm{H,u}} = \min\left\{\mathcal{C}_{\mathrm{H,AL}}, \mathcal{C}_{\mathrm{H,BL}}\right\}. \tag{3.6}$$

The uplink transmission capacity for a user served by an SBS in the FD and HD mode can be obtained similarly.

Composite Shadowing and Fading Channel The generalized-$\mathcal{K}$ distribution jointly models the shadowing and fading channels. The distribution can be approximated with a more tractable Gamma distribution using the moment matching method, i.e., $\mathcal{K}_G(m_c, m_s, \Omega) \approx \text{Gamma}(\kappa, \Theta)$ [30]. By matching the first and second moments of the two distributions, the corresponding values of κ and Θ can be given as $\kappa = \frac{m_c m_s}{m_c + m_s + 1 - m_c m_s \epsilon}, \Theta = \frac{\Omega}{\kappa}$, where ϵ is an adjustment parameter. Thus, ζ_A, ζ_B, and χ will be considered as Gamma RVs throughout the chapter.

3.6 Downlink Analysis of a Full/Half-Duplex SBS

In this section, for downlink transmissions (i.e., from MBS), I evaluate the backhaul link, access link, and user capacities (bps/Hz) for FD/HD self-backhauled small-cell. The access and backhaul link capacities are derived using tools from geometric probability.

3.6.1 Backhaul Link Capacity for Full-Duplex SBS

The received signal-to-interference-plus-noise ratio (SINR) at the SBS from the MBS on a given transmission channel is defined as follows:

$$\gamma_s = \frac{P_m D^{-\beta_o} \zeta_B}{R_{\mathrm{SI}} + \sigma^2}, \tag{3.7}$$

Using the scaling law of MGF[3] and noting that $\zeta_B \sim \text{Gamma}(\kappa_{\zeta_B}, \Theta_{\zeta_B})$, the closed-form expression of $\mathcal{M}_{\gamma_s}(t)$ can be derived as $\mathcal{M}_{\gamma_s}(t) = \left(1 + \frac{P_m D^{-\beta_o}}{R_{\text{SI}}+\sigma^2} t\Theta_{\zeta_B}\right)^{-\kappa_{\zeta_B}}$. The capacity of the backhaul link can then be given as [10, 31]:

$$\mathbb{E}[\mathcal{C}_{\text{F,BL}}] = \frac{1}{\ln(2)}\mathbb{E}\left[\ln(1+\gamma_s)\right] \times \mathcal{O} = \int_0^\infty \frac{1-\mathcal{M}_{\gamma_s}(t)}{\ln(2)\ t} e^{-t} dt \times \mathcal{O}. \tag{3.8}$$

Lemma 3.6.1 (Closed-form expression for the backhaul link capacity of FD SBS)**.** *Given the MGF of γ_s from MBS, the backhaul link capacity can be derived for Gamma fading channels as:*

$$\mathbb{E}[\mathcal{C}_{\text{F,BL}}] = \sum_{g=1}^{\kappa_{\zeta_B}} \frac{\mathcal{O}\binom{\kappa_{\zeta_B}}{g}\Gamma(g)}{\ln(2)}\ {}_1F_1\left[g, 1+g-\kappa_{\zeta_B}, \frac{\sigma^2+\frac{P_s}{C_{\text{SI}}}}{P_m\Theta_{\zeta_B}D^{-\beta_o}}\right]. \tag{3.9}$$

Substituting $\kappa_{\zeta_B} = 1$, $\Theta_{\zeta_B} = 1$, $\mathbb{E}[\mathcal{C}_{\text{F,BL}}]$ in (3.9) can be simplified for Rayleigh fading channels as follows:

$$\mathbb{E}[\mathcal{C}_{\text{F,BL}}] = \frac{\mathcal{O}}{\ln(2)} e^{\frac{D^{\beta_o}(\frac{P_s}{C_{\text{SI}}}+\sigma^2)}{P_m}} \Gamma_u\left(0, \frac{(\frac{P_s}{C_{\text{SI}}}+\sigma^2)}{D^{\beta_o}P_m}\right). \tag{3.10}$$

Proof. Consider the integral representation of the backhaul capacity for gamma composite fading channels as given in (3.8). Substituting $\mathcal{M}_{\gamma_s}(t)$, (3.8) can be re-written as:

$$\mathcal{C}_{\text{F,BL}} = \frac{\mathcal{O}}{\ln(2)} \int_0^\infty \frac{1-(1+Xt)^{-\kappa}}{t} e^{-t} dt, \tag{3.11}$$

where $X = P_m\Theta D^{-\beta_o}/(\frac{P_s}{C_{\text{SI}}}+\sigma^2)$. By some algebraic manipulations, (3.11) can be written as follows: $\mathcal{C}_{\text{F,BL}} = \frac{\mathcal{O}}{\ln(2)}\int_0^\infty \frac{(1+Xt)^\kappa-1}{t(1+Xt)^\kappa} e^{-t} dt$. Applying binomial expansion on $(1+Xt)^\kappa$, I can write $(1+Xt)^\kappa = \frac{\mathcal{O}}{\ln(2)}\sum_{g=0}^{\kappa}\binom{\kappa}{g}(Xt)^g$. Substituting this value, the

[3]Given that $Y = bX$, and Y and X are two RVs, the MGF of Y can be derived as $\mathcal{M}_Y(t) = \mathcal{M}_X(bt)$.

integral can be written as:

$$\mathcal{C}_{\mathrm{F,BL}} = \frac{\mathcal{O}}{\ln(2)} \int_0^{\infty} \frac{\sum_{g=1}^{\kappa} \binom{\kappa}{g} (Xt)^g}{t(1+Xt)^{\kappa}} e^{-t} dt,$$
$$= \frac{\mathcal{O}}{\ln(2)} \sum_{g=1}^{\kappa} \binom{\kappa}{g} \int_0^{\infty} \frac{X^g t^{g-1}}{(1+Xt)^{\kappa}} e^{-t} dt. \tag{3.12}$$

The integral in (3.12) can be evaluated, as given in (3.9), by using `MATHEMATICA` or `MAPLE`. □

The backhaul link capacity of HD BSs can be derived as a special case of lemma 1 as mentioned herein.

Special Case 3.6.1 (Closed-form expression for the backhaul link capacity of HD SBS)**.** *Since there is no SI in HD SBS, the capacity of the HD backhaul link can be calculated by substituting $P_s/C_{\mathrm{SI}} = 0$ in Lemma 1 as:*

$$\mathbb{E}[\mathcal{C}_{\mathrm{H,BL}}] = \frac{\mathcal{O}}{2\ln(2)} \sum_{g=1}^{\kappa_{\zeta_B}} \binom{\kappa_{\zeta_B}}{g} \Gamma(g)\, {}_1F_1\left[g, 1+g-\kappa_{\zeta_B}, \frac{\sigma^2 D^{\beta_o}}{P_m \Theta_{\zeta_B}}\right]. \tag{3.13}$$

3.6.2 Access Link Capacity of a Full-Duplex SBS

The received signal power at a user in downlink on a given transmission channel from the SBS is defined as follows:

$$\gamma_u = P_s d^{-\beta_i} \zeta_A. \tag{3.14}$$

For a given value of d in (3.14), the MGF of γ_u can be derived by using the scaling property of MGF as $\mathcal{M}_{\gamma_u}(t) = \left(1 + P_s t d^{-\beta_i} \Theta_{\zeta_A}\right)^{-\kappa_{\zeta_A}}$. The backhaul interference

received at a user from the MBS is defined as:

$$I_u = P_m \tilde{d}^{-\beta_o} \chi, \tag{3.15}$$

where $\tilde{d} = \sqrt{D^2 + d^2 - 2Dd\cos(180^o - \theta)}$ is the distance between MBS and user and χ represents the composite shadowing and fading on the interfering channel. Again, using the scaling property of the MGF, $\mathcal{M}_{I_u}(t)$ can be given as $\mathcal{M}_{I_u}(t) = \left(1 + P_m t \tilde{d}^{-\beta_o} \Theta_\chi\right)^{-\kappa_\chi}$. Given the MGF of I_u and $\mathcal{M}_{\gamma_u}(t)$, the capacity of downlink transmission to a user can be calculated as:

$$\mathbb{E}[\mathcal{C}_{\mathrm{F,AL}}] = \int_0^\infty \frac{\mathcal{M}_{I_u}(t)\Big(1 - \mathcal{M}_{\gamma_u}(t)\Big)}{\ln(2)\ t} e^{-\sigma^2 t} dt \times \mathcal{O}. \tag{3.16}$$

The integral in (3.16) can be evaluated by using `MATHEMATICA`.

Special Case 3.6.2 (Closed-form expression for the access link capacity of HD SBS)**.** *Since there is no backhaul interference in HD SBSs, the HD backhaul capacity can be calculated by substituting* $I_u = 0$ *in* (3.16)*, i.e.,* $\mathcal{M}_{I_u}(t) = 1$ *as:*

$$\mathbb{E}[\mathcal{C}_{\mathrm{H,AL}}] = \frac{\mathcal{O}}{2\ln(2)} \int_0^\infty \frac{1 - \mathcal{M}_{\gamma_u}(t)}{t} e^{-\sigma^2 t} dt. \tag{3.17}$$

A closed-form expression can then be given using Lemma 1 in a straightforward manner.

3.6.3 Transmission Capacity of a Downlink User

The transmission capacity of a downlink user served by an SBS in the FD mode can be defined as:

$$\begin{aligned}\mathbb{E}[\mathcal{C}_{\mathrm{F,u}}] &= \mathbb{E}\left[\min\left\{\mathcal{C}_{\mathrm{F,AL}}, \mathcal{C}_{\mathrm{F,BL}}\right\}\right] \\ &= \frac{\mathcal{O}}{\ln(2)} \begin{cases} \mathcal{C}_{\mathrm{F,AL}}, & \mathcal{C}_{\mathrm{F,AL}} \leq \mathcal{C}_{\mathrm{F,BL}}, \\ \mathcal{C}_{\mathrm{F,BL}}, & \mathcal{C}_{\mathrm{F,AL}} > \mathcal{C}_{\mathrm{F,BL}}, \end{cases} \\ &= \frac{\mathcal{O}}{\ln(2)} \begin{cases} \ln(1+\frac{d^{-\beta_i} P_s \zeta_A}{I_u+\sigma^2}), & \zeta_A \leq C\zeta_B, \\ \ln(1+\frac{D^{-\beta_o} P_s \zeta_B}{R_{\mathrm{SI}}+\sigma^2}), & \zeta_A > C\zeta_B, \end{cases} \end{aligned} \tag{3.18}$$

where[4] $C = \left(\frac{D^{-\beta_o} P_m \left(\mathbb{E}[I_u]+\sigma^2\right)}{(R_{\mathrm{SI}}+\sigma^2) P_s d^{-\beta_i}}\right)$. The average attained capacity of a downlink user can, therefore, be derived as:

$$\begin{aligned}\mathbb{E}[\mathcal{C}_{\mathrm{F,u}}] = \frac{\mathcal{O}}{\ln(2)} \int_0^\infty \Bigg(\int_0^{C\zeta_b} \ln\left(1+\frac{d^{-\beta_i} P_s \zeta_a}{I_u+\sigma^2}\right) f_{\zeta_A}(\zeta_a) d_{\zeta_a} \\ + \ln\left(1+\frac{D^{-\beta_o} P_m \zeta_b}{R_{\mathrm{SI}}+\sigma^2}\right) \frac{\Gamma_u\left(\kappa_{\zeta_a}, \frac{C\ \zeta_b}{\Theta_{\zeta_a}}\right)}{\Gamma\left(\kappa_{\zeta_a}\right)} \Bigg) f_{\zeta_B}(\zeta_b) d_{\zeta_B}(\zeta_b).\end{aligned} \tag{3.19}$$

Similarly, the capacity of a downlink user served by an SBS in the HD model can be given in a straightforward manner by ignoring I_u and R_{SI} in (3.18) and (3.19), respectively, and dividing $\mathcal{O}$ by 2.

[4]For analytical tractability, I approximate the backhaul interference with its statistical average, i.e., $I_u \approx \mathbb{E}[I_u]$.

3.7 Uplink Analysis of a Full/Half-Duplex SBS

The capacity of the uplink FD backhaul link can be evaluated as:

$$\begin{aligned}\mathbb{E}[\mathcal{C}_{\mathrm{F,BL}}] &= \mathcal{O} \times \log_2\Big(1+\frac{P_s D^{-\beta_o}\zeta_B}{I_m+\sigma^2}\Big)\\ &= \int_0^{\infty} \frac{\mathcal{M}_{I_m}(t)\Big(1-\mathcal{M}_{\gamma_m}(t)\Big)}{\ln(2)\ t} e^{-\sigma^2 t} dt \times \mathcal{O}, \end{aligned} \tag{3.20}$$

where $\mathcal{M}_{I_m}(t) = \Big(1+P_u t \tilde{d}^{-\beta_o}\Theta_\chi\Big)^{-\kappa_\chi}$ and $\mathcal{M}_{\gamma_m}(t) = \big(1+P_s t D^{-\beta_o}\Theta_{\zeta_B}\big)^{-\kappa_{\zeta_B}}$. Alike, the HD backhaul capacity can be given by removing I_m in (3.20) and dividing $\mathcal{O}$ by 2.

The capacity of the uplink FD access link can be given as:

$$\begin{aligned}\mathbb{E}[\mathcal{C}_{\mathrm{F,AL}}] &= \mathcal{O} \times \log_2\Big(1+\frac{P_u d^{-\beta_i}\zeta_A}{R_{\mathrm{SI}}+\sigma^2}\Big)\\ &= \sum_{g=1}^{\kappa_{\zeta_A}} \frac{\mathcal{O}\binom{\kappa_{\zeta_A}}{g}\Gamma(g)}{\ln(2)}\ {}_1F_1\left[g, 1+g-\kappa_{\zeta_A}, \frac{\sigma^2+R_{\mathrm{SI}}}{P_u\Theta_{\zeta_A}d^{-\beta_i}}\right]. \end{aligned} \tag{3.21}$$

The capacity of the uplink HD backhaul link can be evaluated easily by removing R_{SI} in (3.21) and dividing $\mathcal{O}$ by 2.

The attained transmission capacity of the uplink user in FD mode can be defined as:

$$\begin{aligned}\mathbb{E}[\mathcal{C}_{\mathrm{F,u}}] &= \mathbb{E}\left[\min\left\{\mathcal{C}_{\mathrm{F,AL}}, \mathcal{C}_{\mathrm{F,BL}}\right\}\right]\\ &= \frac{\mathcal{O}}{\ln(2)} \begin{cases} \ln(1+\frac{d^{-\beta_i}P_u\zeta_A}{R_{\mathrm{SI}}+\sigma^2}), & \zeta_A \le W\zeta_B,\\ \ln(1+\frac{D^{-\beta_o}P_s\zeta_B}{\mathbb{E}[I_m]+\sigma^2}), & \zeta_A > W\zeta_B, \end{cases}\end{aligned} \tag{3.22}$$

where $W = \left(\frac{D^{-\beta_o}P_s\left(R_{\mathrm{SI}}+\sigma^2\right)}{(\mathbb{E}[I_m]+\sigma^2)P_u d^{-\beta_i}}\right)$. The average attained capacity of the uplink user can,

therefore, be derived as:

$$\mathbb{E}[\mathcal{C}_{\mathrm{F,u}}] = \frac{\mathcal{O}}{\ln(2)} \int_0^{\infty} \left(\int_0^{W\zeta_b} \ln\left(1 + \frac{d^{-\beta_i} P_u \zeta_a}{R_{\mathrm{SI}} + \sigma^2}\right) f_{\zeta_A}(\zeta_a) d_{\zeta_a} + \ln\left(1 + \frac{D^{-\beta_o} P_s \zeta_b}{\mathbb{E}\left[I_m\right] + \sigma^2}\right) \frac{\Gamma_u\left(\kappa_{\zeta_a}, \frac{W\ \zeta_b}{\Theta_{\zeta_a}}\right)}{\Gamma\left(\kappa_{\zeta_a}\right)} \right) f_{\zeta_B}(\zeta_b) d_{\zeta_b}. \tag{3.23}$$

Similarly, the transmission capacity of the uplink user in HD mode can be derived easily by ignoring R_{SI} and I_m in (3.22) and (3.23), respectively, and dividing $\mathcal{O}$ by 2.

3.8 Numerical Results and Discussion

This section validates the accuracy of the derived capacity expressions for HD and FD scenarios. I consider generalized-$\mathcal{K}$ composite shadowing and fading, i.e., $f_{\zeta_A}(\zeta_a) \sim$ Gamma$(1/2, 2)$, $f_{\zeta_B}(\zeta_b) \sim$ Gamma$(3, 1/3)$, and $f_{\chi}(\chi) \approx$ Gamma$(1, 1)$. The coverage radii of an MBS and an SBS are $R_m = 500$ m and $R_s = 60$ m, respectively. I set path-loss exponent for small cells $\beta_i = 2.0$, and outdoor path-loss exponent $\beta_o = 3.0$, the thermal noise power density $\sigma^2 = 1 \times 10^{-10}$ W/Hz, the transmission powers of an MBS, an SBS, and a user are set as $P_m = 5$ W, $P_s = 0.1$ W, and $P_u = 0.001$ W, respectively.

3.8.1 Results: Downlink Transmission

***User capacity as a function of** D:* Fig. 3.5 illustrates the effect of distance between the MBS and the SBS on the backhaul link capacity and downlink user capacity considering both the FD and HD SBS. The derived expressions corroborate the Monte-Carlo simulations. As expected, due to increasing in path-loss effects, the capacity of the backhaul link decreases with the increasing distance D between the

MBS and the SBS. This trend remains valid for both FD and HD SBS. However, the backhaul link capacity of HD SBS turns out to be relatively limited compared to FD SBS due to the orthogonal phases for backhauling and information transfer.

Conversely, in FD SBS, the attained user capacity is significantly reduced compared to backhaul capacity at small values of D. The reason is the curse of backhaul interference which does not allow a user to enjoy higher backhaul capacity at small values of D. Note that, in case of HD SBS, the attained user capacity is quite close to HD backhaul capacity and it monotonically decreases with increasing D which is the converse of FD SBS. The reason is the absence of backhaul interference and the dominating effect of path-loss. Interestingly, for small values of D, the user capacity in HD SBS turns out to be higher than that in FD SBS. This fact motivates the need of adaptive full duplexing in self-backhauled small cells that allow SBSs to decide their mode of operation in an opportunistic manner. However, as D increases the user capacity tends to increase due to reduced backhaul interference and becomes limited by the backhaul capacity at a certain point. This is the point beyond which an increase in the access link capacity will not bring any further benefits to user capacity. Therefore, beyond this point, using wireless backhaul links with FD transmission may not be beneficial.

Impact of d on user capacity: Fig. 3.6 demonstrates the degradation in the user capacity in FD SBS with increasing distance d between SBS and user. This degradation is due to the reduction in received signal power of the scheduled user. Surprisingly, the user capacity in HD SBS does not exhibit the same trend. The reason is that the backhaul capacity in HD SBS is less and thus the user capacity becomes limited with the backhaul capacity for very low values of D as shown in Fig. 3.5. As such, efficient scheduling of users may not bring any more benefits with HD

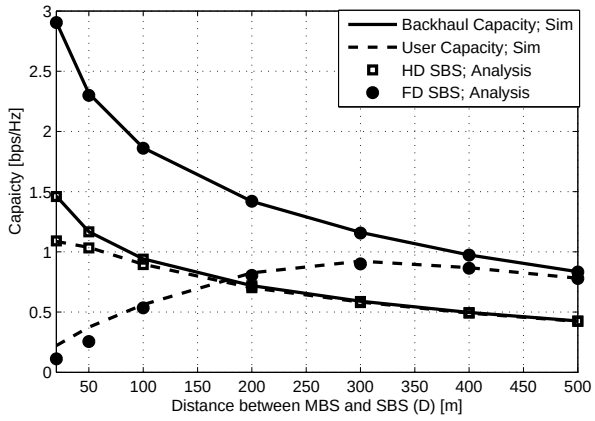

Figure 3.5: Backhaul link and user capacity in the downlink as a function of distance between MBS and SBS for both the HD SBS and FD SBS (for $\theta = 0^o$, $d = 50$ m).

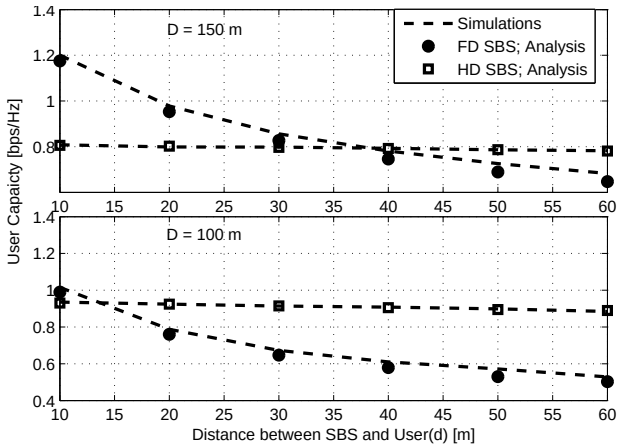

Figure 3.6: User capacity in the downlink as a function of distance between user and SBS for both the HD SBS and FD SBS (for $\theta = 0^o$).

small cells. Moreover, the gains of FD SBS are evident over its HD counterpart for a wide range of d when D is high. On the other hand, the same is not true for low values of D due to high backhaul interference.

Impact of multi-user selection with adaptive FD (AFD) self-backhauling and D ***on user capacity:*** Adaptive FD allows an SBS to switch between FD and HD operation based on the utility gain in each time slot. In other words, it selects the mode which contributes the largest value towards the (i) over-

all throughput of the SBS; (ii) overall fairness of the users. Specifically, in each scheduling interval, the SBS computes for each user the $\mathcal{C}_{\mathrm{F,u}} = \min\{C^{u}_{\mathrm{AL}}, \mathcal{C}_{\mathrm{F,BL}}\}$. and $\mathcal{C}_{\mathrm{H,u}} = \min\{C^{u}_{\mathrm{AL}}, \mathcal{C}_{\mathrm{H,BL}}\}$, where $u = 1, 2, \cdots, U$ and U is the total number of users served by the SBS. Then SBS performs throughput and fairness maximization, respectively, as follows:

- **Throughput maximization (TM)** In each scheduling interval, the AFD scheduler computes $\mathcal{C}_{\mathrm{F,u}}$ and $\mathcal{C}_{\mathrm{H,u}}$ for each user and selects a user with maximum utility as:

$$u^{*}_{\mathrm{AFD,TM}} = \arg\max\{\max\{\mathcal{C}_{\mathrm{F,u}}\}, \max\{\mathcal{C}_{\mathrm{H,u}}\}\}, \quad u \in U. \tag{3.24}$$

- **Fairness maximization (FM)** To maximize the fairness among users, the scheduler selects a user randomly and then computes $\mathcal{C}_{\mathrm{F,u}}$ and $\mathcal{C}_{\mathrm{H,u}}$ for the scheduled user and selects the mode of operation which provides a better user capacity.

Fig. 3.7 demonstrates the impact of distance between MBS and SBS on the capacity of SBS with multiple users considering two user selection schemes, namely, TM and FM. It is observed that the adaptive FD favors the HD mode and the FD mode for low and high values of D, respectively, to achieve high capacity gains for both TM and FM. At small values of D, the user capacity drops abruptly as SBS prefers to operate in HD mode to avoid backhaul interference. The reduction is only due to deterioration in signal strength. The decaying trend continues up to a certain point and then starts to follow the trends of FD. This is the point beyond which FD gains become higher than HD gains. Note that the switching to FD mode operation is beneficial for TM scenario over a wider range as compared to FM scenario.

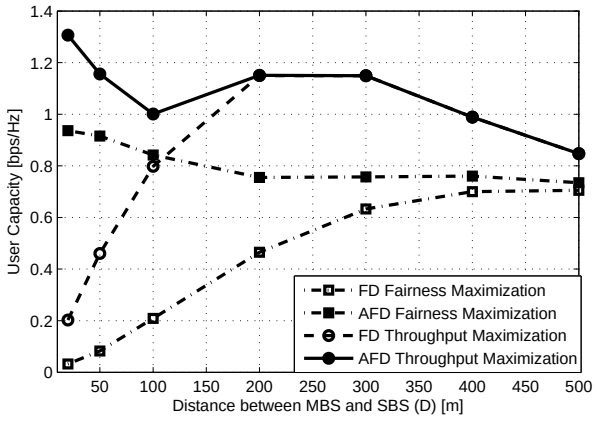

Figure 3.7: Capacity of SBS in the downlink when operating in FD or adaptive FD mode considering both the throughput and fairness maximization scheduling criteria (for $\theta = 0^o$).

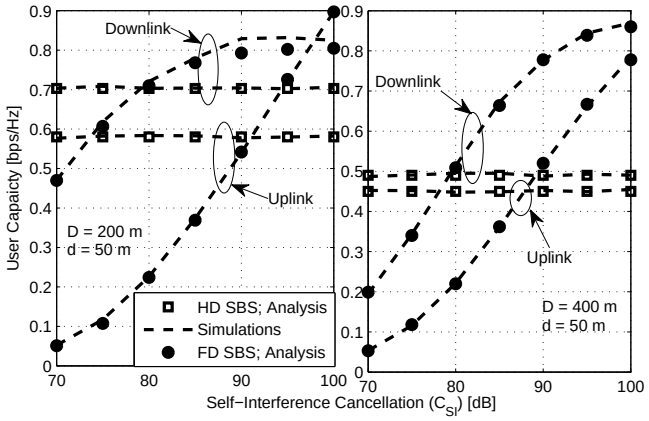

Figure 3.8: Uplink and downlink user capacity as a function of self-interference cancellation value (C_{SI}) (for $\theta = 0^o$).

3.8.2 Results: Downlink and Uplink Transmissions

Fig. 3.8 depicts the effect of SI cancellation value (C_{SI}) on the backhaul and user capacities of an FD and HD SBS considering both the uplink and downlink transmission scenarios. The user capacity of HD SBS is independent of C_{SI} value in either uplink or downlink. As expected, the performance gains of FD increases with increasing C_{SI} due to the reduction in SI. However, the usefulness of FD over HD is evident only

after a certain amount of SI cancellation. This SI cancellation value is a function of the location of FD SBS D and the location of the scheduled user d. In general, the uplink capacity is smaller than the downlink due to lower transmission power of the users; therefore, a high value for C_{SI} is required to achieve FD gains in the uplink. Note that, for high values of D, in both HD and FD mode, the user capacity becomes limited by the backhaul link capacity and thus reduces due to path-loss degradation.

3.9 Chapter Summary

This chapter characterizes the performance of FD self-backhauling considering downlink and uplink transmissions in a two-tier small cell network. It is found that HD self-backhauling is more feasible in the downlink for SBSs located close to an MBS. On the other hand, FD self-backhauling would be a better choice in other cases. Numerical results exhibit the relatively high benefits of implementing adaptive FD for fairness-constrained scheduling schemes.

In this chapter, I have investigated the achievable capacity gains of a user associated to an FD small base station over its HD counterpart assuming that single channel is available. However, for a given spectrum, how much portion of spectrum should be allocated for backhaul transmission and access transmission, respectively, to maximize the network performance, and whether it is feasible to employ FD (referred as in-band full-duplex (IBFD)) over traditional HD (referred as out-of-band full-duplex (OBFD)) backhauling are unexplored questions so far. Consequently, in the next chapter, a comprehensive framework will be presented that investigates the feasibility of IBFD over OBFD backhauling while optimizing their respective spectrum allocations.

Chapter 4

Downlink Spectrum Allocation for Wireless Backhauling in Full-Duplex Small Cells

In-band full-duplex (IBFD) backhauling is a potential technique for wireless backhauling of small cells that allows the use of same spectrum for the backhaul and access links of the SBSs concurrently at the expense of backhaul interference and self-interference (SI). This chapter investigates the problem of optimal access/backhaul spectrum allocation considering IBFD backhauling, out-of-band full-duplex (OBFD) backhauling (in which the access and backhaul transmissions take place on different spectrum), and SBSs with the provisioning for hybrid IBFD/OBFD backhauling. I first formulate a problem to maximize the minimum achievable rate (i.e., minimum of the rates in the backhaul link and the access link) at the SBSs in a hybrid IBFD/OBFD setting. The solution of the centralized spectrum allocation problem, which serves as a benchmark for any sub-optimal solution, is provided by transforming the original problem into an epigraph form. As a special case of the formulated problem, I derive closed-form

optimal solutions for the access/backhaul spectrum allocation of OBFD backhauling as well as IBFD backhauling. I then propose and comparatively analyze the performance of two distributed backhaul spectrum allocation schemes, namely, maximum received signal power (max-RSP) and minimum received signal power (min-RSP) schemes. For these schemes, I theoretically derive the number of allocated backhaul channels, minimum rate coverage probability, and average achievable rate of each SBS given its distance from the centralized wireless backhaul hub (WBH) for both IBFD and OBFD backhauling. Numerical results reveal that the optimal spectrum allocation rules can significantly vary for IBFD and OBFD backhauling. Optimal OBFD backhauling favors more backhaul spectrum for SBSs located far-away from the WBH. With IBFD backhauling, spectrum allocation for SBSs strongly depends on SI. With the reduction in SI, the optimal backhaul spectrum increases/decreases for nearby/farther SBSs. Simulation results comparing the optimal solution with the distributed spectrum allocation solutions based on max-RSP and min-RSP schemes are also presented.

4.1 Introduction

4.1.1 Overview

Wireless backhauling is a viable and cost-effective approach to handle the backhaul connectivity of large number of small cells in the fifth-generation (5G) and beyond cellular networks [54–56]. Traditionally, backhauling of small cells exploits wired connectivity (e.g., optical fiber and digital subscriber line (DSL) connections); however, the massive implementation of the wired backhaul connections seems infeasible for the emerging 5G networks. The reason is the prohibitively high cost and possibly hard-

to-reach locations of the small cell base stations (SBSs) in 5G networks (e.g. SBSs deployed on roof-tops, lamp-posts, street fixtures, etc.). In this context, millimeter (mm) waves have been recently considered for wireless backhauls due to its ample and low cost spectrum [57,58]. However, the significant penetration losses of the mm-wave links may require sophisticated hardware/software modifications at SBSs, e.g., massive antenna implementation [59], advanced precoding techniques, and beam/antenna alignment techniques [43]. On the contrary, traditional radio frequency (RF) spectrum is less-sensitive to channel propagation effects, provides wider coverage due to non line-of-sight (NLOS) propagation, makes the reuse of existing hardware possible, and thus enable simpler operation and maintenance (O&M). Therefore, although the RF spectrum is quite limited compared to mmwave, it is still an attractive solution for backhauling small cells.

Recently, in-band full-duplex (IBFD) technology has been investigated by many research groups to improve spectral efficiency [60–63]. To enable efficient spectrum reuse, IBFD transmission can be exploited to enable simultaneous transmission of access and backhaul information in the same frequency band (see Fig. 1 for graphical illustration). The gains of IBFD transmission are, however, subject to self-interference (SI) which is generated by the transmitter to its own collocated receiver [5]. To date, a significant progress has been made to mitigate SI with a combination of analog and digital cancellation techniques. For example, [64] reported to cancel SI by 110 dB. In [65] a closed-loop echo cancellation technique was used to obtain SI cancellation up to 150 dB. The IBFD backhaul/access transmission in the downlink leads to three-node full-duplex (TNFD) transmission which involves three nodes, i.e., the wireless backhaul hub (WBH) transmits to a given SBS and the SBS transmits to a user[1] (see Fig. 1). In the TNFD mode, a given small cell user suffers from backhaul interference

[1]Interested readers are referred to [5] for the details of TNFD mode of transmission.

(i.e., the interference received from the WBH associated to the serving SBS of that user) whereas the SBS suffers from SI. In the presence of such interferences, the performance of IBFD backhauling needs to be evaluated to determine its usefulness.

4.1.2 Contribution

The spectrum allocation problem for backhauling and access for SBSs is different conceptually as well as mathematically from the traditional spectrum allocation problems. Since the achievable rate for SBSs is given by the minimum of access link capacity and backhaul link capacity, the overall achievable capacity of an SBS can be constrained by its backhaul capacity or the access link capacity. Therefore, the overall achievable rates for SBSs cannot be maximized in a traditional manner. As has been mentioned before, recent research studies have focused mainly on developing iterative game-theoretic algorithms for backhaul spectrum allocation of half-duplex SBSs (referred to as out-of-band full-duplex (OBFD) SBSs in this paper as is named in [31,66,67]) in which the access and backhaul transmissions take place simultaneously on orthogonal spectrum bands. These solutions do not guarantee optimality. To date, there has not been any comprehensive framework that investigates the feasibility of IBFD over traditional OBFD backhauling while optimizing their respective spectrum allocations. Note that the IBFD backhauling may not always be beneficial due to additional interferences such as SI and backhaul interference (as shown in Fig. 1). Therefore, backhaul spectrum resources need to be allocated in an efficient manner.

In the above context, the contributions of this chapter can be summarized as follows:

- I investigate the problem of optimal access/backhaul spectrum allocation for SBSs considering both the IBFD and OBFD (in which the access and backhaul

transmissions take place on different spectrum) backhauling. I introduce spectrum allocation problem for hybrid IBFD/OBFD backhauling in which each SBS can optimally exploit both IBFD and OBFD backhauling such that the minimum achievable rate at the SBSs can be maximized. The solution of the centralized problem, which serves as a benchmark for any sub-optimal solution, is provided by transforming the original problem into an epigraph form.

- I also develop "closed-form" solutions for optimal access/backhaul spectrum allocation for an SBS considering both IBFD and OBFD backhauling. These solutions provide insights into the interplay among system parameters and possible simple backhaul channel allocation schemes. Numerical results obtained using `CVX` validate the accuracy of the closed-form optimal solutions and reveal that the optimal spectrum allocation rules can significantly vary for OBFD and IBFD backhauling.

- I propose and comparatively analyze two distributed backhaul channel allocation schemes, namely, maximum received signal power (*max-RSP*) and minimum received signal power (*min-RSP*) schemes. These decentralized strategies are feasible to implement due to their inherent similarity with current LTE channel allocation schemes such as max-RSP for the access channels [68]. The max-RSP scheme assigns a larger amount of backhaul spectrum to closer SBSs and in turn offers a higher backhaul rate to the SBSs. However, this scheme may not necessarily improve the overall transmission rate of small cell users due to the limited access rate in each small cell and thus the overall network rate may suffer severely due to the starvation of SBSs with weaker backhaul channels. Consequently, inspired from our derived optimal closed-form results, I propose the min-RSP scheme, which allocates more backhaul channels to SBSs that are

located far-away from the WBH (or SBSs with weaker backhaul channel gains). This scheme is shown to outperform the max-RSP scheme.

- Using tools from the theory of order statistics, I first derive the number of backhaul channels allocated to SBSs considering both the max-RSP and min-RSP schemes. Based on this, I provide a complete analytical framework to derive the minimum rate coverage probability and mean achievable rate of each SBS. The framework is general and can be used for different backhaul channel allocation schemes by simply deriving number of allocated channels per SBS (as will be discussed in Section IV). The Monte-Carlo simulations verify the accuracy of the derived expressions for the distributed schemes.

4.2 Related Work

Recently, the problem of backhaul/access spectrum allocation has been investigated in a number of research studies [69–71]. An interesting study was [69] where backhaul spectrum allocation in hybrid mm-wave and sub-6 GHz bands was investigated. The problem was formulated as a one-to-many matching game and considered both the wireless channel characteristics and economic factors. A distributed algorithm was proposed to find a two-sided stable solution that guarantees the quality-of-service (QoS) at the backhaul of SBSs. In [70], a weighted sum-rate (WSR) maximization problem was formulated for the access and backhaul transmissions in a time division duplex (TDD)-based system. By small cell grouping and resource slicing, a sub-optimal rate balancing algorithm was proposed. In [71], a collaborative filtering (CF) scheme was proposed that enables each SBS to estimate the probability of its cached files being requested and in turn its backhaul usage. The bandwidth allocation was updated based on the estimated backhaul usage. Using matching theory, a cache-

aware user association scheme was proposed that minimizes the backhaul usage at each SBS.

In addition, several studies focused on backhaul interference management via resource allocation [51, 72, 73]. In [72], a duplex and spectrum sharing scheme based on co-channel reverse TDD and dynamic soft frequency reuse (SFR), was proposed for backhaul interference management. An optimization problem was formulated to allocate backhaul bandwidth and to optimize user association such that the network sum-rate can be maximized. In [51], interference management was performed for self-organized small cells. The SBSs operate like decode-and-forward relays for the macrocell users and forward their uplink traffic to the macrocell base station (MBS) over heterogeneous backhauls. The problem was formulated as a non-cooperative game and a reinforcement learning approach was used to find an equilibrium. For a single massive MIMO-enabled MBS and small cells deployed on a fixed distance from the MBS, a precoding method was designed in [73] for IBFD backhauling. The precoding method enables complete rejection of the backhaul interference received at a given user from the MBS to which the serving SBS of that user is associated with. Recently, based on stochastic geometry, [74] demonstrated the gains of IBFD over OBFD backhauling in small cells and proposed few backhaul interference mitigation methods.

Notation: Gamma$(\kappa_{(\cdot)}, \Theta_{(\cdot)})$ denotes Gamma distribution with shape parameter κ, scale parameter Θ and $(\cdot)$ is the name of the random variable (RV). $\Gamma(a) = \int_0^\infty x^{a-1}e^{-x}dx$ is the Gamma function, $\Gamma_u(a;b) = \int_b^\infty x^{a-1}e^{-x}dx$ is the upper incomplete Gamma function, and $\Gamma_l(a;b) = \int_0^b x^{a-1}e^{-x}dx$ is the lower incomplete Gamma function. $f(\cdot)$ and $F(\cdot)$ denote the probability density function (PDF) and cumulative density function (CDF), respectively. Vectors are denoted by **bold** letters.

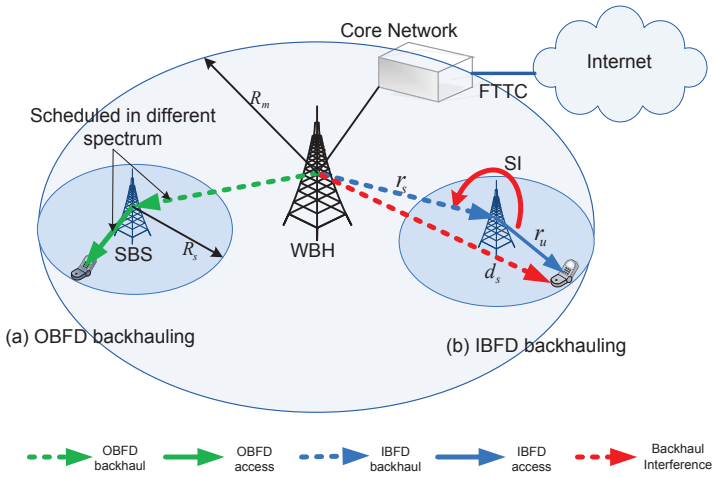

Figure 4.1: Graphical illustration of the downlink backhaul and access transmission in small cells considering in-band full-duplex (IBFD) backhauling and out-of-band full-duplex (OBFD) backhauling.

4.3 System Model and Assumptions

I consider a circular macrocell of coverage radius R_m overlaid with S randomly deployed SBSs. The coverage radius of each SBS is $R_s, \forall s = \{1, 2, \cdots, S\}$. The SBSs operate in the closed-access mode and are connected to the core network through a WBH. The WBH is typically situated at a fiber point-of-presence or where high-capacity line-of-sight (LOS) microwave link is available. An existing MBS can be an example of such a WBH as MBSs are connected to the core network by fiber-to-the-cell (FTTC) links. I assume that WBH, SBSs, and small cell users are equipped with single antenna. I assume that N channels (each channel is analogous to LTE frequency resource blocks) constitute the total spectrum. Each SBS serves one randomly selected user at a time over all available spectrum resources. Different small cell users can be served one after the other in different time slots.

4.3.1 Modes of Backhauling at SBSs

A given SBS can operate in one of the following backhaul transmission modes:

a) **Out-of-Band full-duplex (OBFD) mode:** In this mode, the access and backhaul transmissions use orthogonal spectrum bands. That is, the assigned spectrum to each SBS is further partitioned for access transmission (i.e., *from SBS to the scheduled small cell user*) and backhaul transmission (i.e., *from WBH to SBS*).

b) **In-Band full-duplex (IBFD) mode:** In this mode, the access and backhaul transmissions use the same spectrum band (i.e., the SBSs operate in full-duplex mode). The full-duplex mode at the SBSs can be realized through shared antenna configuration [53, 64, 75]. In shared antenna configuration, only one antenna is used for concurrent transmission and reception using a circulator[2] which connects antenna to the transceiver [76]. In the IBFD mode, there are two types of interferences: (i) SI at the SBS and (ii) the backhaul interference from the WBH to the small cell user as shown in Fig. 4.1. Note that IBFD operation allows transmission as well as reception of a signal at the same time and frequency; however, the transmitted signal (i.e., signal from SBS to its user) and received signal (i.e., signal from WBH to SBS) may not necessarily be the same. This can happen due to internal buffering and processing delay of the SBS receiver circuitry. Also, the backhaul capacity of a given SBS can be significantly different from its access capacity; thus these links may carry different

[2]The circulator is a three-port device which steers the signal through its ports such that the signal comes in at one port and exits from the next port, depending on the direction of rotation. As such, the signal cannot propagate to the opposite direction, which ensures certain isolation between the transmitter and the receiver. The amount of isolation can vary between 20 and 60 dB depending on the size and cost of the circulator whereas the attenuation in the desired direction remains less than half a decibel. Being a passive component, the size of the circulator depends on the wavelength of the operating frequency [76].

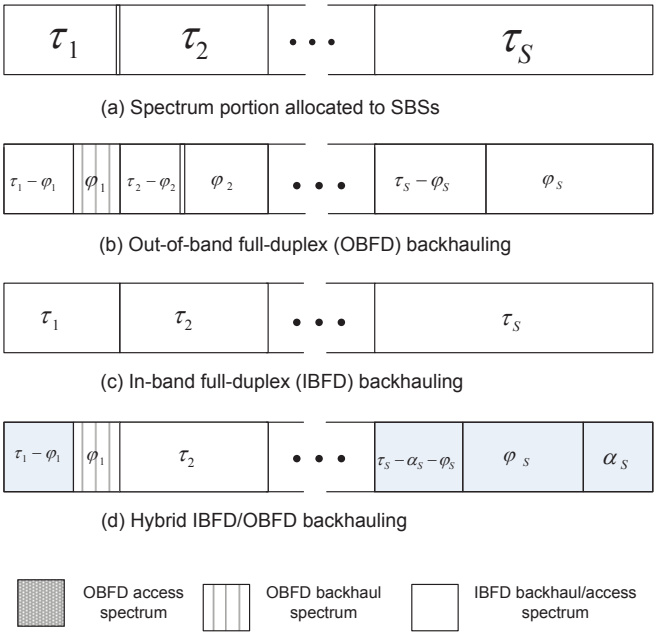

Figure 4.2: Spectrum partitioning for backhaul and access transmissions considering out-of-band full-duplex (OBFD), in-band full-duplex (IBFD), and hybrid IBFD/OBFD backhauling.

amount of data. Due to aforementioned reasons, the signal from WBH to small cell user is typically treated as interference [31, 77].

c) **Hybrid OBFD/IBFD mode:** Hybrid backhauling provides a flexible spectrum allocation in which a SBS may operate completely in the OBFD mode, or completely in the IBFD mode, or in both of these modes in an optimal fashion (see Fig. 4.2 for graphical illustration).

4.3.2 Spectrum Allocation for Different Transmission Modes

As shown in Fig. 4.2(a), each SBS is allocated a portion of spectrum, i.e., $\tau_s, s \in \{1, 2, \cdots, S\}$, where $0 < \tau_s \leq 1$ and $\sum_{s=1}^{S} \tau_s = 1$, for access and backhaul transmissions. Since the SBSs are randomly deployed and the distances between WBH and

SBSs vary, τ_s may significantly differ for various SBSs depending on their distances from the WBH. For instance, an SBS located in cell-center region (near the WBH) may require less spectrum to meet its target rate than the SBS located at the cell-edge (far from the WBH). For a given τ_s, the number of channels allocated to the s^{th} SBS can be calculated as $N_s = \tau_s \times N$. The WBH allocates orthogonal channels to SBSs and more than one channels can be allocated to a given SBS depending on its backhaul/access transmission requirements. The spectrum allocations for access/backhaul transmissions in the OBFD, IBFD, and hybrid OBFD/ IBFD modes are illustrated in Fig. 4.2 and described in the following.

a) **OBFD Backhauling:** In this case, the portion of spectrum assigned to the s^{th} SBS, i.e., τ_s is partitioned into backhaul spectrum φ_s ($0 < \varphi_s < \tau_s$) and access spectrum $\tau_s - \varphi_s$, as illustrated in Fig. 2(b). Accordingly, the channels available for the backhaul and access transmissions are $\varphi_s N$ and $N_s - \varphi_s N = (\tau_s - \varphi_s)N$, respectively.

b) **IBFD Backhauling:** Here, the fraction of spectrum assigned to s^{th} SBS, i.e., τ_s is fully shared for backhaul and access transmissions as illustrated in Fig. 4.2(c). Accordingly, the available channels for backhaul and access transmissions are calculated as $N_s = \tau_s N$.

c) **Hybrid IBFD/OBFD Backhauling:** In this case, the assigned spectrum to s^{th} SBS is partitioned optimally into three portions, i.e., α_s for IBFD backhaul/access transmission, φ_s for OBFD backhaul transmission, and $\tau_s - \alpha_s - \varphi_s$ for OBFD access transmissions (see Fig. 4.2(d)). It can be seen that when $\alpha_s \to 0$ the SBS s will favor OBFD backhauling whereas when $\alpha_s \to \tau_s$ or $\varphi_s \to 0$ the SBS s will favor IBFD backhauling. Subsequently, τ_s can be

flexibly utilized solely for OBFD backhauling or IBFD backhauling or hybrid IBFD/OBFD backhauling. The ranges of φ_s and α_s are interdependent, i.e., $0 < \varphi_s < \tau_s - \alpha_s$ and $0 < \alpha_s < \tau_s - \varphi_s$. The number of channels for IBFD backhaul and access transmissions are given as $\alpha_s N$. Similarly, the number of channels for OBFD backhaul and access transmissions are given as $\varphi_s N$, and $(\tau_s - \alpha_s - \varphi_s)N$, respectively.

4.3.3 Performance Metric: Rate Calculations

a) **OBFD Backhauling:** With OBFD backhauling, for the s^{th} SBS, the achievable rates in the backhaul and access links can be defined, respectively, as follows:

$$\mathcal{R}_{\text{s,b}}^{(\text{OB})} = \varphi_s N \log_2\left(1 + \text{V}_{\text{s,b}}^{(\text{OB})}\right), \quad \mathcal{R}_{\text{s,a}}^{(\text{OB})} = (\tau_s - \varphi_s) N \log_2\left(1 + \text{V}_{\text{s,a}}^{(\text{OB})}\right), \quad (4.1)$$

where

$$\text{V}_{\text{s,b}}^{(\text{OB})} = \frac{Y_{\text{s,b}}}{\sigma^2} = \frac{P_m \; r_s^{-\beta_o} \; \chi_s}{\sigma^2}, \quad \text{V}_{\text{s,a}}^{(\text{OB})} = \frac{Y_{\text{s,a}}}{\sigma^2} = \frac{P_s \; r_u^{-\beta_i} \; \zeta_u}{\sigma^2}. \quad (4.2)$$

Note that $Y_{\text{s,b}}$ is the received signal power at SBS s from the WBH, $Y_{\text{s,a}}$ is the received signal power by the small cell user served by SBS s during a transmission interval, P_m is the fixed transmit power of the WBH per backhaul channel, P_s is the available transmit power of SBS s per access channel, r_s is the distance between WBH and s^{th} SBS, r_u is the distance between a given SBS and its user, β_o and β_i are the outdoor (WBH to SBS) and indoor (SBS to user) path-loss exponents, respectively, and χ_s and ζ_u denote the channel power gain due to shadowing at the backhaul and at access links of SBS s, respectively. The path-

loss between indoor SBS and its user is modeled as $r_s^{-\beta_i}$, where $1.5 \leq \beta_i \leq 3.5$. The path-loss between indoor SBS and outdoor WBH is modeled as $r_u^{-\beta_o}$, where $3.5 \leq \beta_o \leq 6.5$ [78]. The overall channel power gains for the backhaul and access links are given as $|h_b|^2 = r_s^{-\beta_o}\ \chi_s$ and $|h_a|^2 = r_u^{-\beta_i}\ \zeta_u$, respectively. I model χ_s and ζ_u as Gamma distributed RVs, i.e., $\chi_s \sim \text{Gamma}(\kappa_{\chi_s}, \Theta_{\chi_s})$ and $\zeta_u \sim \text{Gamma}(\kappa_{\zeta_u}, \Theta_{\zeta_u})$. I consider that χ_s remains the same (on average) over all backhaul channels allocated to an SBS s and ζ_u remains the same (on average) over all access channels allocated to a user in SBS s. The downlink transmission rate of s^{th} SBS in OBFD mode can then be given as

$$\mathcal{R}_s^{(\text{OB})} = \min\{\mathcal{R}_{\text{s,b}}^{(\text{OB})}, \mathcal{R}_{\text{s,a}}^{(\text{OB})}\}. \tag{4.3}$$

b) **IBFD Backhauling:** With IBFD backhauling, for the s^{th} SBS, the achievable rates in the backhaul and access links can be defined, respectively, as

$$\mathcal{R}_{\text{s,b}}^{(\text{IB})} = N_s\ \log_2\left(1 + \text{V}_{\text{s,b}}^{(\text{IB})}\right), \quad \mathcal{R}_{\text{s,a}}^{(\text{IB})} = N_s\ \log_2\left(1 + \text{V}_{\text{s,a}}^{(\text{IB})}\right), \text{ where} \tag{4.4}$$

$$\text{V}_{\text{s,b}}^{(\text{IB})} = \frac{Y_{\text{s,b}}}{\text{R}_{\text{SI}} + \sigma^2} = \frac{P_m\ r_s^{-\beta_o}\ \chi_s}{\text{R}_{\text{SI}} + \sigma^2}, \quad \text{V}_{\text{s,a}}^{(\text{IB})} = \frac{Y_{s,a}}{\text{I}_{\text{s}} + \sigma^2} = \frac{P_s\ r_u^{-\beta_i}\ \zeta_u}{P_m\ d_s^{-\beta_o}\ \zeta_s + \sigma^2}, \tag{4.5}$$

in which d_s is the distance between the user being served by SBS s and the WBH, and ζ_s is the channel power gain (due to shadowing) in the link between the WBH and the user. ζ_s is assumed to be same (on average) over all backhaul interfering channels for SBS s. Since the SBS receives backhaul data (from the WBH) and transmits (to the user) simultaneously, the SI experienced by the user is given as $R_{\text{SI}} = \frac{P_s}{C_{\text{SI}}}$. Note that SI depends on P_s and here I assume

a linear model to define the residual SI power as given in [36, 74, 79–81]. $\frac{1}{C_{\mathrm{SI}}}$ is the residual self-interference power that can be characterized based on the cancellation algorithms. For example, after digital domain cancellation, the residual self-interfering channel gain can be obtained by taking the difference of self-interfering channel and its estimate. Consequently, $\frac{1}{C_{\mathrm{SI}}}$ can be modeled as the estimation error variance, which is a constant [60, 80, 82–84]. With IBFD mode, for the s^{th} SBS, the achievable downlink transmission rate can then be given as

$$\mathcal{R}_s^{(\mathrm{IB})} = \min\{\mathcal{R}_{\mathrm{s,b}}^{(\mathrm{IB})}, \mathcal{R}_{\mathrm{s,a}}^{(\mathrm{IB})}\}. \tag{4.6}$$

c) **Hybrid IBFD-OBFD Backhauling:** With hybrid IBFD/OBFD backhauling, the achievable rate of s^{th} SBS can be given by first defining the total backhaul and access spectrum, respectively, as

$$\begin{aligned}\mathcal{R}_{\mathrm{s,b}}^{(\mathrm{H})} =& \alpha_s N \log_2\left(1+\mathrm{V}_{\mathrm{s,b}}^{(\mathrm{IB})}\right) + \varphi_s N \log_2\left(1+\mathrm{V}_{\mathrm{s,b}}^{(\mathrm{OB})}\right)\\ \mathcal{R}_{\mathrm{s,a}}^{(\mathrm{H})} =& \alpha_s N \log_2\left(1+\mathrm{V}_{\mathrm{s,a}}^{(\mathrm{IB})}\right) + (\tau_s-\varphi_s-\alpha_s) N \log_2\left(1+\mathrm{V}_{\mathrm{s,a}}^{(\mathrm{OB})}\right).\end{aligned} \tag{4.7}$$

The achievable downlink transmission rate can then be given as

$$\mathcal{R}_s^{(\mathrm{H})} = \min\{\mathcal{R}_{\mathrm{s,b}}^{(\mathrm{H})}, \mathcal{R}_{\mathrm{s,a}}^{(\mathrm{H})}\}. \tag{4.8}$$

In the next section, I will formulate and solve the problem of optimal spectrum allocation in a small cell considering hybrid IBFD/OBFD backhauling and its special cases (i.e., IBFD backhauling and OBFD backhauling) in closed-form. A list of important variables is provided in Table 4.1.

Table 4.1: Chapter 4:Summary of the main variables and their definitions

Variable	**Definition**	**Variable**	**Definition**
$(\cdot)$	$(\cdot)$ = (OB) for OBFD backhauling mode and $(\cdot)$ = (IB) for IBFD backhauling mode	τ_s	Portion of spectrum allocated to SBS s for backhaul and access transmissions
φ_s	Portion of spectrum allocated to SBS s for backhaul transmission in OBFD mode	α_s	Portion of spectrum allocated to SBS s for IBFD backhaul/access transmission in hybrid backhauling mode
$V_{\mathrm{s,b}}^{(\cdot)}$	Received backhaul SINR at SBS s	$V_{\mathrm{s,a}}^{(\cdot)}$	Received access SINR at SBS s
$\mathcal{R}_{\mathrm{s,a}}^{(\cdot)}$, $\mathcal{R}_{\mathrm{s,b}}^{(\cdot)}$	Rate of SBS s at access and backhaul spectrum, respectively	R_{th}	Minimum achievable rate per SBS
$Y_{\mathrm{s,b}}$, $Y_{\mathrm{s,a}}$	Signal power at the backhaul and access of SBS s	$Y_{(\mathrm{s}),\mathrm{b}}$, $Y_{(\mathrm{s}),\mathrm{a}}$	Signal power at the backhaul and access of s^{th} ranked SBS
$\hat{p}_{(\mathrm{s})}$	Backhaul channel allocation probability of s^{th} ranked SBS for max-RSP	$\bar{p}_{(\mathrm{s})}$	Backhaul channel allocation probability of s^{th} ranked SBS for min-RSP
$\hat{N}_{(\mathrm{s}),\mathrm{b}}^{(\cdot)}$, $\bar{N}_{(\mathrm{s}),\mathrm{b}}^{(\cdot)}$	Number of channels allocated to s^{th} ranked SBS for backhaul transmission with max-RSP and min-RSP, respectively	$N_{(\mathrm{s}),\mathrm{a}}^{(\mathrm{OB})}$	Number of channels allocated to s^{th} ranked SBS for access transmission with min-RSP and max-RSP, respectively, in OBFD mode
$\hat{N}_{(\mathrm{s}),\mathrm{a}}^{(\mathrm{IB})}$	Number of channels allocated to s^{th} ranked SBS for access transmission with max-RSP in IBFD mode	$\bar{N}_{(\mathrm{s}),\mathrm{a}}^{(\mathrm{IB})}$	Number of channels allocated to s^{th} ranked SBS for access transmission with min-RSP in IBFD mode
$\hat{\mathcal{C}}_{(\mathrm{s}),\mathrm{b}}^{(\cdot)}$, $\bar{\mathcal{C}}_{(\mathrm{s}),\mathrm{b}}^{(\cdot)}$	Backhaul rate coverage of s^{th} ranked SBS for max-RSP and min-RSP, respectively	$\hat{\mathcal{C}}_{(\mathrm{s}),\mathrm{a}}^{(\cdot)}$, $\bar{\mathcal{C}}_{(\mathrm{s}),\mathrm{a}}^{(\cdot)}$	Access rate coverage of s^{th} ranked SBS for max-RSP and min-RSP, respectively
$\hat{\mathcal{C}}_{(\mathrm{s})}^{(\cdot)}$, $\bar{\mathcal{C}}_{(\mathrm{s})}^{(\cdot)}$	Rate coverage of s^{th} ranked SBS for max-RSP and min-RSP, respectively	$\hat{\mathcal{C}}^{(\cdot)}$, $\bar{\mathcal{C}}^{(\cdot)}$	Minimum network rate for max-RSP and min-RSP, respectively
$\hat{\eta}_{(\mathrm{s}),\mathrm{b}}^{(\mathrm{OB})}$,$\bar{\eta}_{(\mathrm{s}),\mathrm{b}}^{(\mathrm{OB})}$	Backhaul threshold of s^{th} ranked SBS with max-RSP and min-RSP, respectively, in OBFD mode	$\eta_{(\mathrm{s}),\mathrm{a}}^{(\mathrm{OB})}$	Access threshold of s^{th} ranked SBS with max-RSP and min-RSP in OBFD mode
$\hat{\eta}_{(\mathrm{s})}^{(\mathrm{IB})}$	Backhaul and access threshold of s^{th} ranked SBS with max-RSP in IBFD mode	$\bar{\eta}_{(\mathrm{s})}^{(\mathrm{IB})}$	Backhaul and access threshold of s^{th} ranked SBS with min-RSP in IBFD mode

4.4 Centralized Access/Backhaul Spectrum Allocation

The main objective of the considered spectrum allocation problem is to optimize the allocation of spectrum for backhaul and access links such that the minimum achievable downlink transmission rate of SBSs can be maximized. In this section, I first formulate an optimization problem for the hybrid IBFD/OBFD backhauling where the achievable downlink transmission rate in a small cell is defined as the minimum of the backhaul transmission rate at the corresponding SBS and the access rate in that small cell (as described in Section II). Provided the spectrum allocated to SBSs be $\boldsymbol{\tau} = [\tau_1, \tau_2, \cdots, \tau_S]$, the backhaul/access spectrum allocated to SBSs for IBFD backhauling be $\boldsymbol{\alpha} = [\alpha_1, \alpha_2, \cdots, \alpha_S]$, and the backhaul spectrum allocated to SBSs for OBFD backhauling be $\boldsymbol{\varphi} = [\varphi_1, \varphi_2, \cdots, \varphi_S]$, the problem can be formulated as follows:

$$\begin{aligned} \textbf{(P)} \quad & \underset{\boldsymbol{\tau},\, \boldsymbol{\alpha},\, \boldsymbol{\varphi}}{\text{maximize}} \quad \min_{s} \quad \left(\mathcal{R}^{\mathrm{H}}_{\mathrm{s,b}},\ \mathcal{R}^{\mathrm{H}}_{\mathrm{s,a}}\right) \\ & \text{subject to} \quad \sum_{s=1}^{S} \tau_s = 1, \quad \alpha_s + \varphi_s \leq \tau_s, \quad \alpha_s > 0, \varphi_s > 0, \quad \forall s, \end{aligned} \tag{4.9}$$

where $\mathcal{R}^{\mathrm{H}}_{\mathrm{s,b}}$, and $\mathcal{R}^{\mathrm{H}}_{\mathrm{s,a}}$ are defined in (4.7). By introducing a variable for minimum achievable target rate R_{th}, the original problem **(P)** can be formulated in epigraph

form as follows:

$$
\begin{aligned}
\textbf{(P1)} \quad & \underset{\mathrm{R_{th}},\, \boldsymbol{\tau},\, \boldsymbol{\alpha},\, \boldsymbol{\varphi}}{\text{maximize}} \quad \mathrm{R_{th}} \\
& \text{subject to} \\
& C_1 : \alpha_s N \log_2\left(1 + \mathrm{V}_{\mathrm{s,b}}^{(\mathrm{IB})}\right) + \varphi_s N \log_2\left(1 + \mathrm{V}_{\mathrm{s,b}}^{(\mathrm{OB})}\right) \geq \mathrm{R_{th}}, \quad \forall\, s, \\
& C_2 : \alpha_s N \log_2\left(1 + \mathrm{V}_{\mathrm{s,a}}^{(\mathrm{IB})}\right) + \left(\tau_s - \alpha_s - \varphi_s\right) N \log_2\left(1 + \mathrm{V}_{\mathrm{s,a}}^{(\mathrm{OB})}\right) \geq \mathrm{R_{th}}, \quad \forall\, s, \\
& C_3 : \sum_{s=1}^{S} \tau_s = 1, \\
& C_4 : \alpha_s + \varphi_s \leq \tau_s, \quad \forall s, \\
& C_5 : \alpha_s > 0, \varphi_s > 0, \quad \forall s.
\end{aligned}
\tag{4.10}
$$

Constraints C_1 **and** C_2 ensure rate of each SBS at backhaul and access spectrum to be greater than $\mathrm{R_{th}}$. Note that the total achievable backhaul rate at a SBS s depends on the available portions of spectrum α_s and φ_s. The variables α_s and φ_s in constraint C_1 are inversely related to each other. As α_s (portion of in-band backhaul/access spectrum) increases, φ_s (portion of out-of-band backhaul spectrum) might decrease in order to fulfill **Constraint** C_4. Similarly, from **Constraint** C_2, higher values of α_s reduce the spectrum portion for OBFD access transmissions, i.e., $\tau_s - \alpha_s - \varphi_s$. **Constraint** C_3 implies that sum of portions of spectrum allocated to each SBS should not exceed unity. Finally, **Constraint** C_4 implies that the portion of backhaul spectrum in IBFD and OBFD modes for SBS s cannot exceed its total available portion of spectrum τ_s. As can be seen, Problem **(P1)** is in an epigraph form; therefore, the optimal solution can be derived by successively solving the feasibility problem **(F1)** and updating R_{th} using Bisection search algorithm [85]. The considered

feasibility problem is as follows:

$$\begin{aligned} \textbf{(F1)} \quad & \text{Find} \quad (\boldsymbol{\tau}, \boldsymbol{\alpha}, \boldsymbol{\varphi}) \\ & \text{subject to} \\ & C_1 - C_5 \quad \text{of problem } \textbf{(P1)} \end{aligned} \tag{4.11}$$

Let $\mathrm{R}_{\mathrm{th}}^{*}$ denote the optimal value of **(P1)**. I assume the problem **(F1)** is feasible, and start with an interval $[\mathrm{R}_{\min}, \mathrm{R}_{\max}]$ known to contain the optimal value $\mathrm{R}_{\mathrm{th}}^{*}$. The problem is solved at its midpoint $\mathrm{R}_{\mathrm{th}} = (\mathrm{R}_{\min} + \mathrm{R}_{\max})/2$, to determine whether the optimal value is in the lower half or upper half of the interval and I can update the interval accordingly. If the feasibility problem **(F1)** is feasible, then I have $\mathrm{R}_{\mathrm{th}}^{*} \geq \mathrm{R}_{\mathrm{th}}$. Contrarily, if the problem **(F1)** is infeasible, then $\mathrm{R}_{\mathrm{th}}^{*} \leq \mathrm{R}_{\mathrm{th}}$ [85]. This generates a new interval, which also contains the optimal value, but has half the width of the initial interval. This algorithm repeats until the width of the interval is small enough. The details of the algorithm are presented in **Algorithm 1**. Once the optimal $\mathrm{R}_{\mathrm{th}}^{*}$ is achieved, the optimal values of the primal variables can be taken from the solution of the feasibility problem **(F1)**. The number of iteration requires for the convergence of **Algorithm 1** is $\log_2\left((\mathrm{R}_{\max} - \mathrm{R}_{\min})/\eta\right)$.

Algorithm 1 Algorithm for Centralized Solution

Initialize $\mathrm{R}_{\min} = 0$, $\mathrm{R}_{\max} > \mathrm{R}_{\mathrm{th}}^{*}$, $\eta > 0$

Repeat

1. $\mathrm{R}_{\mathrm{th}} := \frac{1}{2}\left(\mathrm{R}_{\min} + \mathrm{R}_{\max}\right)$
2. Solve the convex feasibility problem (4.11).
3. **if** (4.11) is feasible set $\mathrm{R}_{\min} := \mathrm{R}_{\mathrm{th}}$, **else** $\mathrm{R}_{\max} := \mathrm{R}_{\mathrm{th}}$,

until $\mathrm{R}_{\max} - \mathrm{R}_{\min} \leq \eta$

In the following, I will consider deriving closed-form optimal solutions for the special cases of **(P1)**, i.e., IBFD backhauling in **(P2)** and OBFD backhauling in

(P3).

Special Case 4.4.1 (Spectrum Allocation for IBFD Backhauling)**.** *When $\alpha_s \to \tau_s$ then $\varphi_s = 0$ and **(P1)** reduces to IBFD spectrum allocation problem **(P2)** as follows:*

$$
\begin{aligned}
(\mathbf{P2}) \quad & \underset{\mathrm{R_{th}},\, \boldsymbol{\tau}}{\text{maximize}} \quad \mathrm{R_{th}} \\
& \text{subject} \quad \text{to} \\
& C_1: \ \tau_s \ N \ \log_2\left(1+\mathrm{V}_{\mathrm{s,b}}^{(\mathrm{IB})}\right) \geq \mathrm{R_{th}}, \quad \forall\, s, \\
& C_2: \ \tau_s \ N \ \log_2\left(1+\mathrm{V}_{\mathrm{s,a}}^{(\mathrm{IB})}\right) \geq \mathrm{R_{th}}, \quad \forall\, s, \\
& C_3: \ \sum_{s=1}^{S} \tau_s = 1, \\
& C_4: \ \tau_s > 0,
\end{aligned}
\tag{4.12}
$$

Solving the KKT conditions for **(P2)** results in the following optimal solution for τ_s^* and R_{th}^*.

Corollary 4.4.1 (Optimal Spectrum and Minimum Achievable Rate (τ_s^* and R_{th}^*) per SBS for IBFD Backhauling)**.** *Provided the gains for access/backhaul channels, the optimal portion of spectrum for SBS s can be derived as:*

$$
\tau_s^* = \begin{cases}
\frac{\mathrm{R_{th}^*}}{N \ \log_2\left(1+\mathrm{V}_{\mathrm{s,a}}^{(\mathrm{IB})}\right)}, & \mathrm{V}_{\mathrm{s,b}}^{(\mathrm{IB})} > \mathrm{V}_{\mathrm{s,a}}^{(\mathrm{IB})} \\
\frac{\mathrm{R_{th}^*}}{N \ \log_2\left(1+\mathrm{V}_{\mathrm{s,b}}^{(\mathrm{IB})}\right)}, & \mathrm{V}_{\mathrm{s,b}}^{(\mathrm{IB})} < \mathrm{V}_{\mathrm{s,a}}^{(\mathrm{IB})} \\
\frac{\mathrm{R_{th}^*}}{N \ \log_2\left(1+\mathrm{V}_{\mathrm{s,b}}^{(\mathrm{IB})}\right)} \text{or} \frac{\mathrm{R_{th}^*}}{N \ \log_2\left(1+\mathrm{V}_{\mathrm{s,b}}^{(\mathrm{IB})}\right)}, & \mathrm{V}_{\mathrm{s,b}}^{(\mathrm{IB})} = \mathrm{V}_{\mathrm{s,a}}^{(\mathrm{IB})}
\end{cases}
$$

Equivalently, $\tau_s^* = \frac{\mathrm{R_{th}^*}}{N \ \log_2\left(1+\mathrm{V}_{\mathrm{s,a}}^{(\mathrm{IB})}\right)} \mathbb{1}_{\left(\mathrm{V}_{\mathrm{s,b}}^{(\mathrm{IB})} > \mathrm{V}_{\mathrm{s,a}}^{(\mathrm{IB})}\right)} + \frac{\mathrm{R_{th}^*}}{N \ \log_2\left(1+\mathrm{V}_{\mathrm{s,b}}^{(\mathrm{IB})}\right)} \mathbb{1}_{\left(\mathrm{V}_{\mathrm{s,a}}^{(\mathrm{IB})} < \mathrm{V}_{\mathrm{s,a}}^{(\mathrm{IB})}\right)} + \frac{\mathrm{R_{th}^*}}{N \ \log_2\left(1+\mathrm{V}_{\mathrm{s,b}}^{(\mathrm{IB})}\right)} \mathbb{1}_{\left(\mathrm{V}_{\mathrm{s,b}}^{(\mathrm{IB})} = \mathrm{V}_{\mathrm{s,a}}^{(\mathrm{IB})}\right)}$, *where $\mathbb{1}(\cdot)$ is an indicator function which takes a binary value either 0 or 1. Note that R_{th}^* is not known apriori; however, using C_3 the optimal*

$\mathrm{R}_{\mathrm{th}}^{*}$ *can be determined as follows:*

$$\mathrm{R}_{\mathrm{th}}^{*}=\frac{N}{\sum_{s=1}^{S}\left(\frac{\mathbb{1}\left(\mathrm{V}_{\mathrm{s,b}}^{(\mathrm{IB})}>\mathrm{V}_{\mathrm{s,a}}^{(\mathrm{IB})}\right)}{\log_2\left(1+\mathrm{V}_{\mathrm{s,a}}^{(\mathrm{IB})}\right)}+\frac{\mathbb{1}\left(\mathrm{V}_{\mathrm{s,b}}^{(\mathrm{IB})}<\mathrm{V}_{\mathrm{s,a}}^{(\mathrm{IB})}\right)}{\log_2\left(1+\mathrm{V}_{\mathrm{s,b}}^{(\mathrm{IB})}\right)}+\frac{\mathbb{1}\left(\mathrm{V}_{\mathrm{s,b}}^{(\mathrm{IB})}=\mathrm{V}_{\mathrm{s,a}}^{(\mathrm{IB})}\right)}{\log_2\left(1+\mathrm{V}_{\mathrm{s,b}}^{(\mathrm{IB})}\right)}\right)},\tag{4.13}$$

Proof. Given the Lagrangian of **(P2)** as $\mathcal{L}\left(\boldsymbol{\tau},\mathrm{R}_{\mathrm{th}},\boldsymbol{\lambda},\boldsymbol{\nu},\omega\right)=\mathrm{R}_{\mathrm{th}}+\sum_{s=1}^{S}\lambda_s\left(\tau_s\ N\ \log_2\left(1+\mathrm{V}_{\mathrm{s,b}}^{(\mathrm{IB})}\right)-\mathrm{R}_{\mathrm{th}}\right)+\sum_{s=1}^{S}\nu_s\left(\tau_s\ N\ \log_2\left(1+\mathrm{V}_{\mathrm{s,a}}^{(\mathrm{IB})}\right)-\mathrm{R}_{\mathrm{th}}\right)+\omega\left(1-\sum_{s=1}^{S}\tau_s\right)$, the KKT conditions include primal feasibility conditions K_1-K_3, which are same as constraints C_1-C_3 of **(P2)**, the Lagrangian stationarity conditions, complementarity slackness conditions, and dual feasibility conditions. The Lagrangian stationarity conditions, complementarity slackness conditions, and dual feasibility conditions are listed, respectively, in the following:

$$\begin{aligned}
&K_4:\ \frac{\partial\mathcal{L}}{\partial\tau}=\lambda_s N\ \log_2\left(1+\mathrm{V}_{\mathrm{s,b}}^{(\mathrm{IB})}\right)+\nu_s N\ \log_2\left(1+\mathrm{V}_{\mathrm{s,a}}^{(\mathrm{IB})}\right)-\omega=0,\\
&K_5:\ \frac{\partial\mathcal{L}}{\partial\mathrm{R}_{\mathrm{th}}}=1-\lambda_s-\nu_s=0,\\
&K_6:\ \lambda_s\left(\tau_s\ N\ \log_2\left(1+\mathrm{V}_{\mathrm{s,b}}^{(\mathrm{IB})}\right)-\mathrm{R}_{\mathrm{th}}\right)=0,\\
&K_7:\ \nu_s\left(\tau_s\ N\ \log_2\left(1+\mathrm{V}_{\mathrm{s,a}}^{(\mathrm{IB})}\right)-\mathrm{R}_{\mathrm{th}}\right)=0,\\
&K_8:\ \lambda_s,\nu_s\geq 0.
\end{aligned}\tag{4.14}$$

Since **(P2)** comprises of two inequality constraints (C_1,C_2) for each SBS s, I have two complementary slackness KKT conditions for each SBS s which implies following four conditions to be considered.

- **Case (i)** When $\lambda_s=\nu_s=0$, K_5 gives $1=0$ which is obviously not true.
- **Case (ii)** When $\lambda_s=0$ and $\nu_s>0$, all KKT conditions are satisfied. From K_4,K_5, and K_7, respectively, I have $\nu_s\ N\ \log_2\left(1+\mathrm{V}_{\mathrm{s,a}}^{(\mathrm{IB})}\right)-\omega=0,\quad 1-\nu_s=$

$0, \quad \tau_s\ N\ \log_2\left(1+\mathrm{V}_{\mathrm{s,a}}^{(\mathrm{IB})}\right)-\mathrm{R}_{\mathrm{th}}=0$. In this case, the optimal value of τ_s^* can be determined as $\tau_s^*=\frac{\mathrm{R}_{\mathrm{th}}}{N\ \log_2\left(1+\mathrm{V}_{\mathrm{s,a}}^{(\mathrm{IB})}\right)}$ from K_7. As $\lambda_s=0$, the second part of K_6 must be be greater than zero, i.e., $\left(\tau_s\ N\ \log_2\left(1+\mathrm{V}_{\mathrm{s,b}}^{(\mathrm{IB})}\right)-\mathrm{R}_{\mathrm{th}}\right)>0$ to satisfy the complementary slackness condition. This states that $\mathrm{V}_{\mathrm{s,b}}^{(\mathrm{IB})}$ will be greater than $2^{\mathrm{R}_{\mathrm{th}}/(\tau_s\ N)}$. On the other hand, as $\nu_s>0$ then second part of K_7 must be equal to zero, i.e., $\tau_s\ N\ \log_2\left(1+\mathrm{V}_{\mathrm{s,a}}^{(\mathrm{IB})}\right)-\mathrm{R}_{\mathrm{th}}=0$ which means $\mathrm{V}_{\mathrm{s,a}}^{(\mathrm{IB})}$ will be equal to $2^{\mathrm{R}_{\mathrm{th}}/(\tau_s\ N)}$. Therefore, this case is true <u>iff</u> $\mathrm{V}_{\mathrm{s,b}}^{(\mathrm{IB})}>\mathrm{V}_{\mathrm{s,a}}^{(\mathrm{IB})}$.

- **Case (iii)** When $\lambda_s>0$ and $\nu_s=0$, all KKT conditions are satisfied. From K_4, K_5, and K_6, respectively, I have $\lambda_s\ N\ \log_2\left(1+\mathrm{V}_{\mathrm{s,b}}^{(\mathrm{IB})}\right)-\omega=0, \quad 1-\lambda_s=0, \quad \tau_s\ N\ \log_2\left(1+\mathrm{V}_{\mathrm{s,b}}^{(\mathrm{IB})}\right)-\mathrm{R}_{\mathrm{th}}=0$. In this case, the optimal τ_s^* can be calculated as $\tau_s^*=\frac{\mathrm{R}_{\mathrm{th}}}{N\ \log_2\left(1+\mathrm{V}_{\mathrm{s,b}}^{(\mathrm{IB})}\right)}$. Using the similar arguments as for case (ii) I can show that this case is true <u>iff</u> when $\mathrm{V}_{\mathrm{s,b}}^{(\mathrm{IB})}<\mathrm{V}_{\mathrm{s,a}}^{(\mathrm{IB})}$.

- **Case (iv)** When $\lambda_s>0, \nu_s>0$, all KKT conditions are satisfied. From K_6 and K_7, respectively, I have $\tau_s\ N\ \log_2\left(1+\mathrm{V}_{\mathrm{s,b}}^{(\mathrm{IB})}\right)-\mathrm{R}_{\mathrm{th}}=0, \quad \tau_s\ N\ \log_2\left(1+\mathrm{V}_{\mathrm{s,a}}^{(\mathrm{IB})}\right)-\mathrm{R}_{\mathrm{th}}=0$. From both equations, it can be seen that they will be valid <u>iff</u> $\mathrm{V}_{\mathrm{s,b}}^{(\mathrm{IB})}=\mathrm{V}_{\mathrm{s,a}}^{(\mathrm{IB})}$. That is, when backhaul SINR ($\mathrm{V}_{\mathrm{s,b}}^{(\mathrm{IB})}$) and access SNR ($\mathrm{V}_{\mathrm{s,a}}^{(\mathrm{IB})}$) of a given SBS s are identical. The optimal value of τ_s^* can thus be obtained either from K_6, i.e.,$\tau_s^*=\frac{\mathrm{R}_{\mathrm{th}}}{N\ \log_2\left(1+\mathrm{V}_{\mathrm{s,b}}^{(\mathrm{IB})}\right)}$ or from K_7, i.e., $\tau_s^*=\frac{\mathrm{R}_{\mathrm{th}}}{N\ \log_2\left(1+\mathrm{V}_{\mathrm{s,a}}^{(\mathrm{IB})}\right)}$.

Summing up all conclusions derived from the cases (ii)-(iv) for each SBS s, the proof of (4.13) is self-explanatory. □

Special Case 4.4.2 (Spectrum Allocation for OBFD Backhauling)**.** *When* $\alpha_s\rightarrow\tau_s$

*then $\varphi_s = 0$, **(P1)** reduces to OBFD spectrum allocation problem **(P3)** as follows:*

$$
\begin{aligned}
(\mathbf{P3}) \quad & \underset{\mathrm{R_{th}},\, \boldsymbol{\varphi},\, \boldsymbol{\tau}}{\text{maximize}} \quad \mathrm{R_{th}} \\
& \text{subject} \quad \text{to} \\
& C_1: \ \varphi_s \ N \ \log_2\left(1+\mathrm{V}_{\mathrm{s,b}}^{(\mathrm{OB})}\right) \geq \mathrm{R_{th}}, \quad \forall\, s, \\
& C_2: \ (\tau_s - \varphi_s) \ N \ \log_2\left(1+\mathrm{V}_{\mathrm{s,a}}^{(\mathrm{OB})}\right) \geq \mathrm{R_{th}}, \quad \forall\, s, \\
& C_3: \ \sum_{s=1}^{S} \tau_s = 1, \\
& C_4: \ \varphi_s \leq \tau_s, \quad \varphi_s > 0 \quad \forall s.
\end{aligned}
\tag{4.15}
$$

Solving the KKT conditions for **(P3)** results in the following optimal solution for τ_s^*, φ_s^*, and R_{th}^*.

Corollary 4.4.2 (Optimal Spectrum and Minimum Achievable Rate (τ_s^*, φ_s^*, and R_{th}^*) per SBS for OBFD Backhauling)**.** *Provided the gains for access/backhaul channels, the optimal portion of spectrum for SBS s can be derived as:*

$$
\tau_s^* = \frac{\mathrm{R_{th}^*}}{N}\left(\frac{1}{\log_2\left(1+\mathrm{V}_{\mathrm{s,b}}^{(\mathrm{OB})}\right)} + \frac{1}{\log_2\left(1+\mathrm{V}_{\mathrm{s,a}}^{(\mathrm{OB})}\right)}\right), \tag{4.16}
$$

and the optimal portion of backhaul spectrum of SBS s can be derived as

$$
\varphi_s^* = \frac{\mathrm{R_{th}}}{N \ \log_2\left(1+\mathrm{V}_{\mathrm{s,b}}^{(\mathrm{OB})}\right)} \tag{4.17}
$$

By substituting (4.16) *in C_3, I obtain optimal $\mathrm{R_{th}^*}$ as follows:*

$$
\mathrm{R_{th}^*} = \frac{N}{\sum_{s=1}^{S}\left(\frac{1}{\log_2\left(1+\mathrm{V}_{\mathrm{s,b}}^{(\mathrm{OB})}\right)} + \frac{1}{\log_2\left(1+\mathrm{V}_{\mathrm{s,a}}^{(\mathrm{OB})}\right)}\right)}. \tag{4.18}
$$

Proof. Provided the Lagrangian of **(P3)** as $\mathcal{L}\left(\boldsymbol{\tau}, \mathrm{R_{th}}, \boldsymbol{\varphi}, \boldsymbol{\lambda}, \boldsymbol{\nu}, \omega, \boldsymbol{\epsilon}\right) = \mathrm{R_{th}} + \sum_{s=1}^{S} \lambda_s \left(\varphi_s N \log_2\left(1+\mathrm{V}_{\mathrm{s,b}}^{(\mathrm{OB})}\right) - \mathrm{R_{th}}\right) + +\omega\left(1-\sum_{s=1}^{S}\tau_s\right) + \sum_{s=1}^{S}\epsilon_s\left(\tau_s-\varphi_s\right) + \sum_{s=1}^{S}\nu_s\left(\left(\tau_s-\varphi_s\right) N \log_2\left(1+\mathrm{V}_{\mathrm{s,a}}^{(\mathrm{OB})}\right) - \mathrm{R_{th}}\right)$, the KKT conditions $K_1 - K_4$ are same as constraints $C_1 - C_4$ of **(P3)**, respectively, and the Lagrangian stationarity conditions, complementarity slackness conditions, and dual feasibility conditions are listed, respectively, in the following:

$$
\begin{aligned}
&K_5: \frac{\partial \mathcal{L}}{\partial \tau} = \nu_s\, N \log_2\left(1+\mathrm{V}_{\mathrm{s,a}}^{(\mathrm{OB})}\right) - \omega + \epsilon_s = 0,\\
&K_6: \frac{\partial \mathcal{L}}{\partial \mathrm{R_{th}}} = 1 - \lambda_s - \nu_s = 0,\\
&K_7: \frac{\partial \mathcal{L}}{\partial \varphi} = \lambda_s\, N \log_2\left(1+\mathrm{V}_{\mathrm{s,b}}^{(\mathrm{OB})}\right) - \nu_s N \log_2\left(1+\mathrm{V}_{\mathrm{s,a}}^{(\mathrm{OB})}\right) - \epsilon_s = 0,\\
&K_8: \lambda_s\left(\varphi_s\, N \log_2\left(1+\mathrm{V}_{\mathrm{s,b}}^{(\mathrm{OB})}\right) - \mathrm{R_{th}}\right) = 0,\\
&K_9: \nu_s\left(\left(\tau_s-\varphi_s\right) N \log_2\left(1+\mathrm{V}_{\mathrm{s,a}}^{(\mathrm{OB})}\right) - \mathrm{R_{th}}\right) = 0,\\
&K_{10}: \epsilon_s\left(\tau_s-\varphi_s\right) = 0,\\
&K_{11a}: \lambda_s, \nu_s \geq 0, \quad K_{11b}: \epsilon_s = 0.
\end{aligned}
$$

Since **(P3)** comprises of three inequality constraints (C_1, C_2, C_4) for each SBS s, I have three complementary slackness KKT conditions for each SBS s which implies following eight conditions to be considered.

- **Case (i)** When $\lambda_s = \nu_s = \epsilon_s = 0$, K_6 gives $1 = 0$ which is not true.
- **Case (ii)** When $\lambda_s > 0, \nu_s = \epsilon_s = 0$, substitution in K_7 makes the backhaul rate zero which is indeed a positive value in order for the problem to be feasible.
- **Case (iii)** When $\lambda_s = \nu_s = 0, \epsilon_s > 0$, K_6, K_{10}, and K_{11b} are violated. Substituting $\lambda_s = \nu_s = 0$ in K_6 gives $1 = 0$ which is obviously not true. When $\epsilon_s > 0$ then $\tau_s - \varphi_s$ should be equal to zero to satisfy K_{10} which is not possible. The

reason is when $\tau_s - \varphi_s = 0$ it means that all spectrum τ_s is used for backhaul ($\tau_s = \varphi_s$) and there is no spectrum for access transmission which makes the problem infeasible.

- **Case (iv-v)** When $\lambda_s = 0, \nu_s > 0, \epsilon > 0$ and $\lambda_s > 0, \nu_s = 0, \epsilon_s > 0$ then each case violates K_7, K_{10} and K_{11b}. The reason of violation of K_7 and K_{10} is same as explained in Case (ii) and Case (iii), respectively.

- **Case (vi)** $\lambda_s > 0, \nu_s > 0, \epsilon_s > 0$. This condition violates K_{10} and K_{11b}.

- **Case (vii)** $\lambda_s = \epsilon_s = 0, \nu_s > 0$. It violates $K7$. The reason is same as explained in Case (ii).

- **Case (viii)** When $\lambda_s > 0$, $\nu_s > 0$, $\epsilon_s = 0$, then all KKT conditions are satisfied. Since $\lambda_s > 0$, the second term of K_8 must be equal to zero, i.e., $\varphi_s \; N \; \log_2\left(1 + \mathrm{V}_{\mathrm{s,b}}^{(\mathrm{OB})}\right) - \mathrm{R}_{\mathrm{th}} = 0$. From this, I can obtain $\varphi_s^* = \frac{\mathrm{R}_{\mathrm{th}}}{N \; \log_2\left(1+\mathrm{V}_{\mathrm{s,b}}^{(\mathrm{OB})}\right)}$. Similarly, as $\nu_s > 0$, the second term of K_9 must be equal to zero, i.e., $(\tau_s - \varphi_s) \; N \; \log_2\left(1 + \mathrm{V}_{\mathrm{s,a}}^{(\mathrm{OB})}\right) - \mathrm{R}_{\mathrm{th}} = 0$. By substituting φ_s^* obtained from K_8 into K_9 and K_3 and then doing simple algebraic manipulations, I obtain optimal τ_s^* in terms of $\mathrm{R}_{\mathrm{th}}^*$ as given in **Corollary 2**.

□

To reduce the overhead involved in solving the centralized problem (due to the complete knowledge of access/backhaul channel state information of all SBSs) and to gain system design insights, in the subsequent sections, I will investigate two distributed and light-weight backhaul channel scheduling schemes, i.e., *max-RSP* and *min-RSP* schemes. For both schemes, I will determine the spectrum allocated to each SBS, the rate coverage, and achievable downlink transmission rate for a small cell user.

4.5 Distributed Backhaul/Access Spectrum Allocation Schemes

The max-RSP scheme allocates more backhaul channels to cell-center SBSs (or SBSs with higher backhaul channel gains) while the min-RSP scheme allocates more backhaul channels to SBSs with weaker backhaul channel gains. Intuitively, the max-RSP scheme will offer a higher backhaul rate to their respective users. However, since the access link can be a bottleneck, this scheme may not necessarily maximize the achievable downlink transmission rate for small cell users. Further, the overall network rate may suffer due to the starvation of SBSs with weaker backhaul channels. Note that since the access rate experienced at nearby and farther SBSs could be nearly the same due to similar coverage radii, allocating more backhaul channels to farther SBSs can be more beneficial, which motivates the design of min-RSP scheme. The min-RSP scheme is also inspired by the results in **Corollary 2** in which the backhaul spectrum portion is inversely proportional to the backhaul channel conditions.

I comparatively analyze the performance of max-RSP and min-RSP schemes defined as follows:

- **Maximum Received Signal Power (max-RSP)** scheme: The WBH allocates a given backhaul channel j to an SBS with maximum received signal power. Mathematically, this criterion can be written as:

$$Y_{\mathrm{s,b}}^{*} = \arg\max\{Y_{\mathrm{s,b}}^{(j)}\}, \forall s = \{1, \cdots, S\}, \tag{4.19}$$

  where $Y_{\mathrm{s,b}}^{(j)} = P_m \; r_s^{-\beta_o} \; \chi_s^{(j)}$ is the received signal power of an SBS on backhaul channel j from the WBH.

- **Minimum Received Signal Power (min-RSP)** scheme: The WBH allocates

a given backhaul channel j to an SBS with minimum received signal power. Mathematically, this criterion can be written as:

$$Y^{*}_{\mathrm{s,b}} = \arg\min\{Y^{(j)}_{\mathrm{s,b}}\}, \forall s = \{1, \cdots, S\}. \tag{4.20}$$

With OBFD backhauling, the available spectrum (i.e., N channels) is partitioned for backhaul and access link transmissions (i.e., N_b and $N - N_b$ are the total number of backhaul and access channels, respectively). I divide the access spectrum equally among all SBSs. This is based on the results in **Corollary 2**. Note that the access and backhaul spectrum are the same in case of IBFD backhauling. With OBFD backhauling and max-RSP scheme, I outline the methodology to evaluate the downlink achievable rate per SBS in the following.

- Rank all SBSs according to their distances from the WBH.
- Derive the probability of allocating a backhaul channel to a ranked SBS s. This is a fundamental step toward defining the rate coverage of users served by a given SBS.
- Determine the number of backhaul channels allocated to each SBS s.
- The achievable rate in the access link (i.e., access rate) is given as $\mathcal{R}^{(OB)}_{(s),a} = N^{(\mathrm{OB})}_{(\mathrm{s}),\mathrm{a}} \log_2\left(1 + \frac{P_s r_u^{-\beta_i} \zeta_u}{\sigma^2}\right)$ and the backhaul rate as $\hat{\mathcal{R}}^{(\mathrm{OB})}_{(s),b} = \hat{N}^{(\mathrm{OB})}_{(\mathrm{s}),\mathrm{b}} \log_2\left(1 + \frac{P_m\ r_{(s)}^{-\beta_o} \chi_s}{\sigma^2}\right)$, where $\hat{N}^{(\mathrm{OB})}_{(\mathrm{s}),\mathrm{b}}$ and $N^{(\mathrm{OB})}_{(\mathrm{s}),\mathrm{a}}$ are the number of channels allocated to ranked SBS s for backhaul and access transmission, respectively.
- Derive access and backhaul rate coverage probability of s^{th} ranked SBS and finally, determine the achievable downlink transmission rate for the small cell users.

Following these steps, the achievable downlink transmission rate for OBFD backhauling with min-RSP scheme and IBFD backhauling with both max-RSP and min-RSP schemes will also be analyzed in the subsequent sections.

4.5.1 Distance-based Ranking of SBSs

Since the SBSs are uniformly distributed, the PDF of the distance between SBS s and WBH can be defined as $f_{r_s}(r_s) = \frac{2r_s}{R_m^2}$, where $0 \leq r_s \leq R_m$. The CDF of r_s can be given as $F_{r_s}(r_s) = \int_0^{r_s} f_{r_s}(u)du = r_s^2/R_m^2$. For given PDF and CDF of r_s, the SBSs can be ranked w.r.t their distances from the WBH. The PDF of the s^{th} ranked SBS can therefore be defined, using ordered statistics [86], as follows:

$$f_{r_{(s)}}(r_{(s)}) = \frac{S!\,(1 - F_{r_s}(r_s))^{S-s}\, f_{r_s}(r_s)}{(F_{r_s}(r_s))^{1-s}\,(s-1)!(S-s)!}. \tag{4.21}$$

Substituting the PDF and CDF of r_s and by applying the Binomial expansion, (5.9) can be written as:

$$f_{r_{(s)}}(r_{(s)}) = \sum_{n=0}^{S-s} \frac{2\ S!\ (-1)^{S-s+n}\ r_s^{2S-2n-1} R_m^{2(n-S)}}{(s-1)!\ (S-s-n)!\ n!}. \tag{4.22}$$

4.5.2 Probability of Backhaul Channel Allocation

In this subsection, I first derive the PDF and CDF of received signal power at a given backhaul channel. Then I derive the probability of allocating a backhaul channel to a ranked SBS s for both max-RSP and min-RSP schemes. Subsequently, I determine the number of backhaul channels allocated to the ranked SBS s for both the schemes. The received signal power at a given backhaul channel of s ranked SBS can be defined as $Y_{(\text{s}),\text{b}} = P_m r_{(s)}^{-\beta_o} \chi_s$. It was shown that Gamma distribution models shadowing as

close as the log-normal distribution [87] and that the composite shadow-fading can be modeled as Gamma distribution [74]. Note that after multiplying $r_{(s)}^{-\beta_o}$ with an RV χ_s, $Y_{(\mathrm{s}),\mathrm{b}}$ is no longer a ranked RV. The received signal power at the access link of s ranked SBS is defined as $Y_{(\mathrm{s}),\mathrm{a}} = P_s r_u^{-\beta_i} \zeta_u$. Now conditioning on the distribution of $r_{(s)}$, doing transformation of RV, i.e., $f_{Y_{(\mathrm{s}),\mathrm{b}}}(y_{(\mathrm{s}),\mathrm{b}}|r_{(s)}) = \frac{r_{(s)}^{\beta_o}}{P_m} f_{\chi_s}\left(\frac{y_{(\mathrm{s}),\mathrm{b}} r_{(s)}^{\beta_o}}{P_m}\right)$, and finally averaging over the PDF of $r_{(s)}$, I can write:

$$f_{Y_{(\mathrm{s}),\mathrm{b}}}(y_{(\mathrm{s}),\mathrm{b}}) = \sum_{n=0}^{S-s} \frac{A(n)\Gamma_l\left(\kappa_{\chi_s} - \frac{2(n-S)}{\beta_o}, B y_{(\mathrm{s}),\mathrm{b}}\right)}{y_{(s),b}^{1-\frac{2(n-S)}{\beta_o}}}, \tag{4.23}$$

where $B = \frac{R_m^{\beta_o}}{P_m \Theta_{\chi s}}$ and

$$A(n) = \frac{2S!(-1)^{S-s+n} B^{\frac{2(n-S)}{\beta_o}}}{(s-1)!(S-s-n)!n!\Gamma(\kappa_{\chi_s})\beta_o}. \tag{4.24}$$

The CDF of $Y_{(\mathrm{s}),\mathrm{b}}$ can be derived as follows:

$$F_{Y_{(\mathrm{s}),\mathrm{b}}}(y_{(\mathrm{s}),\mathrm{b}}) = \sum_{n=0}^{S-s} \frac{A(n)\beta_o}{2(n-S)} \left(y_{(s),b}^{\frac{2(n-S)}{\beta_o}} \Gamma_l\left(\kappa_{\chi_s} - \frac{2(n-S)}{\beta_o}, B\ y_{(\mathrm{s}),\mathrm{b}}\right) - \frac{\Gamma_l\left(\kappa_{\chi s}, B y_{(\mathrm{s}),\mathrm{b}}\right)}{B^{-\frac{2(S-n)}{\beta_o}}} \right). \tag{4.25}$$

Given the PDF and CDF of the received signal power $Y_{(\mathrm{s}),\mathrm{b}}$, the backhaul channel allocation probability for max-RSP and min-RSP scheme can be derived as explained below.

Maximum Received Signal Power (max-RSP)

The conditional probability of a given backhaul channel to be allocated to the s rank SBS can be derived as:

$$\hat{p}_{(s)|Y_{(s),\mathrm{b}}} = \Pr(\underset{\substack{g=1,\ldots,S\\ g\neq s}}{Y_{(\mathrm{g}),\mathrm{b}}} \leq Y_{(\mathrm{s}),\mathrm{b}}) = \prod_{\substack{g=1\\ g\neq s}}^{S} F_{Y_{(\mathrm{g}),\mathrm{b}}}(y_{(\mathrm{s}),\mathrm{b}}). \tag{4.26}$$

The unconditional $\hat{p}_{(s)}$ can then be derived by averaging over the distribution of $Y_{(\mathrm{s}),\mathrm{b}}$ as follows:

$$\hat{p}_{(s)} = \int_0^{\infty} \prod_{\substack{g=1\\ g\neq s}}^{S} F_{Y_{(\mathrm{g}),\mathrm{b}}}(y_{(\mathrm{s}),\mathrm{b}}) f_{Y_{(\mathrm{s}),\mathrm{b}}}(y_{(\mathrm{s}),\mathrm{b}}) dy_{(\mathrm{s}),\mathrm{b}}, \tag{4.27}$$

where PDF and CDF of $Y_{(\mathrm{s}),\mathrm{b}}$ are given in (5.12) and (5.14), respectively. (5.16) can be evaluated numerically using standard mathematical software packages.

Minimum Received Signal Power (min-RSP)

The conditional probability of a given backhaul channel to be allocated to the s rank SBS can be derived as:

$$\begin{aligned}\bar{p}_{(s)|Y_{(s),\mathrm{b}}} &= \Pr(\underset{\substack{g=1,2,\ldots,S\\ g\neq s}}{Y_{(\mathrm{g}),\mathrm{b}}} > Y_{(\mathrm{s}),\mathrm{b}}) = \left(1-\Pr(Y_{(1),b} \leq Y_{(\mathrm{s}),\mathrm{b}})\right)\cdots\left(1-\Pr(Y_{(\mathrm{S}),\mathrm{b}} \leq Y_{(\mathrm{s}),\mathrm{b}})\right),\\ &= \prod_{\substack{g=1\\ g\neq s}}^{S}\left(1-F_{Y_{(\mathrm{g}),\mathrm{b}}}(y_{(\mathrm{s}),\mathrm{b}})\right).\end{aligned} \tag{4.28}$$

The unconditional $\bar{p}_{(s)}$ can be derived by averaging over the distribution of $Y_{(\mathrm{s}),\mathrm{b}}$ as follows:

$$\bar{p}_{(s)} = \int_0^{\infty} \prod_{\substack{g=1 \\ g \neq s}}^{S} \left(1 - F_{Y_{(\mathrm{g}),\mathrm{b}}}(y_{(\mathrm{s}),\mathrm{b}})\right) f_{Y_{(\mathrm{s}),\mathrm{b}}}(y_{(\mathrm{s}),\mathrm{b}}) dy_{(\mathrm{s}),\mathrm{b}}, \tag{4.29}$$

where (5.18) can be evaluated numerically using standard mathematical software packages.

4.5.3 Number of Allocated Backhaul/Access Channels

In the OBFD mode, the number of channels allocated to ranked SBS s for backhaul transmission considering max-RSP and min-RSP schemes can be determined, respectively, as $\hat{N}^{(\mathrm{OB})}_{(\mathrm{s}),\mathrm{b}} = N_{\mathrm{b}} \times \hat{p}_{(\mathrm{s})}$, $\bar{N}^{(\mathrm{OB})}_{(\mathrm{s}),\mathrm{b}} = N_{\mathrm{b}} \times \bar{p}_{(\mathrm{s})}$, where $\hat{p}_{(\mathrm{s})}$ and $\bar{p}_{(\mathrm{s})}$ are the probabilities of backhaul channel allocation to s^{th} ranked SBS with max-RSP and min-RSP schemes, respectively, and N_b is the total number of backhaul channels. Since I consider equal distribution of access spectrum among all SBSs in OBFD backhauling, $N^{(\mathrm{OB})}_{(\mathrm{s}),\mathrm{a}} = \frac{N - N_{\mathrm{b}}}{S}$. Note that the $N^{(\mathrm{OB})}_{(\mathrm{s}),\mathrm{a}}$ is same for both the max-RSP and min-RSP schemes due to equal distribution of access spectrum in both cases. In the IBFD mode, the number of channels allocated to ranked SBS s for backhaul in max-RSP and min-RSP schemes is given, respectively, as $\hat{N}^{(\mathrm{IB})}_{(\mathrm{s}),\mathrm{b}} = N \times \hat{p}_{(\mathrm{s})}, \quad \bar{N}^{(\mathrm{IB})}_{(\mathrm{s}),\mathrm{b}} = N \times \bar{p}_{(\mathrm{s})}$. In the IBFD mode, since the backhaul channels allocated to an SBS are same as the access channels, for max-RSP, $\hat{N}^{(\mathrm{IB})}_{(\mathrm{s}),\mathrm{b}} = \hat{N}^{(\mathrm{IB})}_{(\mathrm{s}),\mathrm{a}}$ and for min-RSP, $\bar{N}^{(\mathrm{IB})}_{(\mathrm{s}),\mathrm{b}} = \bar{N}^{(\mathrm{IB})}_{(\mathrm{s}),\mathrm{a}}$.

4.6 Rate Coverage Analysis for IBFD/OBFD Backhauling With Distributed Spectrum Allocation

In this section, I derive the rate coverage probability of a small cell user (which depends on the rate coverage probabilities of the access and backhaul links) and achievable downlink transmission rate by a small cell user considering max-RSP and min-RSP schemes in the IBFD and OBFD backhauling modes.

4.6.1 OBFD Backhauling

To achieve a user rate of R_{th} in a given small cell, both the backhaul and access rate for the corresponding SBS must be at least R_{th}. The rate coverage probability for the ranked SBS s is therefore defined as the probability that the backhaul and access rates are higher than a minimum achievable rate R_{th}. I assume that the channel statistics between the WBH and a given SBS remains the same over all allocated channels. Therefore, the backhaul rate of an SBS s with max-RSP scheme can be defined as follows:

$$\hat{\mathcal{R}}^{(\text{OB})}_{(\text{s}),\text{b}} = \hat{N}^{(\text{OB})}_{(\text{s}),\text{b}} \log_2 \left(1 + \frac{P_m \; r_{(s)}^{-\beta_o} \chi_s}{\sigma^2}\right). \tag{4.30}$$

Similarly, the backhaul rate of an SBS s with min-RSP scheme ($\bar{\mathcal{R}}^{(\text{OB})}_{(\text{s}),\text{b}}$) can be obtained by replacing $\hat{N}^{(\text{OB})}_{(\text{s}),\text{b}}$ with $\bar{N}^{(\text{OB})}_{(\text{s}),\text{b}}$ in (4.30). To achieve R_{th} at the backhaul spectrum, $P_m \; r_{(s)}^{-\beta_o} \chi_s / \sigma^2$ must be greater than a prescribed threshold, which is defined for max-RSP and min-RSP schemes as follows:

$$\hat{\eta}^{(\text{OB})}_{(\text{s}),\text{b}} = 2^{R_{\text{th}}/(\hat{N}^{(\text{OB})}_{(\text{s}),\text{b}})} - 1, \bar{\eta}^{(\text{OB})}_{(\text{s}),\text{b}} = 2^{R_{\text{th}}/(\bar{N}^{(\text{OB})}_{(\text{s}),\text{b}})} - 1. \tag{4.31}$$

The access rate at the s^{th} SBS can thus be given as: $\mathcal{R}^{(\text{OB})}_{(\text{s}),\text{a}} = N^{(\text{OB})}_{(\text{s}),\text{a}} \log_2\left(1+\frac{P_s r_u^{-\beta_i}\zeta_u}{\sigma^2}\right)$, and $P_s r_u^{-\beta_i}\zeta_u/\sigma^2$ must be greater than another prescribed threshold $\eta^{(\text{OB})}_{(\text{s}),\text{a}}$, which is defined as follows:

$$\eta^{(\text{OB})}_{(\text{s}),\text{a}} = 2^{R_{\text{th}}/N^{(\text{OB})}_{(\text{s}),\text{a}}} - 1. \tag{4.32}$$

Since the spectrum band used for the access links is equally distributed in the max-RSP and min-RSP schemes, the threshold remains the same for both schemes.

a) **Rate Coverage for Transmission in the Access Link:** With the max-RSP scheme, the rate coverage probability for the access link of s ranked SBS can be given as:

$$\mathcal{C}^{(\text{OB})}_{(\text{s}),\text{a}} = \mathbb{P}\left(\frac{P_s\ r_u^{-\beta_i}\ \zeta_u}{\sigma^2} > \eta^{(\text{OB})}_{(\text{s}),\text{a}}\right) = \mathbb{P}\left(Y_{(\text{s}),\text{a}} > \eta^{(\text{OB})}_{(\text{s}),\text{a}}\sigma^2\right) = 1 - \text{F}_{\text{Y}_{(\text{s}),\text{a}}}\left(\eta^{(\text{OB})}_{(\text{s}),\text{a}}\sigma^2\right), \tag{4.33}$$

where $Y_{(\text{s}),\text{a}} = P_s r_u^{-\beta_i}\zeta_u$. The PDF of $Y_{(\text{s}),\text{a}}$, i.e., $f_{Y_{(\text{s}),\text{a}}}\left(y_{(\text{s}),\text{a}}\right)$ can be derived as given in [88, eq. 29]. Consequently,

$$F_{Y_{(\text{s}),\text{a}}}\left(\eta^{(\text{OB})}_{(\text{s}),\text{a}}\sigma^2\right) = \int_0^{\eta^{(\text{OB})}_{(\text{s}),\text{a}}\sigma^2} f_{y_{(\text{s}),\text{a}}}(u)\,du = \frac{K^{2/\beta_i}\Gamma_l\left(\kappa_{\zeta_u}, K\right) - \Gamma_l\left(\kappa_{\zeta_u}+\frac{2}{\beta_i}, K\right)}{R_s^2\Gamma(\kappa_{\zeta_u})\left(\frac{K}{R_s^{\beta_i}}\right)^{-2/\beta_i}}. \tag{4.34}$$

b) **Rate Coverage for Transmission in the Backhaul Link:** With the max-RSP scheme, the rate coverage probability for the backhaul link of s ranked

SBS can be derived as follows:

$$\hat{\mathcal{C}}^{(\mathrm{OB})}_{(\mathrm{s}),\mathrm{b}} = \mathbb{P}\left(\frac{P_m\ r^{-\beta_o}_{(s)}\ \chi_s}{\sigma^2} > \hat{\eta}^{(\mathrm{OB})}_{(\mathrm{s}),\mathrm{b}}\right) = 1 - \mathbb{P}\left(Y_{(\mathrm{s}),\mathrm{b}} \leq \hat{\eta}^{(\mathrm{OB})}_{(\mathrm{s}),\mathrm{b}}\sigma^2\right),$$
$$= 1 - \mathrm{F}_{\mathrm{Y}_{(\mathrm{s}),\mathrm{b}}}\left(\hat{\eta}^{(\mathrm{OB})}_{(\mathrm{s}),\mathrm{b}}\sigma^2\right), \tag{4.35}$$

where $Y_{(\mathrm{s}),\mathrm{b}} = P_m\ r^{-\beta_o}_{(s)}\ \chi_s$. The PDF of $Y_{(\mathrm{s}),\mathrm{b}}$ is given in (5.12). Hence, for Gamma distributed channels, $F_{Y_{(\mathrm{s}),\mathrm{b}}}\left(\hat{\eta}^{(\mathrm{OB})}_{(\mathrm{s}),\mathrm{b}}\sigma^2\right)$ is given by replacing $(Y_{(\mathrm{s}),\mathrm{b}})$ with $(\hat{\eta}^{(\mathrm{OB})}_{(\mathrm{s}),\mathrm{b}}\sigma^2)$ in (5.14).

c) **Overall Rate Coverage and Achievable Downlink Transmission Rate:**

With the max-RSP scheme, the overall rate coverage probability $\hat{\mathcal{C}}^{(\mathrm{OB})}_{(\mathrm{s})}$ for the SBS at rank s is defined as:

$$\hat{\mathcal{C}}^{(\mathrm{OB})}_{(\mathrm{s})} = \hat{\mathcal{C}}^{(\mathrm{OB})}_{(\mathrm{s}),\mathrm{b}} \times \mathcal{C}^{(\mathrm{OB})}_{(\mathrm{s}),\mathrm{a}}, \tag{4.36}$$

where $\hat{\mathcal{C}}^{(\mathrm{OB})}_{(\mathrm{s}),\mathrm{b}}$ and $\mathcal{C}^{(\mathrm{OB})}_{(\mathrm{s}),\mathrm{a}}$ are given in (4.35) and (4.33), respectively. Then the achievable downlink transmission rate for a user served by the SBS at rank s can be determined as $\hat{\mathcal{C}}^{(\mathrm{OB})}_{(s)} \times \mathrm{R}_{\mathrm{th}}$, where $\hat{\mathcal{C}}^{(\mathrm{OB})}_{(s)}$ is given in (4.36). Accordingly, the total achievable downlink transmission rate in all the small cells (i.e., network rate) is given by

$$\hat{\mathcal{R}}^{(\mathrm{OB})} = \sum_{s=1}^{S} \hat{\mathcal{C}}^{(\mathrm{OB})}_{(s)} \times \mathrm{R}_{\mathrm{th}}. \tag{4.37}$$

Remark: For the min-RSP scheme, the backhaul rate coverage probability $(\bar{\mathcal{C}}^{\mathrm{OB}}_{(\mathrm{s}),\mathrm{b}})$ for SBS s can be obtained by replacing $\hat{\eta}^{(\mathrm{OB})}_{(\mathrm{s}),\mathrm{b}}$ with $\bar{\eta}^{(\mathrm{OB})}_{(\mathrm{s}),\mathrm{b}}$in (4.35). The access rate coverage probability $\mathcal{C}^{\mathrm{OB}}_{(\mathrm{s}),\mathrm{a}}$ for SBS s will be the same as that in case of max-RSP.

Consequently, the network rate ($\bar{\mathcal{R}}^{\mathrm{OB}}$) can be obtained by replacing $\hat{\mathcal{C}}^{\mathrm{OB}}_{(\mathrm{s})}$ with $\bar{\mathcal{C}}^{\mathrm{OB}}_{(\mathrm{s})} = \bar{\mathcal{C}}^{\mathrm{OB}}_{(\mathrm{s}),\mathrm{b}} \times \mathcal{C}^{\mathrm{OB}}_{(\mathrm{s}),\mathrm{a}}$ in (4.37), where the achievable rate for a user served by the SBS at rank s is $\bar{\mathcal{C}}^{(\mathrm{OB})}_{(s)} \times \mathrm{R}_{\mathrm{th}}$.

4.6.2 IBFD Backhauling

With the max-RSP scheme, the backhaul rate for s^{th} ranked SBS in IBFD mode can be defined as:

$$\hat{\mathcal{R}}^{(\mathrm{IB})}_{(\mathrm{s}),\mathrm{b}} = \hat{N}^{(\mathrm{IB})}_{(\mathrm{s}),\mathrm{b}} \log_2 \left(1 + \frac{P_m \; r^{-\beta_o}_{(s)} \; \chi_s}{\mathrm{R}_{\mathrm{SI}} + \sigma^2}\right). \tag{4.38}$$

Similarly, for the min-RSP scheme, the backhaul rate ($\bar{\mathcal{R}}^{(\mathrm{IB})}_{(\mathrm{s}),\mathrm{b}}$) of s^{th} ranked SBS can be obtained by replacing $\hat{N}^{(\mathrm{IB})}_{(\mathrm{s}),\mathrm{b}}$ with $\bar{N}^{(\mathrm{IB})}_{(\mathrm{s}),\mathrm{b}}$ in (4.38). Therefore, to achieve a target rate of R_{th} in the backhaul link, $\frac{P_m \; r^{-\beta_o}_{(s)} \; \chi_s}{\mathrm{R}_{\mathrm{SI}}+\sigma^2}$ must be greater than a prescribed threshold, which is defined for the max-RSP and min-RSP schemes, respectively, as follows:

$$\hat{\eta}^{(\mathrm{IB})}_{(\mathrm{s})} = 2^{R_{\mathrm{th}}/(\hat{N}^{(\mathrm{IB})}_{(s),b})} - 1, \quad \bar{\eta}^{(\mathrm{IB})}_{(\mathrm{s})} = 2^{R_{\mathrm{th}}/(\bar{N}^{(\mathrm{IB})}_{(s),b})} - 1. \tag{4.39}$$

On the other hand, with the max-RSP scheme, the access rate can be defined as follows:

$$\hat{\mathcal{R}}^{(\mathrm{IB})}_{(\mathrm{s}),\mathrm{a}} = \hat{N}^{(\mathrm{IB})}_{(\mathrm{s}),\mathrm{a}} \log_2 \left(1 + \frac{P_s \; r^{-\beta_i}_{u} \; \zeta_u}{P_m \; d^{-\beta_o}_{(s)} \; \zeta_s + \sigma^2}\right), \tag{4.40}$$

where $d_{(s)}$ is the distance between the WBH and the user being served by the s ranked SBS. Similarly, with the min-RSP scheme, the access rate ($\bar{\mathcal{R}}^{(\mathrm{IB})}_{(\mathrm{s}),\mathrm{a}}$) for the s^{th} ranked SBS is given by replacing $\hat{N}^{(\mathrm{IB})}_{(\mathrm{s}),\mathrm{a}}$ with $\bar{N}^{(\mathrm{IB})}_{(\mathrm{s}),\mathrm{a}}$ in (4.40).

Note: Since in IBFD backhauling, $\hat{N}^{(\mathrm{IB})}_{(\mathrm{s}),\mathrm{a}} = \hat{N}^{(\mathrm{IB})}_{(\mathrm{s}),\mathrm{b}}$, the desired SINR threshold is the same for both the access and backhaul links, i.e., $\hat{\eta}^{(\mathrm{IB})}_{(\mathrm{s})}$ for max-RSP and $\bar{\eta}^{(\mathrm{IB})}_{(\mathrm{s})}$ for min-RSP.

a) **Rate Coverage for Transmission in Access Link:** With the max-RSP scheme, the rate coverage probability for the access link of s ranked SBS can be derived as follows:

$$\begin{aligned}\hat{\mathcal{C}}^{(\mathrm{IB})}_{(\mathrm{s}),\mathrm{a}} &= \mathbb{P}\left(\frac{P_s\ r_u^{-\beta_i}\ \zeta_u}{P_m\ d_{(s)}^{-\beta_o}\zeta_s + \sigma^2} > \hat{\eta}^{(\mathrm{IB})}_{(\mathrm{s})}\right) = \mathbb{P}\left(P_s\ r_u^{-\beta_i}\ \zeta_u > \hat{\eta}^{(\mathrm{IB})}_{(\mathrm{s})}\left(P_m d_{(s)}^{-\beta_o}\zeta_s + \sigma^2\right)\right), \\ &= 1 - \mathbb{P}\left(Y_{(\mathrm{s}),\mathrm{a}} \leq \hat{\eta}^{(\mathrm{IB})}_{(\mathrm{s})}\left(I_{(s)} + \sigma^2\right)\right), \\ &= 1 - \mathrm{F}_{\mathrm{Y}_{(\mathrm{s}),\mathrm{a}}}\left(\hat{\eta}^{(\mathrm{IB})}_{(\mathrm{s})}\left(I_{(s)} + \sigma^2\right)\right), \\ &= 1 - \int_0^\infty \mathrm{F}_{\mathrm{Y}_{(\mathrm{s}),\mathrm{a}}}\left(\hat{\eta}^{(\mathrm{IB})}_{(\mathrm{s})}\left(I_{(s)} + \sigma^2\right)\right) f_{I_{(s)}}(I)dI, \end{aligned} \tag{4.41}$$

where $\mathrm{F}_{\mathrm{Y}_{(\mathrm{s}),\mathrm{a}}}\left(\hat{\eta}^{(\mathrm{IB})}_{(\mathrm{s})}\left(I_{(s)} + \sigma^2\right)\right)$ can be obtained by putting $K = \frac{R_s^{\beta_i}\hat{\eta}^{(\mathrm{IB})}_{(\mathrm{s})}\left(I_{(s)}+\sigma^2\right)}{P_s\Theta_{\zeta_u}}$ in (4.34). Since the distance between a small cell user and its SBS is very small, $d_{(s)}$ can be approximated by the distance between s ranked SBS and WBH ($r_{(s)}$), i.e., $d_{(s)} \approx r_{(s)}$. The PDF of exact interference, i.e., $f_{I(s)}(I)$ can be derived as given in [31, eq. 40]. However, keeping in view the complicated expression in [31], I approximate the interference received at small cell user of s ranked SBS from WBH. The approximated interference distribution can thus be given as:

$$f_{I_{(s)}}(I) \approx \sum_{n=0}^{S-s} \frac{A(n)\Gamma_l\left(\kappa_{\zeta_s} - \frac{2(n-S)}{\beta_o}, BI\right)}{I^{1-\frac{2(n-S)}{\beta_o}}}, \tag{4.42}$$

where $B = \frac{R_m^{\beta_o}}{P_m \Theta_{\zeta_s}}$ and $A(n) = \frac{2S!(-1)^{S-s+n} B^{\frac{2(n-S)}{\beta_o}}}{(s-1)!(S-s-n)!n!\Gamma(\kappa_{\zeta_s})\beta_o}$. Thus (4.41) can be evaluated by using standard mathematical software such as Matlab and Mathematica.

b) **Rate Coverage for Transmission in Backhaul Link:**

With the max-RSP scheme, the backhaul coverage probability for s ranked SBS can be derived as:

$$\begin{aligned}\hat{\mathcal{C}}_{(\mathrm{s}),\mathrm{b}}^{(\mathrm{IB})} &= \mathbb{P}\left(\frac{P_m\ r_{(s)}^{-\beta_o}\ \chi_s}{\mathrm{R_{SI}} + \sigma^2} > \hat{\eta}_{(\mathrm{s}),\mathrm{b}}^{(\mathrm{IB})}\right), \\ &= 1 - \mathbb{P}\left(Y_{(\mathrm{s}),\mathrm{b}}^{(\mathrm{IB})} \leq \hat{\eta}_{(\mathrm{s}),\mathrm{b}}^{(\mathrm{IB})}\left(\mathrm{R_{SI}} + \sigma^2\right)\right), \\ &= 1 - \mathrm{F}_{\mathrm{Y}_{(\mathrm{s}),\mathrm{b}}}\left(\hat{\eta}_{(\mathrm{s}),\mathrm{b}}^{(\mathrm{IB})}\left(\mathrm{R_{SI}} + \sigma^2\right)\right), \end{aligned} \tag{4.43}$$

where $\mathrm{F}_{\mathrm{Y}_{(\mathrm{s}),\mathrm{b}}}\left(\hat{\eta}_{(\mathrm{s}),\mathrm{b}}^{(\mathrm{IB})}\left(\mathrm{R_{SI}} + \sigma^2\right)\right)$ can be obtained by replacing $Y_{(\mathrm{s}),\mathrm{b}}$ with $\hat{\eta}_{(\mathrm{s}),\mathrm{b}}^{(\mathrm{IB})}\left(\mathrm{R_{SI}} + \sigma^2\right)$ in (5.14).

c) **Overall Rate Coverage and Achievable Downlink Transmission Rate:**

With the max-RSP scheme, the overall rate coverage probability $\hat{\mathcal{C}}_{(\mathrm{s})}^{(\mathrm{IB})}$ for a given SBS at rank s can be given as: $\hat{\mathcal{C}}_{(\mathrm{s})}^{(\mathrm{IB})} = \hat{\mathcal{C}}_{(\mathrm{s}),\mathrm{b}}^{(\mathrm{IB})} \times \hat{\mathcal{C}}_{(\mathrm{s}),\mathrm{a}}^{(\mathrm{IB})}$, where $\hat{\mathcal{C}}_{(\mathrm{s}),\mathrm{b}}^{(\mathrm{IB})}$ and $\hat{\mathcal{C}}_{(\mathrm{s}),\mathrm{a}}^{(\mathrm{IB})}$ are given in (4.43) and (4.41), respectively. Accordingly, the achievable downlink transmission rate for a user served by the ranked SBS s is given as $\hat{\mathcal{C}}_{(s)}^{(\mathrm{IB})} \times \mathrm{R_{th}}$. Therefore, with the max-RSP scheme, the total achievable transmission rate in all the small cells (i.e., network rate) can be determined as $\hat{\mathcal{R}}^{(\mathrm{IB})} = \sum_{s=1}^{S} \hat{\mathcal{C}}_{(s)}^{(\mathrm{IB})} \times \mathrm{R_{th}}$.

Remark: With the min-RSP scheme, the backhaul rate coverage probability ($\bar{\mathcal{C}}_{(\mathrm{s}),\mathrm{b}}^{\mathrm{IB}}$) and access rate coverage probability ($\bar{\mathcal{C}}_{(\mathrm{s}),\mathrm{a}}^{\mathrm{IB}}$) for a given SBS at rank s can be

determined, respectively, by replacing $\hat{\eta}_{(\mathrm{s})}^{(\mathrm{IB})}$ with $\bar{\eta}_{(\mathrm{s})}^{(\mathrm{IB})}$ in (4.43) and (4.41). Subsequently, the overall rate coverage probability for the ranked SBS s can be obtained as $\bar{\mathcal{C}}_{(\mathrm{s})}^{\mathrm{IB}} = \bar{\mathcal{C}}_{(\mathrm{s}),\mathrm{b}}^{\mathrm{IB}} \times \bar{\mathcal{C}}_{(\mathrm{s}),\mathrm{a}}^{\mathrm{IB}}$. Accordingly, the achievable downlink rate for small cell users served by SBS s is given as $\bar{\mathcal{R}}^{\mathrm{IB}} = \bar{\mathcal{C}}_{(s)}^{(\mathrm{IB})} \times \mathrm{R}_{\mathrm{th}}$.

4.7 Numerical Results and Discussion

This section provides a comparative analysis of IBFD backhauling, OBFD backhauling, and hybrid IBFD/OBFD backhauling using the derived spectrum allocation solutions. CVX is used to validate the accuracy of the derived optimal solutions in Section IV. Insights are extracted related to the optimal backhaul and access spectrum allocation in a variety of system scenarios. Further, this section quantitatively analyzes the performance of distributed min-RSP and max-RSP schemes in both IBFD and OBFD backhauling scenarios and compares them to the centralized IBFD and OBFD backhauling solutions. Finally, the numerical results verify the accuracy of the derived rate coverage expressions and the minimum achievable average rate per SBS via Monte-Carlo simulations.

I assume number of SBSs $S = 6$, number of total available channels $N = 20$, $f_{\chi_s}(\chi_s) = \mathrm{Gamma}\,(0.5, 3.8)$, $f_{\zeta_s}(\zeta_s) = \mathrm{Gamma}\,(2, 1)$, and $f_{\zeta_u}(\zeta_u) = \mathrm{Gamma}\,(2, 1)$. The coverage radii of the WBH and SBSs are $R_m = 300$ m and $R_s = 30$ m, respectively. I set the indoor path-loss exponent within small cells $\beta_i = 2.1$, outdoor path-loss exponent $\beta_o = 3.9$, and the thermal noise power density $\sigma^2 = 1 \times 10^{-15}$ W/Hz. The transmit powers of the WBH and SBSs are set as $P_m = 1$ W and $P_s = 0.1$ W, respectively, per channel. The SI cancellation value is set to $C_{\mathrm{SI}} = 130$ dB [65]. The values of the aforementioned parameters remain the same unless stated otherwise.

4.7.1 Optimized Spectrum Allocation - Centralized Solution

Spectrum Allocation for SBSs: Fig. 4.3 shows the impacts of different backhauling schemes (i.e., OBFD, IBFD, and hybrid OBFD/IBFD backhauling) on the access and backhaul spectrum allocation to SBSs (ranked based on their distances from WBH). The channels allocated to a ranked SBS can be obtained by multiplying the proportion of channels with total available channels, i.e., $N = 20$. For example, in Fig. 3(a), the proportion of channels allocated to 6^{th} ranked SBS using IBFD backhauling is 0.2. Thus the number of channels allocated to this SBS can be calculated as $0.2 \times 20 = 4$ channels. In case the product is not an integer, I take the rounded value.

With OBFD backhauling, since the backhaul spectrum is allocated to a given SBS based on its distance from the WBH, which can be significantly larger compared to access link distances, a large proportion of available spectrum is allocated for backhaul transmissions. The larger the distance from the WBH, the higher would be the required backhaul spectrum (in order to overcome their weak backhaul signal). On the other hand, for access link transmissions, optimal spectrum to all SBSs is similar. This is justified since the average received signal power in the access link is nearly the same for all SBSs irrespective of their ranking from the WBH.

With IBFD backhauling, the access spectrum is the same as backhaul spectrum and the portion of access/backhaul spectrum slightly increases with the increasing distances of SBSs from the WBH. Finally, hybrid OBFD/IBFD backhauling favors IBFD backhauling for reduced SI (e.g., for $C_{\mathrm{SI}} = 120$ dB) and OBFD backhauling for higher SI (e.g., for $C_{\mathrm{SI}} = 110$ dB). Also, if SI is relatively low (e.g., $C_{\mathrm{SI}} = 120$dB), the hybrid scheme allocates a large portion of available spectrum to the access links of nearby SBSs to compensate the impact of backhaul interference at the access links

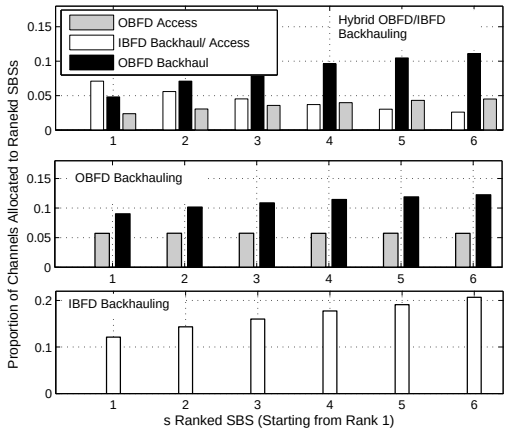

(a) $C_{\mathrm{SI}} = 110$ dB

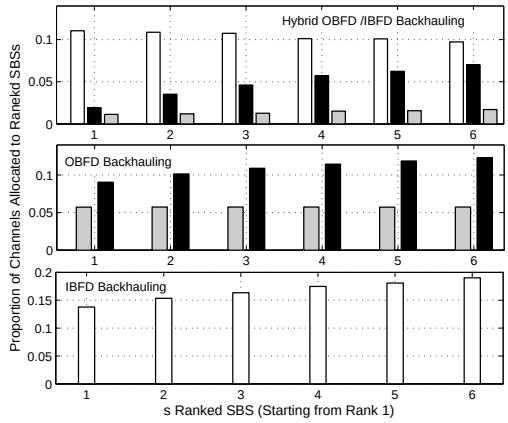

(b) Perfect $C_{\mathrm{SI}} = 120$ dB

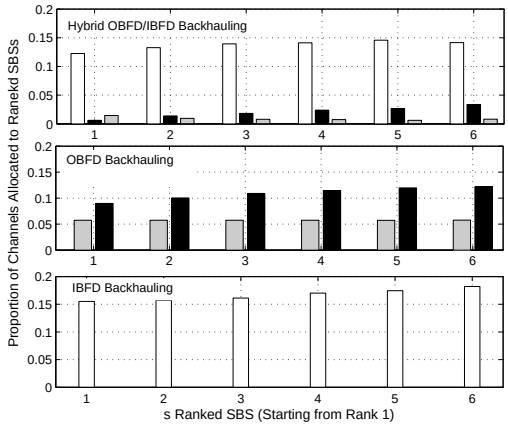

(c) Perfect $C_{\mathrm{SI}} = 130$ dB

Figure 4.3: Access and backhaul spectrum allocation to SBSs ranked according to their distance from the WBH.

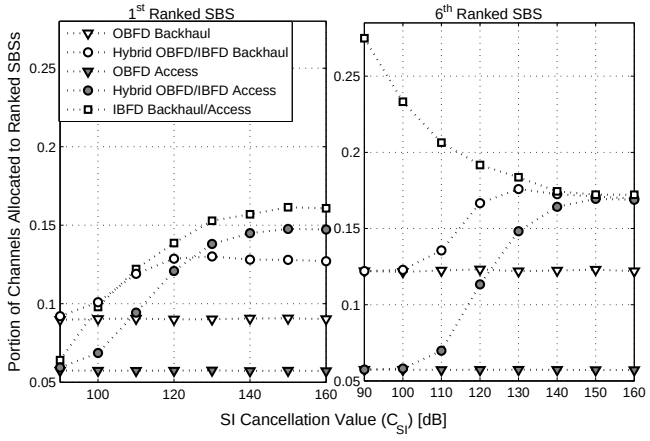

Figure 4.4: Spectrum allocation to the cell-center SBS (1^{st} ranked) and cell-edge SBS (6^{th} ranked) as a function of C_{SI} considering OBFD backhauling, IBFD backhauling, and hybrid OBFD/IBFD backhauling. The portion of spectrum for hybrid backhaul (hybrid access) is obtained by summing up the portions of spectrum for IBFD and OBFD backhaul (IBFD and OBFD access).

and thus allows to improve the access rate along with the backhaul rate. However, if SI is high, overcoming backhaul interference may not be useful due to the backhaul rate limitation. As such, in this case, nearly the same spectrum is assigned to all SBSs.

Spectrum Allocation for the Nearest and Farthest SBS as a function of C_{SI}***:*** Fig. 4.4 shows the impact of SI cancellation value on the backhaul and access spectrum of ranked SBSs. To gain insights, I consider two extremes, i.e., closest SBS (1^{st} ranked) and farthest SBS (6^{th} ranked). It can be seen that OBFD backhauling is independent of C_{SI}; however, the amount of backhaul spectrum required for the farthest SBS is higher (compared to cell-center SBS) due to its weak backhaul signal strength. The access spectrum however remains the same.

With IBFD backhauling, the required spectrum (backhaul/access spectrum) for the closest and farthest SBSs shows the opposite trend. That is, contrary to the farthest SBS, spectrum requirement of the closest SBS increases with increasing SI

cancellation. The reason is that the closer SBS is limited by backhaul interference (which limits the access rate). Therefore, as SI reduces, the backhaul rate starts to improve. Now in order to improve user rate, access rate needs to be improved as well which requires more access spectrum. On the other hand, the user rate in the farthest SBS is limited by the SI. That is, the user rate is limited by the backhaul rate. Therefore, as SI reduces, a higher backhaul rate can be attained with reduced backhaul spectrum.

With hybrid IBFD/OBFD backhauling, an increase in C_{SI} (i.e., reduction in SI) increases the access/backhaul spectrum which leads to a higher achievable rate R_{th}^{*}, as will be shown in Fig. 4.5. The spectrum requirement for hybrid backhauling follows that for IBFD backhauling when C_{SI} is high and that for OBFD backhauling when C_{SI} is low. Further, it is observed that for the farthest SBS (for which the backhaul rate is limited), the backhaul spectrum requirement is always higher than the access spectrum. Conversely, for the closest SBS, if I keep reducing SI, there is a point after which the the SBS becomes access rate limited. Then the access spectrum requirement exceeds the backhaul spectrum requirement. *Since the backhaul interference affects more the access links of SBSs, which are closer to the WBH, and SI affects more the backhaul links of farther SBSs, the optimal spectrum allocation rules can significantly vary for different SBSs.*

4.7.2 Optimum Achievable Downlink Rate - Centralized Solution

Impact of SI Cancellation Value: Fig. 4.5 shows the impact of SI cancellation value (C_{SI}) on the optimized achievable downlink rate (R_{th}^{*}) for a small cell user considering OBFD, IBFD, and hybrid OBFD/IBFD backhauling. Since there is no SI in the OBFD mode, R_{th}^{*} is independent of the C_{SI} value. With IBFD backhauling,

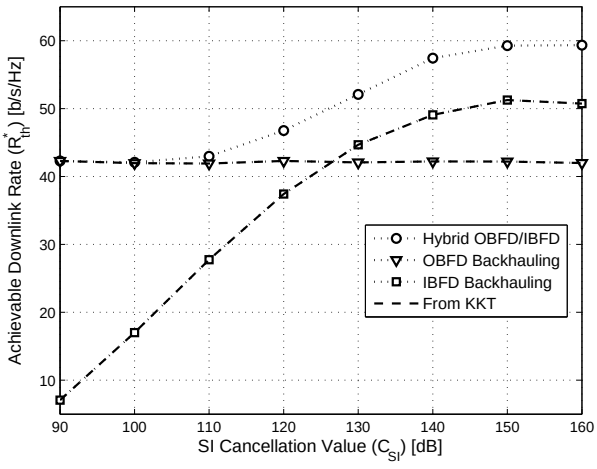

Figure 4.5: Optimized achievable downlink rate (R_{th}) in a small cell as a function of the self-interference cancellation value C_{SI} in OBFD, IBFD, and hybrid OBFD/IBFD backhauling.

as expected, R^*_{th} increases significantly with increasing C_{SI}. This is due to the reduction of SI which increases the rate at the backhaul link. However, after a certain limit, R^*_{th} will not increase any further even with increasing C_{SI}. This is the point beyond which the backhaul rate gets saturated and the achievable rate depends on the access link rate. It can be clearly observed that the benefits of IBFD over OBFD backhauling are evident only after a certain amount of SI cancellation. Finally, the hybrid IBFD/OBFD backhauling exploits the benefits of both the OBFD and IBFD backhauling in low and high SI cancellation scenarios, respectively.

Impact of Transmit Power of SBS: Fig. 4.6 illustrates the effect of increasing transmit power of SBSs P_s on (R^*_{th}) considering C_{SI} = 125 dB and C_{SI} = 130 dB. With OBFD backhauling, R^*_{th} increases slightly with P_s due to the improved access link rate; whereas, with IBFD backhauling, an interesting trade-off can be seen at C_{SI} = 130 dB. Increasing P_s first improves R^*_{th} due to higher signal power in the access link transmission. However, after a certain limit, R^*_{th} starts degrading due to higher

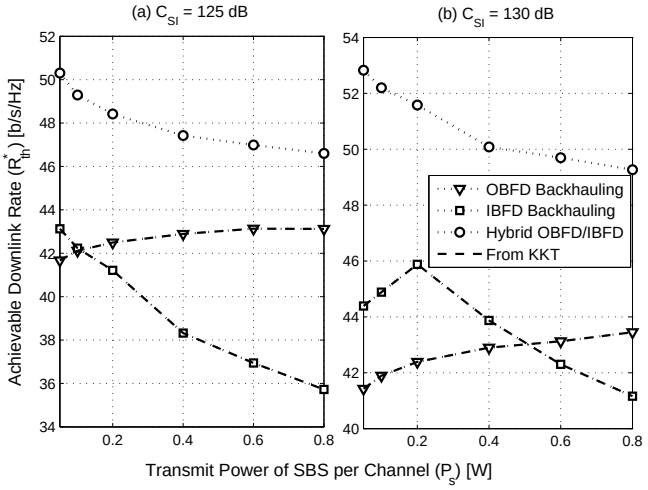

Figure 4.6: Optimized achievable downlink rate (R_{th}) of a small cell user as a function of the transmit power of SBS per channel P_s in OBFD, IBFD, and hybrid OBFD/IBFD backhauling by setting (a) $C_{\text{SI}} = 125$ dB, and (b) $C_{\text{SI}} = 130$ dB.

SI caused to the backhaul link transmission. It is also important to note that this trade-off is prominent only for relatively higher values of SI cancellation (e.g., $C_{\text{SI}} = 130$ dB) and disappears completely for relatively low levels of SI cancellation (e.g., $C_{\text{SI}} = 125$ dB) as shown in Fig. 4.5. The reason is that the backhaul rate degradation is more dominant for low values of C_{SI}; therefore performance gains at the access link do not affect the achievable downlink rate.

Further, it can be noted that IBFD outperforms OBFD typically for small values of P_s; however, the higher the SI cancellation, the range of P_s (at which IBFD outperforms OBFD) extends. Finally, Fig. 4.6 shows that hybrid OBFD/IBFD backhauling outperforms both the OBFD and IBFD backhauling due to the flexibility of mode selection and its respective spectrum allocation. Nonetheless, the performance of hybrid OBFD/IBFD backhauling follows the trend of IBFD backhauling, which is expected at high SI cancellation values (or low SI values).

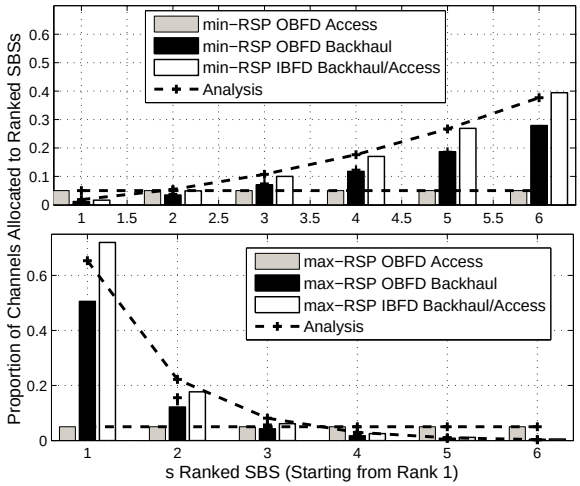

Figure 4.7: Portion of spectrum for OBFD and IBFD backhauling with max-RSP and min-RSP schemes by setting $N_b = 14$ channels

4.7.3 Spectrum Allocation - Distributed Solution

Fig. 4.7 shows the portions of spectrum allocated for OBFD and IBFD backhauling with max-RSP and min-RSP schemes. The portions of backhaul spectrum allocated for OBFD backhauling are determined as $(\hat{p} \times N_b)/N$ and $(\bar{p} \times N_b)/N$, respectively. For IBFD backhauling, the portions are given by $(\hat{p} \times N)/N = \hat{p}$ and $(\bar{p} \times N)/N = \bar{p}$, respectively. With the max-RSP scheme, for both OBFD and IBFD backhauling, the backhaul spectrum is high for cell-center SBSs. With the min-RSP scheme, the backhaul spectrum is high for cell-edge SBSs. With OBFD backhauling the access channel allocation probability is identical for all SBSs irrespective of min-RSP and max-RSP schemes. This is due to the equal distribution of fixed access spectrum among all SBSs. However, the probability of allocation of access channel depends on the amount of available access spectrum. For instance, in this figure, I have $N_a = 6$ channels, so each SBS will receive one channel, which is 0.05% of the total spectrum.

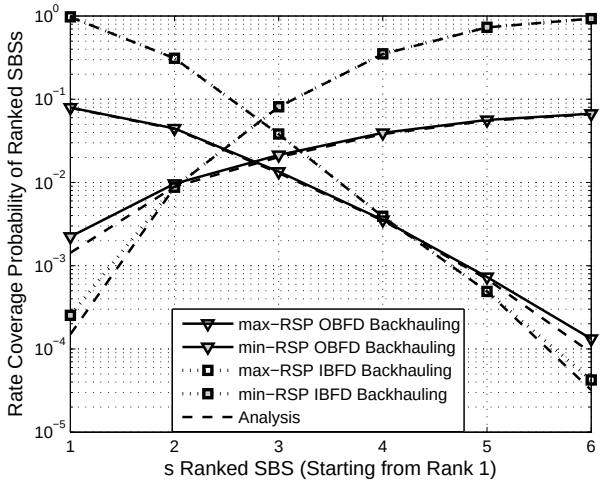

Figure 4.8: Rate coverage probability of ranked SBSs considering OBFD backhauling and IBFD backhauling for max-RSP and min-RSP schemes ($N_b = 14$ channels).

4.7.4 Rate Coverage Probability - Distributed Solution

Fig. 4.8 shows the effect of max-RSP and min-RSP schemes on the rate coverage probability of ranked SBSs considering OBFD backhauling and IBFD backhauling. With max-RSP scheme, the rate coverage probability decreases as the distance of an SBS increases from WBH regardless of OBFD or IBFD backhauling mode. This happens due to the decrease in backhaul spectrum with the increase in distance from WBH. On the other hand, the rate coverage probability increases as the distance of an SBS increases from WBH due to the same reason as mentioned above. The rate coverage probability of cell-center SBSs with IBFD backhauling is significantly higher compared to OBFD backhauling. In general, the rate coverage of IBFD backhauling outperforms the rate coverage of OBFD backhauling due to higher spectral reuse.

Fig. 4.9 compares the average minimum rate of a ranked SBS obtained using distributed schemes such as max-RSP scheme and min-RSP scheme with the average optimal minimum rate obtained from optimization problems (**P2**) and (**P3**) for IBFD and OBFD backhauling, respectively. For distributed schemes, the average minimum

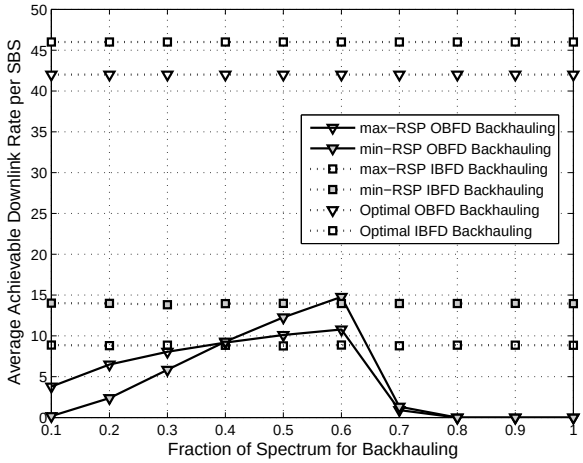

Figure 4.9: Average minimum rate per ranked SBS as a function of fraction of backhaul spectrum considering both OBFD backhauling and IBFD backhauling for max-RSP and min-RSP schemes, respectively, by setting: R^*_{th} for OBFD backhauling = 42, R^*_{th} for IBFD backhauling = 46 taken from Fig. 5.

rate per ranked SBS is calculated by dividing the minimum network rate with the available number of SBSs. As the fraction of backhaul spectrum increases, average rate with max-RSP scheme and min-RSP scheme considering OBFD backhauling also increases due to the increase in backhaul rate. However, after a certain point, the average rate starts to decrease and becomes zero. This decrease is due to the decrease in access spectrum. It can be noted that min-RSP with IBFD backhauling performs better compared to other distributed schemes. Optimal rate with OBFD backhauling and IBFD backhauling outperforms the rate achieved with distributed schemes.

4.7.5 Extensions to Spectrum Sharing Scenarios

To mitigate intra-cell interference, orthogonal channel allocation is being considered in emerging wireless cellular standards such as Long Term Evolution (LTE) [89]. For instance, in OFDMA networks, orthogonal channels are allocated among multiple users in a cell to avoid intra-cell interference. Following the same motivation, I con-

sider orthogonal backhaul channel allocation among SBSs that are located with in a cell. With the IBFD backhauling mode, since the same spectrum band is used for both backhaul and access links, orthogonal channels in the backhaul links imply orthogonal channels in the access links of SBSs. However, in the case of OBFD backhauling, spectrum sharing can be exploited in the access links. Let the proportion of backhaul/access spectrum allocated to SBSs for IBFD backhauling is $\alpha = [\alpha_1, \alpha_2, \cdots, \alpha_S]$ and the proportion of backhaul spectrum allocated to SBSs for OBFD backhauling is $\varphi = [\varphi_1, \varphi_2, \cdots, \varphi_S]$. For the OBFD mode, the spectrum allocated to SBSs for transmissions in the access links is shared and the proportion can be given by $1 - \sum_{s=1}^{S}(\alpha_s + \varphi_s)$. The optimization problem **P1** can then be formulated as follows:

$$
\begin{aligned}
\textbf{(P1)} \quad & \text{maximize} \quad \mathrm{R_{th}} \\
& \text{subject to} \\
& C_1 : \alpha_s N \log_2\left(1 + \mathrm{V}_{\mathrm{s,b}}^{(\mathrm{IB})}\right) + \varphi_s N \log_2\left(1 + \mathrm{V}_{\mathrm{s,b}}^{(\mathrm{OB})}\right) \geq \mathrm{R_{th}}, \quad \forall\, s, \\
& C_2 : \alpha_s N \log_2\left(1 + \mathrm{V}_{\mathrm{s,a}}^{(\mathrm{IB})}\right) + \left(1 - \sum_{s=1}^{S}(\alpha_s + \varphi_s)\right) N \log_2\left(1 + \mathrm{V}_{\mathrm{s,a}}^{(\mathrm{OB})}\right) \geq \mathrm{R_{th}}, \quad \forall\, s, \\
& C_3 : \alpha_s > 0, \varphi_s > 0, \ \ \forall s,
\end{aligned}
\tag{4.44}
$$

where $\mathrm{V}_{\mathrm{s,a}}^{(\mathrm{OB})} = \frac{Y_{\mathrm{s,a}}}{I_u + \sigma^2} = \frac{P_s\ r_u^{-\beta_i}\ \zeta_u}{\sum_{s'=1, s' \neq s}^{S} P_{s'}\ r_{s',u}^{-\beta_o}\ \zeta_{s',u} + \sigma^2}$, $P_{s'}$ represents the transmit power of interfering SBS s', $r_{s',u}$ represents the distance between the small cell user being served in SBS s and the interfering SBS s', $\zeta_{s',u}$ represents channel power gain due to shadowing in the link between the small cell user in SBS s and the interfering SBS s', and I_u denotes the interference at the user being served in SBS s from all other SBSs s'. The constraints C_1 and C_2 ensure that, for each SBS, the achievable rates at the backhaul and access links are greater than $\mathrm{R_{th}}$. The constraints C_3 defines the non-negativity conditions of α_s and φ_s. This problem can be solved optimally by

using the bisection approach as described Section III.

The rate coverage analysis for OBFD backhauling can be performed as follows:

- number of available access channels per SBS as $N - N_b$ instead of $\frac{N-N_b}{S}$
- deriving the characteristic function (CF) of the interference experienced at a small cell user from other OBFD backhauled SBSs. The CF $\phi_{Y_{(\mathrm{s}),\mathrm{a}}}(\omega)$ of the received signal power at the small cell user can be derived as given in [88, Eq. 27] by replacing $t = -i\omega$. Similarly, the CF $\phi_{I_u}(\omega)$ of the interference at the small cell user can be derived as given in [31, Eq. 20] by replacing $t = i\omega$.
- rate coverage probability at the access link of s ranked SBS can be given using Gil-Pelaez theorem as

$$\begin{aligned}\mathcal{C}_{(s),a}^{(\mathrm{OB})} &= \mathbb{P}\left(\mathrm{V}_{\mathrm{s,a}}^{(\mathrm{OB})} > \eta_{(\mathrm{s}),\mathrm{a}}^{(\mathrm{OB})}\right) = \mathbb{P}\left(\frac{P_s\, r_u^{-\beta_i}\, \zeta_u}{I_u + \sigma^2} > \eta_{(\mathrm{s}),\mathrm{a}}^{(\mathrm{OB})}\right), \\ &= \frac{1}{2} + \frac{1}{\pi}\int_0^\infty \mathrm{Im}\left(e^{-\epsilon_a \sigma^2}\phi_{Y_{(\mathrm{s}),\mathrm{a}}}(\omega)\phi_{I_u}(\omega)\right)\frac{d\omega}{\omega}, \end{aligned} \tag{4.45}$$

where $\epsilon_a = i\ \eta_{(\mathrm{s}),\mathrm{a}}^{(\mathrm{OB})}\ \omega$, and $\eta_{(\mathrm{s}),\mathrm{a}}^{(\mathrm{OB})} = 2^{\frac{R_{th}}{N_{(s),a}^{(\mathrm{OB})}}} - 1$. $N_{(s),a}^{(\mathrm{OB})}$ denotes the number of channels for shared access transmissions and can be obtained as $N_{(s),a}^{(\mathrm{OB})} = N - N_{(s),b}^{(\mathrm{OB})}$. Multiplying (4.45) with the backhaul rate coverage probability of s ranked SBS given in (35), $\hat{\mathcal{C}}_{(s)}^{(\mathrm{OB})}$ can be derived.

4.8 Chapter Summary

I have formulated and solved a minimum rate maximization problem for the full-duplex small cells with provisioning for wireless backhauling, i.e., OBFD backhauling, IBFD backhauling, and hybrid IBFD/OBFD backhauling. The optimal spectrum allocations for IBFD and OBFD backhauling have been calculated in closed-form using

KKT optimality conditions. The optimal solutions have been used as a guideline to develop two distributed max-RSP and min-RSP based backhaul channel allocation schemes. For the distributed schemes, I have theoretically derived the number of allocated backhaul channels, minimum rate coverage probability, and average downlink rate of each SBS given its distance from the centralized WBH for both IBFD and OBFD backhauling. Numerical results have revealed that the optimal spectrum allocation rules can significantly vary for OBFD and IBFD backhauling. OBFD backhauling favors more backhaul spectrum for SBSs located far-away from the WBH. With IBFD backhauling and increasing SI cancellation, the backhaul/access spectrum allocation for the SBSs located nearby and far-away from WBH increases and decreases, respectively. The benefits of IBFD over OBFD backhauling become evident only after a certain amount of SI cancellation. Further, the hybrid IBFD/OBFD backhauling exploits the benefits of both OBFD and IBFD backhauling in low and high SI cancellation scenarios, respectively. Finally, simulation results have shown the performance gap between the centralized optimal solution and the distributed solutions for spectrum allocation. The framework can be extended to optimize power allocations so that the performance gain of IBFD backhauling can be further enhanced. Also, the enhancements like a RAKE receiver may also be considered at the small cell user to further improve the system performance at the cost of receiver processing [90]. Deploying massive MIMO at the WBH and anchor BSs within the cellular region along with time-division duplexing are relevant extensions of this framework for massive wireless backhauling scenarios.

In this chapter, the problem of optimal access/backhaul spectrum allocation for SBSs considering both IBFD and OBFD backhauling has been investigated. It has been assumed that power per backhaul channel is fixed. In the next chapter, the

problem of optimal resource (access/backhaul spectrum as well as power) allocation for OBFD SBSs will be explored. Accordingly, I will formulate a problem to optimize the allocation of backhaul/access channel and the power per backhaul channel such that the minimum throughput (or common throughput) at each SBS can be guaranteed and maximized.

Chapter 5

Downlink Resource Allocation for Wireless Backhauling in Full-Duplex Small Cells

The anticipated massive deployment of the small cells entail wireless backhauling for 5G cellular networks. However, the scarcity of radio frequency (RF) spectrum in the licensed bands is a major limitation which necessitates efficient spectrum planning for backhaul/access links of 5G small cells. In this chapter I investigate the problem of channel assignment in the backhaul/access of small cells. I first formulate a problem to maximize the common achievable rate at the backhaul and access links of the small cells. Due to exponential time complexity of the problem, the original problem is transformed into a less complex convex programming problem and solved it numerically. Then, I propose and comparatively analyze the performance of two simple distributed backhaul channel allocation criteria, namely, maximum received signal power (max-RSP) and minimum received signal power (min-RSP) criteria. For these criteria, I theoretically derive the number of allocated backhaul channels and

coverage probability for a given target rate of each small cell given its distance from the centralized wireless backhaul hub. Simulation results provide insights about the performance gap between the centralized and distributed schemes. Further, it is observed that the min-RSP criterion outperforms the max-RSP criterion which implies that more backhaul channels should be allocated to small cells that are located near the cell-edge.

5.1 Introduction

5.1.1 Overview

Wireless backhauling has been emerging as a viable and cost-effective approach to handle the backhaul connectivity of large number of small cells in 5G cellular networks [4]. By definition, the small cell backhaul connections are used to (i) forward/receive the end-user (small cell user) data to/from the core network and (ii) exchange mutual information among different small cells over X2 interface [54]. In this chapter, I will be focusing on the small cell backhaul connections that are referred with respect to the core network. In such a case, system operators need to support the backhauls of several small cell base stations (SBSs) at the same time; thus, a pool of spectrum resources needs to be efficiently selected for backhaul transmissions.

5.1.2 Contribution

The contributions of this chapter can be summarized as follows.

- I consider the problem of downlink access/backhaul resource (channel and power) allocation for multiple small cells.

- I formulate a problem to maximize the common achievable rate at the access and backhaul links of all SBSs.

- Due to exponential time complexity of the problem, I approximate the nominal problem by relaxing few conditions and the resultant approximated problem becomes less complex convex programming problem which is solved numerically.

- I then propose and comparatively analyze the performance of two simple and distributed backhaul channel allocation criteria, namely, maximum received signal power (max-RSP) and minimum received signal power (min-RSP) criteria.

- For max-RSP and min-RSP criteria, I theoretically derive the number of allocated backhaul channels and target rate coverage probability of each SBS given its distance from the wireless backhaul hub (WBH).

5.2 Related Work

Recently backhaul/access spectrum optimization has been dealt with in a variety of research studies [69–71]. In [70], a weighted sum-rate (WSR) maximization problem is formulated to optimize the subchannel and power allocation as well as the transmission time for the access and backhaul transmissions in a time-division duplex (TDD)-based system. By small cell grouping and resource slicing, a sub-optimal rate balancing algorithm is proposed. In [71], a collaborative filtering (CF) scheme is proposed that enables each SBS to estimate the probability of its cached files being requested and in turn its backhaul usage. The bandwidth allocation is updated based on the estimated backhaul usage. Given the available bandwidth, using matching theory, a cache-aware user association scheme is proposed that minimizes the backhaul usage at each SBS.

Another interesting study is [69] where backhaul resource allocation is investigated in hybrid mm-wave and sub-6 GHz bands. The problem is formulated as a one-to-many matching game and considers both the wireless channel characteristics and economic factors within the resource allocation problem. A distributed algorithm is proposed to find a two-sided stable solution that guarantees the quality of service (QoS) at the backhaul links of SBSs. Two in-band backhaul bandwidth allocation schemes, namely, unified bandwidth allocation and per-SBS bandwidth allocation schemes, are investigated in [91], considering SBSs with massive antenna arrays.

In summary, the proposed algorithms to date are expensive from time/computational perspective, requires significant signaling information, and are suboptimal with no comparisons to appropriate benchmarking schemes. Also, it is difficult to gain general design insights from these algorithms.

5.3 System Model and Assumptions

I consider a circular macrocell of coverage radius R_m overlaid with S randomly deployed SBSs with coverage radius $R_s, \forall s = \{1, 2, \cdots, S\}$. All SBSs operate in the closed-access mode and are connected to the core network through a WBH. The WBH is typically situated at a fiber point-of-presence or where high-capacity line-of-sight (LOS) microwave link is available. An existing MBS, which is connected to the core network by fiber-to-the-cell (FTTC) links, can be an example of such a WBH. I assume that the WBH, SBSs, and small cell users are equipped with single antenna.

The spectrum is composed of $N = N_a + N_b$ frequency channels of which N_a and N_b channels are allocated for access and backhaul link transmissions, respectively. SBSs conduct access and backhaul link transmissions concurrently at orthogonal channels. α represents the spectrum partitioning factor. For a given α, the number of channels

for backhaul link and access link transmissions can be determined as $N_b = \alpha \times N$, and $N_a = (1 - \alpha) \times N$, respectively. WBH allocates orthogonal channels to SBSs for backhauling and more than one channels can be allocated to a given SBS. Each SBS serves single user and chooses any of the N_a available access channels for downlink transmission. The same channel can be shared by multiple SBSs that may lead to co-channel interference on the access link. The maximum allowable transmit power of WBH is P_m over all backhaul channels and the minimum target throughput for each SBS at backhaul and access links is denoted by R_{th}.

The received signal power at the SBS from WBH on a given backhaul channel is defined as:

$$\gamma_{s,b} = p_{s,b}\ r_s^{-\beta_o}\ \chi_s, \tag{5.1}$$

where $p_{s,b}$ is the transmit power of WBH for the SBS s on a given backhaul channel, r_s is the distance between WBH and s^{th} SBS, β_o is the outdoor path-loss exponent, and χ_s is the fading gain at the backhaul link. Similarly, the received signal power at a given small cell user is given as:

$$\gamma_{s,a} = P_s\ r_u^{-\beta_i}\ \zeta_u, \tag{5.2}$$

where P_s is the transmit power of SBS s, r_u is the distance between SBS s and its user, β_i is the indoor pathloss exponent, ζ_u is the Gamma-distributed fading gain at the access link.

The received interference power at any small cell user in SBS s is given as:

$$I_u = \sum_{s'=1, s \neq s'}^{\bar{S}} P_{s'}\ d_{s'}^{-\beta_o}\ \bar{\zeta}_{s'}, \tag{5.3}$$

where $d_{s'}$ is the distance between a user in SBS s and an interfering SBS s', $\bar{S}$ is the number of interfering SBSs , $\bar{\zeta}_{s'}$ is the Gamma-distributed fading at interfering links.

5.4 Maximization of Common Achievable Rate per SBS: Centralized Approach

The main objective of subchannel/power allocation problem is to optimize the allocation of backhaul/access channel and the power per backhaul channel such that the minimum throughput (or common throughput) at each SBS can be guaranteed and maximized. The channel allocation indicator for backhaul and access links are binary decision variables $x_{s,a}^{(j)}, x_{s,b}^{(j)} \in \{0,1\}$, where

$$x_{s,a}^{(j)} = \begin{cases} 1, & \text{if } j^{th} \text{ channel is allocated to the access link of SBS } s \\ 0, & \text{otherwise.} \end{cases}$$
$$x_{s,b}^{(j)} = \begin{cases} 1, & \text{if } j^{th} \text{ channel is allocated to the backhaul link of SBS } s \\ 0, & \text{otherwise.} \end{cases} \tag{5.4}$$

The objective of the considered resource allocation problem is to obtain the power allocation for backhaul channels and channel allocation matrices for access and backhaul links, respectively, such that R_{th} is maximized. The channel and power allocation matrices are represented as follows:

$$\mathbf{X}_{s,(\cdot)} = \begin{bmatrix} x_{s,(\cdot)}^{(1)} & ... & x_{s,(\cdot)}^{(N)} \\ . & ... & . \\ . & ... & . \\ . & ... & . \\ x_{S,(\cdot)}^{(1)} & ... & x_{S,(\cdot)}^{(N)} \end{bmatrix}, \mathbf{P}_{s,b} = \begin{bmatrix} p_{s,b}^{(1)} & ... & p_{s,b}^{(N)} \\ . & ... & . \\ . & ... & . \\ . & ... & . \\ p_{S,b}^{(1)} & ... & p_{S,b}^{(N)} \end{bmatrix},$$

where $(\cdot) = a$ for access and $(\cdot) = b$ for backhaul link.

The optimization problem can be formulated as follows:

$$
\begin{aligned}
\textbf{(P1)} \quad & \underset{R_{th},\ x_{s,a}^{(j)},\ x_{s,b}^{(j)}, p_{s,b}^{(j)}}{\text{maximize}} \quad R_{\text{th}} \\
& \text{subject to} \\
& C_1: \sum_{j\in N} x_{s,a}^{(j)} \log_2\left(1+\text{SINR}_{s,a}^{(j)}\right) \geq R_{\text{th}}, \quad \forall\, s, \\
& C_2: \sum_{j\in N} x_{s,b}^{(j)} \log_2\left(1+\text{SNR}_{s,b}^{(j)}\right) \geq R_{\text{th}}, \quad \forall\, s, \\
& C_3: \sum_{s\in S} x_{s,b}^{(j)} \leq 1, \quad \forall\, j, \\
& C_4: \sum_{s\in S} x_{s,a}^{(j)} \geq 0, \quad \forall\, j, \\
& C_5: \sum_{j\in N} x_{s,a}^{(j)} \leq 1, \quad \forall\, s, \\
& C_6: x_{s,a}^{(j)} + \sum_{s\in S} x_{s,b}^{(j)} \leq 1, \quad \forall\, j, s, \\
& C_7: \sum_{j\in N} x_{s,a}^{(j)} \leq x_{s,b}^{(j)}, \quad \forall\, j, s, \\
& C_8: \sum_{s\in S}\sum_{j\in N} x_{s,b}^{(j)} p_{s,b}^{(j)} \leq P_m, \\
& C_9: \ x_{s,a}^{(j)}, x_{s,b}^{(j)} \in \{0,1\}, \quad \forall\, j, s, \\
& C_{10}: p_{s,b}^{(j)} \geq 0, \quad \forall\, j,
\end{aligned}
\tag{5.5}
$$

where $\text{SINR}_{s,a}^{(j)} = \frac{\gamma_{s,a}^{(j)}}{\sum_{s=1}^{S} P_s x_{s,a}^{(j)}\ d_s^{-\beta_o}\ \bar{\zeta}_s + \sigma^2}$ and $\text{SNR}_{s,b}^{(j)} = \frac{p_{s,b}^{(j)} r_s^{-\beta_o} \chi_s^j}{\sigma^2}$. Constraints C_1 and C_2 ensure the rate at access link and backhaul link of SBS s to be greater than R_{th}. C_3 indicates that at most one SBS can use a given channel for backhaul link, i.e., orthogonal backhaul channel allocation among SBSs. C_4 ensures that more than one SBSs can share a given channel for their access link transmission. C_5 indicates

that each SBS can use at most one channel for the access link. C_6 ensures that channels allocated to SBSs for backhaul and access links will also be orthogonal. The constraint C_7 ensures that (i) SBSs with allocated backhaul channel(s) will have an allocated channel for access link. Each SBS can have at most one channel for an access link transmission, and (ii) if an SBS has no backhaul channel, no access channel will be allocated to him. C_8 ensures that transmit power allocated to all backhaul channels does not exceed the maximum transmit power of WBH. C_9 represents the binary decision variables for backhaul and access channel allocation. C_{10} defines the non-negativity condition of the transmit power.

Note that, the constraints C_1 and C_9 turn the optimization problem to a mixed-integer non-linear program (MINLP) with non-convex feasible set. Therefore, the formulation described in **P1** has exponential time complexity. I relax the optimization problem by replacing the non-convex constraints to convex. First, I relax the constraint C_1 by assuming no interference. Then, I replace the non-convex constraints C_8 with the convex constraints $0 \leq x_{s,a}^{(j)} \leq 1$ and $0 \leq x_{s,b}^{(j)} \leq 1$ where $x_{s,a}^{(j)}$ and $x_{s,b}^{(j)}$ denote the portion of time that channel is allocated to an SBS for access and backhaul link transmissions, respectively. I then introduce a new variable $W_{s,b}^{(j)} = x_{s,b}^{(j)} p_{s,b}^{(j)} \geq 0$, which represents the actual transmit power of the WBH on backhaul channel j [92].

The relaxed problem can then be stated as

$$
\begin{aligned}
\textbf{(P2)} \quad & \underset{R_{\text{th}},\, x_{s,a}^{(j)},\, W_{s,b}^{(j)}}{\text{maximize}} \quad R_{\text{th}} \\
& \text{subject to} \\
& C_3 - C_7, C_{10} \text{ and} \\
& C_{11}: \sum_{s\in S}\sum_{j\in J} W_{s,b}^{j} \leq P_m, \\
& C_{12}: \sum_{j\in\mathcal{N}} x_{s,b}^{(j)} \log_2\left(1+\text{SNR}_{s,b}^{(j)}\right) \geq R_{\text{th}}, \quad \forall\, s, \\
& C_{13}: \sum_{j\in\mathcal{N}} x_{s,a}^{(j)} \log_2\left(1+\text{SINR}_{s,a}^{(j)}\right) \geq R_{\text{th}}, \quad \forall\, s, \\
& C_{14}: 0 \leq x_{s,a}^{(j)} \leq 1, 0 \leq x_{s,b}^{(j)} \leq 1, \quad \forall\, j, s,
\end{aligned}
\tag{5.6}
$$

where $\text{SINR}_{s,a}^{(j)} = \frac{\gamma_{s,a}^{(j)}}{\sigma^2}$, and $\text{SNR}_{s,b}^{(j)} = \frac{W_{s,b}^{(j)} r_s^{-\beta_o} \chi_s^{(j)}}{x_{s,b}^{(j)}\ \sigma^2}$. The constraint C_{12} is concave and the remaining constraints $C_3 - C_7$, C_{10}, and C_{13} are affine. As such, the problem **P2** turns out to be linear convex problem that can be solved using standard interior point methods.

To reduce complexity and gain system design insights, in the next section, I will investigate two distributed backhaul channel scheduling schemes, i.e., max-RSP and min-RSP schemes, for a given backhaul/access spectrum partitioning factor α. The coverage analysis will be performed for target rate R_{th} per SBS and its maximum can be determined numerically using the derived expressions. For the sake of tractability, I consider that the WBH distributes its total power budget equally among all backhaul channels.

5.5 Distributed Backhaul Channel Scheduling: Target Rate Coverage Analysis

This section presents an analysis of rate coverage considering the two following backhaul channel allocation schemes:

- **Maximum Received Signal Power (max-RSP) Scheme:** The WBH allocates a given backhaul channel to an SBS with maximum received signal power at the backhaul link. Mathematically, this criterion can be written as

$$\gamma_{s,b}^{*} = \arg\max\{\gamma_{s,b}^{(j)}\}, \quad \forall s = \{1, 2, \cdots, S\}, \tag{5.7}$$

  where $\gamma_{s,b}^{(j)}$ is the received signal power of an SBS on backhaul channel j from the WBH and is defined in (5.1).

- **Minimum Received Signal Power (min-RSP) Scheme:** The WBH allocates a given backhaul channel to an SBS with minimum received signal power. Mathematically, this criterion can be written as

$$\gamma_{s,b}^{*} = \arg\min\{\gamma_{s,b}^{(j)}\}, \quad \forall s = \{1, 2, \cdots, S\}. \tag{5.8}$$

In the following, I outline the methodology to evaluate the downlink network rate coverage:

- I rank all SBSs according to their distances from WBH.
- I derive the probability of allocating a backhaul channel to a ranked SBS s for both schemes. Subsequently, we determine the number of backhaul channels allocated to a given ranked SBS s for both schemes.

- I derive the rate coverage at the access link $\mathcal{R}_{(s),a}$ and backhaul link $\mathcal{R}^{(\cdot)}_{(s),b}$ of ranked SBS s, where $(\cdot)$ is max for max-RSP and min for min-RSP scheme.

- Finally, I derive the rate coverage of s^{th} ranked SBS, i.e., $\mathcal{R}^{(\cdot)}_{(s)} = \mathcal{R}^{(\cdot)}_{(s),b} \times \mathcal{R}_{(s),a}$ and the network rate coverage, i.e., $\mathcal{R}^{(\cdot)} = \sum_{s=1}^{S} \mathcal{R}^{(\cdot)}_{(s)} \times R_{\text{th}}$, for both schemes.

Notation: Gamma$(\kappa_{(\cdot)}, \Theta_{(\cdot)})$ denotes Gamma distribution with shape parameter κ, scale parameter Θ and $(\cdot)$ is the name of the random variable (RV). $\Gamma(a) = \int_0^\infty x^{a-1}e^{-x}dx$ is the Gamma function and $\Gamma_u(a;b) = \int_b^\infty x^{a-1}e^{-x}dx$ is the upper incomplete Gamma function. ${}_2F_1[\cdot,\cdot,\cdot,\cdot]$ is the Gauss hypergeometric function. $f(\cdot)$ and $F(\cdot)$ denotes the probability density function (PDF) and cumulative density function, respectively. $\mathbb{E}[\cdot]$ denotes the expectation operator.

5.5.1 Distance-Based Ranking of SBSs

Since SBSs are uniformly distributed, the PDF of the distance between SBS s and WBH can be defined as $f_{r_s}(r_s) = \frac{2r_s}{R_m^2}$, where $0 \leq r_s \leq R_m$. The CDF of r_s can be given as $F_{r_s}(r_s) = \int_0^{r_s} f_{r_s}(u)du = r_s^2/R_m^2$. For given PDF and CDF of r_s, the SBSs can be ranked w.r.t their distances from the WBH. The PDF of the s^{th} ranked SBS can be defined as

$$f_{r_{(s)}}(r_{(s)}) = \frac{S!\,(F_{r_s}(r_s))^{s-1}\,(1-F_{r_s}(r_s))^{S-s}\,f_{r_s}(r_s)}{(s-1)!(S-s)!}. \tag{5.9}$$

Substituting the PDF and CDF of r_s and by applying the Binomial expansion, (5.9) can be written as

$$f_{r_{(s)}}(r_{(s)}) = \sum_{n=0}^{S-s} \frac{2\ S!\ (-1)^{S-s+n}\ r_s^{2S-2n-1}}{(s-1)!\ (S-s-n)!\ n!\ R_m^{2(S-n)}}. \tag{5.10}$$

5.5.2 Probability of Backhaul Channel Allocation

In this subsection, I first derive the PDF and CDF of received signal power for the backhaul link. Then I derive the probability of allocating a backhaul channel to a ranked SBS s for both the schemes. Subsequently, I determine the number of backhaul channels allocated to ranked SBS s for both schemes.

The received signal power at the s ranked SBS on a given backhaul channel can be defined as

$$\gamma_{(s),b} = \frac{P_m}{N_b} r_{(s)}^{-\beta_o} \chi_s. \tag{5.11}$$

Now conditioning on the distribution of $r_{(s)}$, doing transformation of RV, i.e., $f_{\gamma_{(s),b}}(\gamma_{(s),b}|r_{(s)}) = \frac{r_{(s)}^{\beta_o}}{P_m/N_b} f_{\chi_s}\left(\frac{\gamma_{(s),b} r_{(s)}^{\beta_o}}{P_m/N_b}\right)$ with $\chi_s \sim \text{Gamma}(\kappa_{\chi_s}, \Theta_{\chi_s})$, and finally averaging over the PDF of $r_{(s)}$, I can write

$$f_{\gamma_{(s),b}}(\gamma_{(s),b}) = \sum_{n=0}^{S-s} \frac{A(n)\Gamma_l\left(\kappa_{\chi_s} - \frac{2(n-S)}{\beta_o}, B\gamma_{(s),b}\right)}{\gamma_{(s),b}^{1-\frac{2(n-S)}{\beta_o}}}, \tag{5.12}$$

where $B = \frac{R_m^{\beta_o} N_b}{P_m \Theta_{\chi s}}$ and

$$A(n) = \frac{2S!(-1)^{S-s+n} B^{\frac{2(n-S)}{\beta_o}}}{(s-1)!(S-s-n)!n!\Gamma(\kappa_{\chi_s})\beta_o}. \tag{5.13}$$

The CDF of $\gamma_{(s),b}$ can be derived as given in (5.14).

a) **Maximum Received Signal Power (max-RSP):** The conditional probability of a given backhaul channel to be allocated to the s rank SBS can be derived

$$F_{\gamma_{(s),b}}(\gamma_{(s),b}) = \sum_{n=0}^{S-s} \frac{A(n)\beta_o}{2(n-S)} \left(\frac{\Gamma_l\left(\kappa_{\chi_s} - \frac{2(n-S)}{\beta_o}, B\gamma_{(s),b}\right)}{\gamma_{(s),b}^{\frac{-2(n-S)}{\beta_o}}} - \frac{\Gamma_l\left(\kappa_{\chi_s}, B\gamma_{(s),b}\right)}{B^{\frac{2(n-S)}{\beta_o}}} \right). \tag{5.14}$$

as

$$p_{(s)|\gamma_{(s),b}}^{\max} = \Pr\Big(\underset{\substack{g=1,2,\ldots,S \\ g\neq s}}{\gamma_{(g),b}} \leq \gamma_{(s),b} \Big) = \prod_{\substack{g=1 \\ g\neq s}}^{S} F_{\gamma_{(g),b}}(\gamma_{(s),b}). \tag{5.15}$$

The unconditional $p_{(s)}^{\max}$ can then be derived by averaging over the distribution of $\gamma_{(s),b}$ as follows:

$$p_{(s)}^{\max} = \int_0^{\infty} \prod_{\substack{g=1 \\ g\neq s}}^{S} F_{\gamma_{(g),b}}(\gamma_{(s),b}) f_{\gamma_{(s),b}}(\gamma_{(s),b}) d\gamma_{(s),b}, \tag{5.16}$$

where the PDF and CDF of $\gamma_{(s),b}$ are given in (5.12) and (5.14), respectively. (5.16) can be evaluated numerically using standard mathematical software packages.

b) **Minimum Received Signal Power (min-RSP):** The conditional probability of a given backhaul channel to be allocated to the s rank SBS can be derived

as

$$\begin{aligned} p^{\min}_{(s)|\gamma_{(s),b}} &= \Pr\Big(\underset{\substack{g=1,2,\ldots,S \\ g\neq s}}{\gamma_{(g),b}} > \gamma_{(s),b} \Big) \\ &= \big(1 - \Pr(\gamma_{(1),b} \leq \gamma_{(s),b})\big) \cdots \big(1 - \Pr(\gamma_{(S),b} \leq \gamma_{(s),b})\big) \\ &= \prod_{\substack{g=1 \\ g\neq s}}^{S} \Big(1 - F_{\gamma_{(g),b}}(\gamma_{(s),b})\Big). \end{aligned} \tag{5.17}$$

The unconditional $p^{\min}_{(s)}$ can be derived by averaging over the distribution of $\gamma_{(s),b}$ as follows:

$$p^{\min}_{(s)} = \int_0^{\infty} \prod_{\substack{g=1 \\ g\neq s}}^{S} \Big(1 - F_{\gamma_{(g),b}}(\gamma_{(s),b})\Big) f_{\gamma_{(s),b}}(\gamma_{(s),b}) d\gamma_{(s),b}, \tag{5.18}$$

where (5.18) can be evaluated numerically using standard mathematical software packages.

Remark: The number of channels allocated to ranked SBSs for backhauling can be determined as follows:

$$N^{(\cdot)}_{(s),b} = N_b \times p^{\max}_{(s)}, \tag{5.19}$$

where $(\cdot)$ is max for max-RSP and min for min-RSP scheme.

5.5.3 Analysis of Rate Coverage

The rate coverage probability $\mathcal{R}^{(\cdot)}_{(s)}$ of ranked SBS s is defined as the probability of its downlink user rate to be higher than a required target rate R_{th}. To achieve R_{th}, both $\mathcal{R}^{(\cdot)}_{(s),b}$ and $\mathcal{R}_{(s),a}$ must be at least R_{th}. Note that the backhaul rate of an SBS s

can be defined as $\mathcal{R}^{(\cdot)}_{(s),b} = N^{(\cdot)}_{(s),b}\log_2(1+\mathrm{SNR}_{(s),b})$. As such, to achieve a target rate of R_{th} in the backhaul link, $\mathrm{SNR}_{(s),b}$ must be greater than a prescribed threshold $\gamma_{(s),b}$ defined as follows:

$$\gamma^{(\cdot)}_{(s),b} = 2^{\frac{R_{\mathrm{th}}}{N^{(\cdot)}_{(s),b}}} - 1. \tag{5.20}$$

On the other hand, the rate for the access channel can be defined as $\mathcal{R}^{(\cdot)}_{(s),a} = \log_2(1+\mathrm{SINR}_{(s),a})$. $\mathrm{SINR}_{(s),a}$ must be greater than another prescribed threshold $\gamma_{(s),a}$ defined as follows:

$$\gamma_{(s),a} = 2^{R_{\mathrm{th}}} - 1. \tag{5.21}$$

The rate coverage probability $\mathcal{R}^{(\cdot)}_{(s)}$ if a given SBS at rank s can be defined as follows:

$$\mathcal{R}^{(\cdot)}_{(s)} = \mathbb{P}\left(\mathrm{SNR}^{(\cdot)}_{(s),b} > \gamma^{(\cdot)}_{(s),b}\right)\mathbb{P}\left(\mathrm{SINR}_{(s),a} > \gamma_{(s),a}\right). \tag{5.22}$$

a) **Rate Coverage Analysis of Access Links:** Using the definition of the characteristic function, i.e., $\phi_{_X}(\omega) = \int_0^\infty e^{i\omega x} f_{_X}(x)dx$, the characteristic function $\phi_{\gamma_{(s),a}}(\omega)$ of the received signal power at the small cell user can be derived as given in [88, Eq. 27] by replacing $t = -i\omega$. Similarly, the characteristic function $\phi_{I_u}(\omega)$ of the co-tier interference power at the small cell user can be derived as given in [31, Eq. 20] by replacing $t = i\omega$. The coverage probability of the access link of s ranked SBS can be given as

$$\begin{aligned}\mathcal{R}_{(s),a} &= \mathbb{P}\left(\mathrm{SINR}_{(s),a} > \gamma_{(s),a}\right)\\ &= \frac{1}{2} + \frac{1}{\pi}\int_0^\infty \mathrm{Im}\left(e^{-\epsilon_a\sigma^2}\phi_{\gamma_{(s),a}}(\omega)\phi_{I_u}(\omega)\right)\frac{d\omega}{\omega},\end{aligned} \tag{5.23}$$

where $\epsilon_a = i\gamma_{(s),a}\omega$.

b) **Rate Coverage Analysis of Backhaul Links:** Using the definition of characteristic function and PDF ($f_{\gamma_{(s),b}}(\gamma_{(s),b})$), the characteristic function $\phi_{\gamma_{(s),b}}(\omega)$ of the received signal power at the ranked SBS s can be derived as follows:

$$\phi_{\gamma_{(s),b}}(\omega) = \sum_{n=0}^{S-s} A(n)\Gamma\left(\frac{2(n-S)}{\beta_o}\right)\left(\frac{\Gamma\left(\kappa_{\chi_s} - \frac{2(n-s)}{\beta_o}\right)}{(i\omega)^{\frac{2(n-S)}{\beta_o}}} - F(n)\right), \tag{5.24}$$

where $F(n) = \frac{{}_2F_1\left[\kappa_{\chi_s}, \frac{2(n-S)}{\beta_o}, \frac{2(n-S)}{\beta_o}+1, -Bi\omega\right]\Gamma(\kappa_{\chi_s})}{B^{\frac{2(n-S)}{\beta_o}}}$. The coverage probability of the backhaul link of s ranked SBS for any scheme can be derived as

$$\begin{aligned}\mathcal{R}^{(\cdot)}_{(s),b} &= \mathbb{P}\left(\mathrm{SNR}^{(\cdot)}_{(s),b} > \gamma^{(\cdot)}_{(s),b}\right) \\ &= \frac{1}{2} + \frac{1}{\pi}\int_0^\infty \mathrm{Im}\left(e^{-\epsilon_b\sigma^2}\phi_{\gamma_{(s),a}}(\omega)\right)\frac{d\omega}{\omega},\end{aligned} \tag{5.25}$$

where $\epsilon_b = i\gamma^{(\cdot)}_{(s),b}\omega$.

5.6 Numerical Results and Discussion

This section validates the accuracy of the derived rate coverage expressions for the min-RSP and max-RSP schemes. Also, it provides a comparative analysis of min-RSP and max-RSP schemes with the solution derived from **P2**. I consider number of SBSs $S = 6$, $\alpha = 0.8$, $R_{\mathrm{th}} = R^*_{\mathrm{th}}$ taken from the solution of **P2**, and $N = 20$. I consider $f_\zeta(\zeta) \sim \mathrm{Gamma}(1/2, 2)$ and $f_{\chi_s}(\chi_s) \approx \mathrm{Gamma}(1, 1)$. The coverage radii of the WBH and SBSs are $R_m = 300$ m and $R_s = 30$ m, respectively. I set indoor path-loss exponent within small cells $\beta_i = 2.1$, outdoor path-loss exponent $\beta_o = 3.9$, and the thermal noise power density $\sigma^2 = 1 \times 10^{-12}$ W/Hz. The transmit powers of

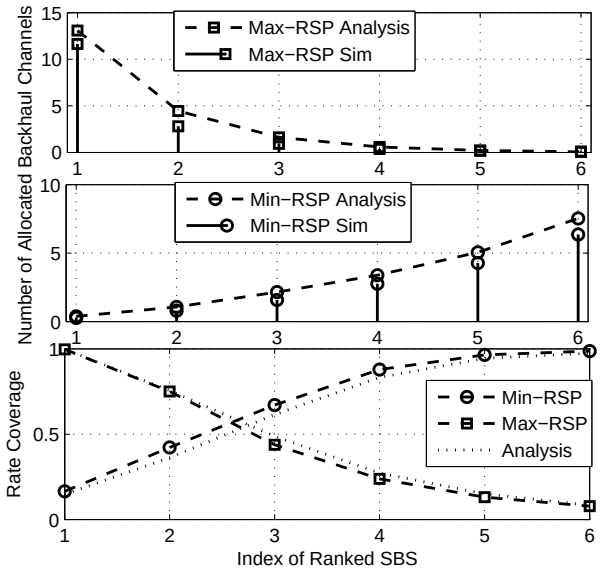

Figure 5.1: (a)-(b) Number of backhaul channels allocated to ranked SBSs with max-RSP and min-RSP schemes, (c) Rate coverage probability of ranked SBSs with max-RSP and min-RSP schemes (for $\alpha = 0.8$, $R_{\text{th}}^{*} = 5.4$).

WBH and SBSs are set as $P_m = 40$ W and $P_s = 1$ W, respectively.

Figs. 5.1(a) and (b) illustrate the number of backhaul channels allocated to SBSs that are ranked with respect to their distances from the WBH considering max-RSP and min-RSP schemes. With max-RSP scheme, a large number of backhaul channels are allocated to the SBSs who have the highest received signal power at the backhaul link (i.e., the scheme favors SBSs located close to WBH). As the received signal power decreases, the number of allocated channels also decreases due to the selection criterion. On the other hand, with min-RSP scheme, more channels are allocated to SBSs that are far away from WBH. Consequently, Fig. 5.1(c) shows the rate coverage of each ranked SBS for both schemes. It can be observed that the allocation of more backhaul channels generally leads to a higher rate coverage of SBSs.

Fig. 5.2 depicts rate of each ranked SBS for centralized min-rate maximization scheme and distributed max-RSP and min-RSP schemes. It can be observed that

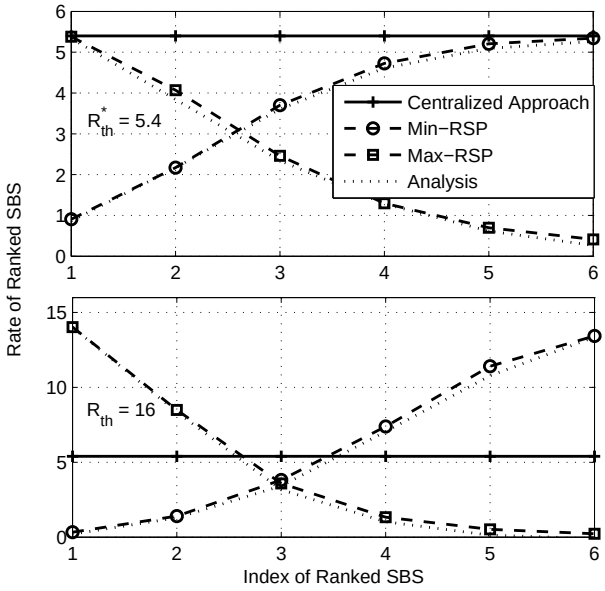

Figure 5.2: Rate of the ranked SBSs for (a) $R^*_{\text{th}} = 5.4$, (b) $R_{\text{th}} = 16$ (for $\alpha = 0.8$, $N = 20$).

allocation of more backhaul channels generally leads to a higher rate as is also observed in Fig. 5.1(c). Moreover, the centralized approach tends to guarantee the minimum achievable rate R^*_{th} at all SBSs whereas the distributed schemes achieve the target rate R_{th} per SBS with a certain probability. It can be seen that when R_{th} of distributed schemes is set to $R^*_{\text{th}} = 5.4$, the centralized scheme significantly outperforms the heuristic schemes.

Fig. 5.3 demonstrates the impact of varying the proportion of backhaul spectrum (out of total available spectrum) on the network rate considering max-RSP and min-RSP schemes. For both schemes, the network rate increases as α increases. Since the rate coverage of an SBS is defined as the minimum of the backhaul and access link rate, the rate of each SBS is constrained by the backhaul link rate which in turn lowers the network rate. Note that when α is small, the system has a fewer number of backhaul channels and more channels are available for access link transmissions.

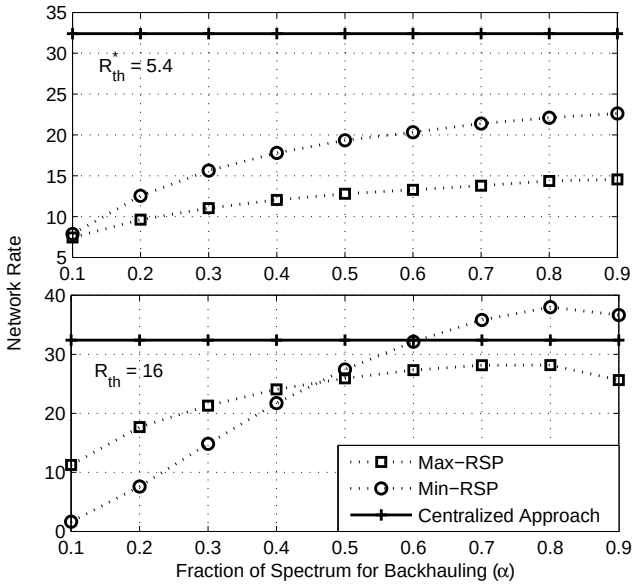

Figure 5.3: Network rate as a function of access/backhaul spectrum partition α (for $N = 20$).

This causes low interference and in turn high rate at access links. Nonetheless, this higher access link rate may not be supported by a very small number of backhaul channels. On the other hand, for high values of α, the interference at access links becomes high and in turn the capacity degrades; therefore, a very high proportion of backhaul channels is not helpful. The significance of optimal spectrum partitioning is thus evident.

Another observation is that the network rate with min-RSP is significantly higher than the max-RSP (especially at higher values of α). The reason is that all SBSs have nearly similar access link transmission capacities on average; however, the cell-edge SBSs suffer more due to their larger distances (in turn poor backhaul channels) from the WBH. Therefore allocating more backhaul channels to cell-edge SBSs is favorable. Finally, it can be observed that the centralized approach outperforms the heuristic schemes in many cases while providing fair rate allocations among all SBSs in the

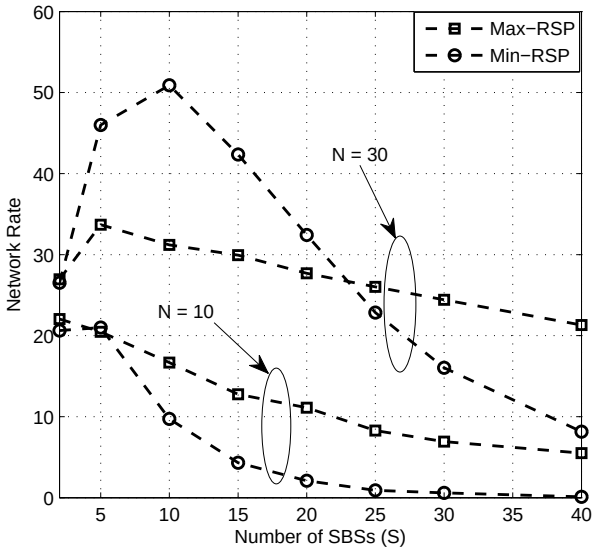

Figure 5.4: Network rate as a function of the number of SBSs for R_{th} =16, $\alpha = 0.8$.

system.

Fig. 5.4 shows the effect of increasing number of SBSs S on the network rate for different values of N considering max-RSP and min-RSP schemes. For given α and N, the network rate increases up to a certain point with S as more SBSs can support more users and access/backhaul transmissions. Nevertheless, the access/backhaul transmissions cannot be supported if S becomes very high. As such the significance of optimum S is evident. For small value of S and/or large number of channels N, the performance of min-RSP is better compared to max-RSP. The reason is the low interference at the access links of all SBSs for high N. This low interference allows a large number of cell-edge SBSs to achieve much better rates provided sufficient backhaul coverage. This sufficient backhaul coverage is possible with the min-RSP scheme which can be observed from Fig. 5.4.

5.7 Chapter Summary

I have formulated a common rate maximization problem for the access and backhaul links of the small cells. Due to the exponential time complexity of the problem, I have transformed and solved a relaxed version of the original problem and used it as a benchmark for the two distributed backhaul channel allocation schemes. It has been observed that allocating more backhaul spectrum for the cell-edge SBSs is beneficial to enhance the overall network rate especially for large number of available channels and high density of small cells given the orthogonality among multiple backhaul streams.

Chapter 6

Conclusion and Future Research Directions

6.1 Conclusion

The massive deployment of small cells over the existing traditional macrocells is deliberated as a key enabling technique for the emerging 5G cellular networks. On one side, the coexistence of base stations (BSs) with different transmit powers lead to unequal distribution of the traffic loads among different BSs when received signal power (RSP)-based user association is taken into consideration. On the other side, to provide an efficient and an economical backhaul transmission for these small cells is a vital issue. To combat this, wireless backhauling is been considered as a viable and cost-effective approach. But the scarcity of radio spectrum in the licensed bands is still a major limitation which requires an efficient spectrum planning for backhaul/access links of small cells. In this thesis, I investigated the key challenges of small cell networks and provided the possible solutions to enhance its performance.

In this chapter, I present a summary of the work presented in this thesis and

discuss my vision for further extensions of the presented work.

a) Channel Access-aware user association for small cell networks

- A channel access-aware (CAA) user association scheme is proposed. CAA scheme exhibits the following features: (i) The channel access probability serves as a dynamic bias towards a given BS regardless of which tier it belongs to. This is different from the conventional BRSP in which a higher bias is given to low-power BSs; (ii) Since the channel access probability reduces with increasing traffic load of a BS, a user may not select a congested BS despite its high received signal power; (iii) For a large number of incoming users, the CAA scheme balances the traffic load among different BSs; (iv) The CAA scheme reduces to RSP-based association if channel access probabilities from all BSs are similar and it reduces to traffic load-based association if the received signal powers from different BSs are alike.
- A mathematical framework is developed that is generalized to
  - Characterize the SE of downlink transmission to a user with CAA-based user association with and without interference coordination at the MBS,
  - Characterize the network-wide SE of downlink transmission,
  - Consider a more general channel fading model, namely, the generalized-$\mathcal{K}$ composite fading which is approximated with Gamma fading channels for tractability reasons,
  - Model the individual traffic load distributions per SBS as well as MBS. In this paper, we consider Poisson traffic load distribution per SBS and MBS. Note that this set-up corresponds to clustered Poisson Point

Processes which are difficult to analyze with the stochastic geometry-based approaches.

- It is observed that the performance gains of BRSP compared to RSP are highly dependent on the bias values and selection of optimal bias is extremely important in order to achieve useful gains. Nevertheless even with the optimal bias selection, CAA scheme is shown to outperform BRSP scheme. This fact highlights the importance of adopting per BS biasing rather than per tier biasing as well as per-tier and per-BS traffic load modeling. Finally, insights are extracted related to selecting the proportion of ABS as a function of traffic load intensities at MBS and SBSs.

b) Wireless backhauling for small cell networks

- An extensive overview of the existing wireless backhaul solutions is provided and their fundamental implementation challenges are discussed.
- While focusing on the radio frequency (RF) backhaul solutions, I theoretically characterize the cellular region in which the downlink transmission capacity of a given half-duplex (HD) small cell is constrained by its backhaul capacity. Then some solution techniques such as full-duplex (FD) backhauling is proposed to overcome the limitation of traditional wireless backhauling for small cells.
- The achievable capacity gains of downlink transmission from the macrocell base station (MBS) to a user associated to an FD self-backhauled small cell are derived and compared to its HD counter part. The results are further outstretched for the uplink transmission.
- It is observed that HD self-backhauling is more feasible in the downlink for

SBSs located near to an MBS. Whereas, FD self-backhauling is a better option in other cases.

c) Downlink spectrum allocation for in-band and out-band wireless Backhauling in full-duplex small cells

- I consider the problem of optimal access/backhaul spectrum allocation for SBSs taking into account both in-band FD (IBFD) backhauling and out-of-band FD (OBFD) backhauling. Further, the spectrum allocation for hybrid IBFD/OBFD backhauling is introduced.
- A problem is formulated to maximize the minimum achievable rate at the SBSs in a hybrid IBFD/OBFD backhaul settings. As a special case, the closed-form optimal solutions for the access/backhaul spectrum allocation of OBFD backhauling and IBFD backhauling are derived.
- Then, two distributed backhaul spectrum allocation schemes are proposed and comparatively analyzed. Using tools from the theory of ordered statistics, the number of backhaul channels allocated to SBSs considering both criteria are derived. Based on this, the minimum rate coverage probability and average minimum achievable rate of each SBS are derived given its distance from the centralized WBH for both the IBFD and OBFD backhauling scenarios.
- It is observed that the optimal spectrum allocation rules significantly vary for OBFD and IBFD backhauling. OBFD backhauling favors more backhaul spectrum for SBSs located far-away from the WBH. With IBFD backhauling and increasing SI cancellation, the backhaul/access spectrum allocation of the SBSs located close to and far-away from WBH increases and

decreases, respectively. The gains of IBFD over OBFD backhauling are obvious only after a certain amount of SI cancellation. So a correct level of SI cancellation is needed to harness the gains of IBFD backhauling. In addition, hybrid IBFD/OBFD backhauling extracts the benefit of both the OBFD and IBFD backhauling in low and high SI cancellation scenarios, respectively.

d) Downlink resource allocation for out-of-band wireless backhauling in full-duplex small cells

- I consider the problem of downlink access/backhaul power and channel scheduling for multiple small cells.
- A problem is formulated to maximize the common achievable rate at the access and backhaul links of all SBSs. Due to exponential time complexity of the problem, the nominal problem is transformed into a less complex convex programming problem and solved it numerically.
- Two simple and distributed backhaul channel allocation criteria, maximum received signal power (max-RSP) and minimum received signal power (min-RSP), are proposed and comparatively analyzed. For both criteria, I theoretically derive the number of allocated backhaul channels and target rate coverage probability of each SBS given its distance from the wireless backhaul hub (WBH).
- It is observed that allocating more backhaul spectrum for the cell-edge SBSs is beneficial to enhance the overall network rate especially for large number of available channels and high density of small cells given the orthogonality among multiple backhaul streams.

6.2 Future Research Directions

Some of the potential research directions for 5G small cell networks are outlined below.

1. *Resource Allocation:* Efficient solutions for backhaul resource allocation need be developed that can adapt according to the locations, channel conditions, and traffic load of different SBSs.Moreover, the backhaul transmissions from SBSs or MBS should be power adaptive depending on the required backhaul capacity per small cell. This will minimize interference while achieving the required backhaul capacity. In dynamic TDD systems, the spectral efficiency of the small cell user can be maximized by optimizing the time allocated for backhaul and transmission given a total time constraint

2. *User association schemes:* With the emerging non-ideal wireless backhaul solutions, the existing user association schemes such as channel-aware, traffic-load-aware, and channel-access-aware schemes may be highly suboptimal. New user association criteria are therefore required that perform cell selection based on the backhaul capacity limitation, backhaul delays, and backhaul interference in addition to traffic load and channel conditions. The traffic load conditions need to be considered now for both the transmission link of an SBS as well as its backhaul link.

3. *Massive MIMO for wireless backhauling:* To serve multiple SBSs at a certain time in the downlink backhauling, the use of multiple antennas or multiple channels is inevitable. From an operator's perspective, deploying large antenna arrays at the MBS to serve massive small cell deployments using the same time-frequency resource could be more attractive than using multiple sets of

channels. With such a deployment, the use of efficient beam-forming techniques can completely cancel the intra-cell backhaul interference.

4. *Full-duplex SBS with satellite backhaul:* The satellite backhaul is a competitive solution to bring small cell services to remote and rural areas. Full-duplex backhauling can be implemented at satellite bands by an SBS to serve simultaneously small-cell users and backhaul data to/from a core network via satellite gateways and, in turn, satellites. Specifically, in the uplink, very small transmit power of the user would not have any impact on the performance of a satellite gateway receiver. In the downlink, the directive feeder antennas at a satellite gateway with possibly additional isolation and processing would cause negligible interference to the small cell user.

Bibliography

[1] "The benefits of cloud-RAN architecture in mobile network expansion," *FUJITSU Network Communications, Inc. White Paper*, Aug. 2014.

[2] B. Nobel and J.W. Daniel, *Applied linear algebra*. Prentice-Hall, 1977.

[3] E. Hossain, M. Rasti, H. Tabassum, and A. Abdelnasser, "Evolution toward 5G multi-tier cellular wireless networks: An interference management perspective," *IEEE Wireless Communications*, vol. 21, no. 3, pp. 118–127, June 2014.

[4] "Small cell backhaul requirements," *NGMN Alliance White Paper*, June 2012.

[5] K. M. Thilina, H. Tabassum, E. Hossain, and D. I. Kim, "Medium access control design for full-duplex wireless systems: Challenges and approaches," *IEEE Communications Magazine*, vol. 53, no. 5, pp. 112–120, May 2015.

[6] M. Duarte, A. Sabharwal, V. Aggarwal, R. Jana, K. K. Ramakrishnan, C. W. Rice, and N. K. Shankaranarayanan, "Design and characterization of a full-duplex multiantenna system for WiFi networks," *IEEE Transactions on Vehicular Technology*, vol. 63, no. 3, pp. 1160–1177, Mar. 2014.

[7] O. Semiari, W. Saad, S. Valentin, M. Bennis, and B. Maham, "Matching theory for priority-based cell association in the downlink of wireless small cell networks," *IEEE International Conference on Acoustics, Speech and Signal Processing (ICASSP'14)*, pp. 444–448, May 2014.

[8] E. Hossain, L. B. Le, and D. Niyato, *Radio resource management in multi-tier cellular wireless networks*, Simon Haykin, Ed. John Wiley and Sons, 2013.

[9] T. Zhou, Y. Huang, and L. Yang, "QoS-aware user association for load balancing in heterogeneous cellular networks," *arXiv:1312.6911 [cs.IT]*, 2013.

[10] K. A. Hamdi, "A useful lemma for capacity analysis of fading interference channels," *IEEE Transactions on Wireless Communications*, vol. 58, no. 2, pp. 411–416, Feb. 2010.

[11] P. Jiyong, J. Wang, W. Dongyao, S. Gang, J. Qi, and L. Jianguo, "Optimized time-domain resource partitioning for enhanced inter-cell interference coordination in heterogeneous networks," *IEEE Wireless Communication and Networking Conference (WCNC'12)*, pp. 1613–1617, Apr. 2012.

[12] Y. Qiaoyang, R. Beiyu, C. Yudong, M. Al-Shalash, C. Caramanis, and J. G. Andrews, "User association for load balancing in heterogeneous cellular networks," *IEEE Transactions on Wireless Communications*, vol. 12, no. 6, pp. 2706–2716, June 2013.

[13] Y. Qiaoyang, M. Al-Shalashy, C. Caramanis, and J. G. Andrews, "On/off macrocells and load balancing in heterogeneous cellular networks," *IEEE Global Communications Conference (Globecom'13)*, pp. 3814–3819, Dec. 2013.

[14] S. Vasudevan, R. N. Pupala, and K. Sivanesan, "Dynamic eICIC: A proactive strategy for improving spectral efficiencies of heterogeneous LTE cellular networks by leveraging user mobility and traffic dynamics," *IEEE Transactions on Wireless Communications*, vol. 12, no. 10, pp. 4956–4969, Oct. 2013.

[15] H. Tang, J. L. Peng, P. L. Hong, and K. P. Xue, "Offloading performance of range expansion in picocell networks: A stochastic geometry analysis," *IEEE Wireless Communication Letters*, vol. 2, no. 5, pp. 511–514, Oct. 2013.

[16] H. S. Jo, Y. J. Sang, P. Xia, and J. G. Andrews, "Outage probability for heterogeneous cellular networks with biased cell association," *IEEE Global Communications Conference (Globecom'11)*, pp. 1–5, Dec. 2011.

[17] S. Mukherjee, and I. Guvenc, "Effects of range expansion and interference coordination on capacity and fairness in heterogeneous networks," *Forty Fifth Asilomar Conference on Signals, Systems and Computers (ASILOMAR'11)*, pp. 1855–1859, Nov. 2011.

[18] A. Merwaday, S. Mukherjee, and I. Guvenc, "On the capacity analysis of HetNets with range expansion and eICIC," *IEEE Global Communications Conference (Globecom'13)*, pp. 4257–4262, Dec. 2013.

[19] C. H. M. de-Lima, M. Bennis, and M. Latva-aho, "Statistical analysis of self-organizing networks with biased cell association and interference avoidance," *IEEE Transactions on Vehicular Technology*, vol. 62, no. 5, pp. 4257–4262, June 2013.

[20] M. Cierny, W. Haining, R. Wichman, D. Zhi, and C. Wijting, "On number of almost blank subframes in heterogeneous cellular networks," *IEEE Transactions on Wireless Communications*, vol. 12, no. 10, pp. 5061–5073, Oct. 2013.

[21] T. D. Novlan, R. K. Ganti, A. Ghosh, and J. G. Andrews, "Analytical evaluation of fractional frequency reuse for heterogeneous cellular networks," *IEEE Transactions on Wireless Communications*, vol. 60, no. 7, pp. 2029–2039, July 2012.

[22] W. Yongbin, J. Hong, and Z. Heli, "Spectrum-efficiency enhancement in small cell networks with biasing cell association and eICIC: An analytical framework," *International Journal of Communication Systems*, Sep. 2014.

[23] J. Andrews, S. Singh, Y. Qiaoyang, L. Xingqin, and H. Dhillon, "An overview of load balancing in hetnets: old myths and open problems," *IEEE Wireless Communications*, vol. 21, no. 2, pp. 18–25, Apr. 2014.

[24] S. Gradshteyn, and I. M. Ryzhik, *Table of integrals, series, and products*, 6th Edition ed. New York: Academic Press, 2000.

[25] B. Zhuang, D. Guo, and M. L. Honig, "Traffic-driven spectrum allocation in heterogeneous networks," *IEEE Journal on Selected Areas in Communications*, vol. 33, no. 10, pp. 2027–2038, Oct. 2015.

[26] B. Rengarajan, and G. de Veciana, "Architecture and abstractions for environment and traffic aware system-level coordination of wireless networks: The downlink case," *IEEE International Conference on Computer Communications*, Apr. 2008.

[27] H. Tabassum, Z. Dawy, M. S. Alouini, and F. Yilmaz, "A generic interference model for uplink OFDMA networks with fractional frequency reuse," *IEEE Transactions on Vehicular Technology*, vol. 63, no. 3, pp. 1491–1497, Mar. 2014.

[28] U. Siddique, H. Tabassum, and E. Hossain, "Channel access-aware user association in two-tier cellular networks," *IEEE International Conference on Communications (ICC'15)*, pp. 1–6, June 2015.

[29] P. Bithas, N. Sagias, P. Mathiopoulos, G. Karagiannidis, and A. Rontogiannis, "On the performance analysis of digital communications over generalized-K fading channels," *IEEE Communication Letters*, vol. 5, no. 10, pp. 353–355, May 2006.

[30] S. Al-Ahmadi, and H. Yanikomeroglu, "On the approximation of the generalized-K distribution by a gamma distribution for modeling composite fading channels," *IEEE Transactions on Wireless Communications*, vol. 9, no. 2, pp. 706–712, Feb. 2010.

[31] H. Tabassum, Z. Dawy, E. Hossain, and M. S. Alouini, "Interference statistics and capacity analysis for uplink transmission in two-tier small cell networks: A geometric probability approach," *IEEE Transactions on Wireless Communications*, vol. 13, no. 7, pp. 3837–3852, July 2014.

[32] H. Tabassum, U. Siddique, E. Hossain, and Md. J. Hossain, "Downlink performance of cellular systems with base station sleeping, user association, and scheduling," *IEEE Transactions on Wireless Communications*, vol. 13, no. 10, pp. 5752–5767, Oct. 2014.

[33] M. N. Islam, A. Sampath, A. Maharshi, O. Koymen, and N. B. Mandayam, "Wireless backhaul node placement for small cell networks," *48th Annual Conference on Information Sciences and Systems (CISS), 2014*, pp. 1–6, Mar. 2014.

[34] J. Zhao, T. Q. S. Quek, and Z. Lei, "Heterogeneous cellular networks using wireless backhaul: Fast admission control and large system analysis," *IEEE Journal on Selected Areas in Communications*, vol. 33, no. 10, pp. 2128–2143, Oct. 2015.

[35] Y. Shi, M. Li, X. Xiong, and G. Han, "A flexible wireless backhaul solution for emerging small cells networks," *IEEE International Conference on Signal Processing, Communications and Computing (ICSPCC)*, pp. 591–596, Aug. 2014.

[36] S. Goyal, L. Pei, S. Panwar, R.A. DiFazio, Y. Rui, L. Jialing, and E. Bala, "Improving small cell capacity with common-carrier full duplex radios," *IEEE International Conference on Communications (ICC'14)*, pp. 4987–4993, June 2014.

[37] S. Barghi, A. Khojastepour, K. Sundaresan, and S. Rangarajan, "Characterizing the throughput gain of single cell MIMO wireless systems with full duplex radios," *10th International Symposium on Modeling and Optimization in Mobile, Ad Hoc and Wireless Networks (WiOpt'12)*, pp. 68–74, May 2012.

[38] D. Nguyen, T. Le-Nam, P. Pirinen, and M. Latva-aho, "On the spectral efficiency of full-duplex small cell wireless systems," *IEEE Transactions on Wireless Communications*, vol. 13, no. 9, pp. 4896–4910, Sep. 2014.

[39] O. Simeone, E. Erkip, and S. Shamai, "Full-duplex cloud radio access networks: An information-theoretic viewpoint," *IEEE Wireless Communication Letters*, vol. 3, no. 4, pp. 413–416, Aug. 2014.

[40] C. H. M. de-Lima, P. H. J. Nardelli, H. Alves, and M. Latva-aho, "Full-duplex communications in interference networks under composite fading channel," *European Conference on Networks and Communication (EuCNC'14)*, pp. 1–5, June 2014.

[41] X. Ge, H. Cheng, M. Guizani, and T. Han, "5G wireless backhaul networks: Challenges and research advances," *IEEE Network*, vol. 28, no. 6, pp. 6–11, Nov. 2014.

[42] R. Taori, and A. Sridharan, "In-band, point to multi-point, mm-Wave backhaul for 5G networks," *IEEE International Conference on Communications Workshops (ICC'14)*, pp. 96–101, June 2014.

[43] "Backhaul technologies for small cells, use cases, requirements and solutions," *Small Cell Forum*, Feb. 2013.

[44] "Spectrum and technology issues for microwave backhaul in Europe," *Innovation Observatory, White Paper*, Nov. 2010.

[45] C. Gerami, N. Mandayam, and L. Greenstein, "Backhauling in TV white spaces," *IEEE Global Telecommunications Conference (GLOBECOM'10)*, pp. 1–6, Dec. 2010.

[46] S. Singh, M. N. Kulkarni, A. Ghosh, and J. G. Andrews, "Tractable model for rate in self-backhauled millimeter wave cellular networks," *IEEE Journal on Selected Areas in Communications*, vol. 33, no. 10, pp. 2196–2211, Oct. 2015.

[47] 3GPP TR 36.842 (V0.2.0), "Study on small cell enhancements for EUTRA and E-UTRAN - Higher layer aspects (Release 12)," 2014.

[48] J. Zhao, and T. Q. S. Quek, and Z. Lei, "Coordinated ulmtipoint transmission with limited backhaul data transfer," *IEEE Transactions on Communications*, vol. 12, no. 6, pp. 2762–2775, June 2013.

[49] D. Chen, T. Q. S. Quek, and M. Kountouris, "Backhauling in heterogeneous cellular networks modeling and tradeoffs," *IEEE Transactions on Wireless Communications*, vol. 14, no. 6, pp. 3194–3206, Jan. 2015.

[50] X. Yi and D. Kerret, and D. Gesbert, "The DoF of network MIMO with backhaul delays," *IEEE International Conference on Communications (ICC'13)*, pp. 3318–3322, June 2013.

[51] S. Samarakoon, M. Bennis, W. Saad, and M. Latva-aho, "Backhaul-aware interference management in the uplink of wireless small cell networks," *IEEE Transactions on Communications*, vol. 12, no. 11, pp. 5813–5825, Nov. 2013.

[52] Gerami, C. and Mandayam, N. and Greenstein, L., "Backhauling in TV White Spaces," *IEEE Global Telecommunications Conference (GLOBECOM'10)*, pp. 1–6, Dec. 2010.

[53] M. E. Knox, "Single antenna full duplex communications using a common carrier," *IEEE Wireless and Microwave Technology Conference (WAMICON'12)*, pp. 1–6, Apr. 2012.

[54] U. Siddique, H. Tabassum, E. Hossain, and D. I. Kim, "Wireless backhauling of 5G small cells: Challenges and solution approaches," *IEEE Wireless Communications Magzine*, vol. 22, no. 5, pp. 22–31, Oct. 2015.

[55] N. Wang, E. Hossain, and V. K. Bhargava, "Backhauling 5G small cells: A radio resource management perspective," *IEEE Wireless Communications*, vol. 22, no. 5, pp. 41–49, Oct. 2015.

[56] R. A. Pitaval, O. Tirkkonen, R. Wichman, K. Pajukoski, E. Lahetkangas, and E. Tirola, "Full-duplex self-backhauling for small-cell 5G networks," *IEEE Wireless Communications*, vol. 22, no. 5, pp. 83–89, Oct. 2015.

[57] Z. Pi and F. Khan, "An introduction to millimeter-wave mobile broadband systems," *IEEE Communications*, vol. 49, no. 6, pp. 101–107, June 2011.

[58] W. Roh, J. Y. Seol, J. Park, B. Lee, J. Lee, Y. Kim, J. Cho, K. Cheun, and F. Aryanfar, "Millimeter-wave beamforming as an enabling technology for 5G cellular communications: Theoretical feasibility and prototype results," *IEEE Communications*, vol. 52, no. 2, pp. 106–113, Feb. 2014.

[59] Z. Gao, L. Dai, D. Mi, Z. Wang, M. A. Imran, and M. Z. Shakir, "MmWave massive-MIMO-based wireless backhaul for the 5G ultra-dense network," *IEEE Wireless Communications*, vol. 22, no. 5, pp. 13–21, Oct. 2015.

[60] M. Duarte, C. Dick, and A. Sabharwal, "Experiment-driven characterization of full-duplex wireless systems," *IEEE Transactions on Wireless Communications*, vol. 11, no. 12, pp. 4296–4307, Sept. 2012.

[61] J. I. Choi, M. Jain, K. Srinivasan, P. Levis, and S. Katti, "Achieving single channel full duplex wireless communication," *in Proc. 16th Annual International Conference on Mobile Computing and Networking*, pp. 1–12, Sep. 2010.

[62] M. Heino, D. Korpi, T. Huusari, E. Antonio-Rodriguez, S. Venkatasubramanian, T. Riihonen, L. Anttila, C. Icheln, K. Haneda, R. Wichman, M. Valkama, "Recent advances in antenna design and interference cancellation algorithms for in-band full duplex relays," *IEEE Communications*, vol. 53, no. 5, pp. 91–101, May 2015.

[63] D. Korpi, Y. S. Choi, T. Huusari, L. Anttila, S. Talwar, and M. Valkama, "Adaptive nonlinear digital self-interference cancellation for mobile in-band full-duplex radio: Algorithms and RF measurements," *IEEE Global Communications Conference (GLOBECOM)*, pp. 1–7, Dec. 2015.

[64] D. Bharadia, E. McMilin, and S. Katti, "Full duplex radios," *Proceedings of ACM SIGCOMM*, 2013.

[65] Y. S. Choi, and H. Shirani-Mehr, "Simultaneous transmission and reception: Algorithm, design and system level performance," *IEEE Transactions on Wireless Communications*, vol. 12, no. 12, pp. 5992–6010, Dec. 2013.

[66] M. K. Hanawal and D. N. Nguyen and M. Krunz, "Jamming attack on in-band full-duplex communications: Detection and countermeasures," *IEEE International Conference on Computer Communications*, pp. 1–9, Dec. 2016.

[67] G. Liu, F. R. Yu, H. Ji, V. C. M. Leung, and X. Li, "In-band full-duplex relaying: A survey, research issues and challenges," *IEEE communications surveys tutorials*, vol. 17, no. 2, pp. 500–524, Jan. 2015.

[68] F. Capozzi, G. Piro, L. A. Grieco, G. Boggia, and P. Camarda, "Downlink packet scheduling in LTE cellular networks: Key design issues and a survey," *IEEE Communications Surveys Tutorials*, vol. 15, no. 2, pp. 678–700, May 2013.

[69] O. Semiari, W. Saad, Z. Daw, and M. Bennis, "Matching theory for backhaul management in small cell networks with mmWave capabilities," *IEEE International Conference on Communications (ICC'15)*, pp. 3460–3465, June 2015.

[70] M. Shariat, E. Pateromichelakis, A. ul Quddus, and R. Tafazolli, "Joint TDD backhaul and access optimization in dense small-cell networks," *IEEE Transactions on Vehicular Technology*, vol. 64, no. 11, pp. 5288–5299, Nov. 2015.

[71] F. Pantisano, M. Bennis, W. Saad, and M. Debbah, "Match to cache: Joint user association and backhaul allocation in cache-aware small cell networks," *IEEE International Conference on Communications (ICC'15)*, pp. 3082–3087, June 2015.

[72] N. Wang, E. Hossain, and V. Bhargava, "Joint downlink cell association and bandwidth allocation for wireless backhauling in two-tier HetNets with large-scale antenna arrays," *IEEE Transactions on Wireless Communications*, vol. 15, no. 5, pp. 3251–3268, Jan. 2016.

[73] B. Li, D. Zhu, and P. Liang, "Small cell in-band wireless backhaul in massive MIMO systems: A cooperation of next-generation techniques," *IEEE Transactions on Wireless Communications*, vol. 14, no. 12, pp. 7057–7069, Dec. 2015.

[74] H. Tabassum, A. H. Sakr, and E. Hossain, "Analysis of massive MIMO-enabled downlink wireless backhauling for full-duplex small cells," *IEEE Transactions on Communications*, vol. 64, no. 6, pp. 2354–2369, June 2016.

[75] H. Ju, E. Oh, and D. Hong, "Improving efficiency of resource usage in two-hop full duplex relay systems based on resource sharing and interference cancellation," *IEEE Transactions on Wireless Communications*, vol. 8, no. 8, pp. 3933–3938, Aug. 2009.

[76] D. Korpi, J. Tamminen, M. Turunen, T. Huusari, Y. S. Choi, L. Anttila, S. Talwar, and M. Valkama, "Full-duplex mobile device: Pushing the limits," *IEEE Communications Magazine*, vol. 54, no. 9, pp. 80–87, Sep. 2016.

[77] B. Li, D. Zhu, and P. Liang, "Small cell in-band wireless backhaul in massive MIMO systems: A cooperation of next-generation techniques," *IEEE Transactions on Wireless Communications*, vol. 14, no. 12, pp. 7057–7069, June 2015.

[78] Andrea Goldsmith, *Wireless communications*. Cambridge Press, New York, 2004.

[79] P. Tehrani, F. Lahouti, and M. Zorzi, "Resource allocation in OFDMA networks with half-duplex and imperfect full-duplex users," *http://arxiv.org/abs/1605.01947*, Jun. 2016.

[80] J. Lee and T. Q. S. Quek, "Hybrid full-/half-duplex system analysis in heterogeneous wireless networks," *IEEE Transactions on Wireless Communications*, vol. 14, no. 5, pp. 2883–2895, May 2015.

[81] M. Al-Imari, M. Ghoraishi, P. Xiao, and R. Tafazolli, "Game theory based radio resource allocation for full-duplex systems," *IEEE 81st Vehicular Technology Conference (VTC Spring)*, vol. 60, no. 5, pp. 1–5, May 2015.

[82] D. W. K. Ng, E. S. Lo, and R. Schober, "Dynamic resource allocation in MIMO-OFDMA systems with full-duplex and hybrid relaying," *IEEE Transactions on Communications*, vol. 60, no. 5, p. 12911304, May 2012.

[83] J. Lee and T. Q. S. Quek, "Effects of channel estimation error on full-duplex two-way networks," *IEEE Transactions on Vehicular Technology*, vol. 62, no. 9, pp. 4666–4672, Nov. 2013.

[84] A. C. Cirik, Y. Rong, and Y. Hua, "Achievable rates of full-duplex MIMO radios in fast fading channels with imperfect channel estimation," *IEEE Transactions on Signal Processing*, vol. 62, no. 15, pp. 3874–3886, Aug. 2014.

[85] S. Boyd and L. Vandenberghe, *Convex optimization*. Cambridge University Press, 2004.

[86] N. Balakrishnan, and A. C. Cohen, *Order statistics and inference*. Academic Press, New York, 1991.

[87] A. Abdi, and M. Kaveh, "Full-duplex transceiver system calculations: Analysis of ADC and linearity challenges," *IEEE Vehicular Technology Conference*, pp. 2308–2312, July 1999.

[88] U. Siddique, H. Tabassum, E. Hossain, and D. I. Kim, "Channel access-aware user association with interference coordination in two-tier downlink cellular networks," *IEEE Transactions on Vehicular Technology*, vol. PP, no. 99, pp. 1–1, Oct. 2015.

[89] C. Cox, *An introduction to LTE: LTE, LTE-advanced, SAE and 4G mobile communications*.

[90] D. P. Moya Osorio, E. E. Bentez Olivo, H. Alves, J. C. S. Santos Filho, and M. Latva-aho, "Exploiting the direct link in full-duplex amplify-and-forward relaying networks," *IEEE Signal Processing Letters*, vol. 22, no. 10, pp. 1766–1770, Oct. 2015.

[91] C. Hoymann, C. Wanshi, J. Montojo, A. Golitschek, C. Koutsimanis, and S. Xiaodong, "Relaying operation in 3GPP LTE: Challenges and solutions," *IEEE Communications Magazine*, vol. 50, no. 2, pp. 156–162, Feb. 2012.

[92] T. Meixia, L. Ying-Chang, and Z. Fan, "Resource allocation for delay differentiated traffic in multiuser OFDM systems," *IEEE Transactions on Wireless Communications*, vol. 7, no. 6, pp. 2190–2201, June 2008.

Appendix A

A.1 PDF and CDF of h_m

The location of the NU is taken as uniformly distributed in the reference macrocell region. On the other hand, the MUs and SUs are uniformly distributed within their corresponding macrocell and small cell coverage area, respectively. Since the NU is uniformly distributed in a reference macrocell, the PDF of r_m is given by:

$$f_{r_m}(r) = \frac{2r}{R_m^2}, \qquad 0 \leq r \leq R_m. \tag{A.1}$$

The PDF of h_m can be derived by conditioning on r_m and U_m in (2.8), doing transformation of RV, i.e., $f_{h_m}(h_m|U_m, r_m) = \frac{r_m^{\beta}(U_m+1)}{P_m} f_{\xi_m}\left(h_m \frac{r_m^{\beta}(U_m+1)}{P_m}\right)$, and averaging over the distributions of U_m and r_m, respectively, as follows:

$$f_{h_m}(h_m) = \sum_{u_m=0}^{\infty} \frac{(u_m+1)\Pr(U_m = u_m)}{P_m} \times \int_0^{R_m} r^{\beta} f_{\xi_m}\left(h_m \frac{r^{\beta}(u_m+1)}{P_m}\right) f_{r_m}(r) dr. \tag{A.2}$$

Since $\xi_m \sim \text{Gamma}(\kappa_{\xi_m}, \Theta_{\xi_m})$, I can rewrite (A.2) by substituting the PDF of r_m given in (A.1), U_m given in (2.1), as well as ξ_m and doing some algebraic manipulations as

follows:

$$f_{h_m}(h_m) = \sum_{u_m=0}^{\infty} \frac{2(\frac{u_m+1}{P_m\Theta_{\xi_m}})^{\kappa_{\xi_m}} \int_0^{R_m} r^{\beta\kappa_{\xi_m}+1} e^{-\frac{h_m(u_m+1)r^{\beta}}{P_m\ \Theta_{\xi_m}}} dr}{e^{\lambda_m}\ u_m!\ R_m^2\ \lambda_m^{-u_m}\ \Gamma(\kappa_{\xi_m}) h_m^{1-\kappa_{\xi_m}}}. \tag{A.3}$$

After solving the integral in (A.3) using [24, 3.381/8], the PDF of h_m can be simplified as given:

$$f_{h_m}(h_m) = \sum_{u_m=0}^{\infty} \frac{2\ \lambda_m^{u_m}(\frac{P_m\Theta_{\xi_m}}{1+u_m})^{\frac{2}{\beta}} \Gamma_l\left(\frac{2+\beta\kappa_{\xi_m}}{\beta}, \frac{h_m\ R_m^{\beta}(1+u_m)}{P_m\Theta_{\xi_m}}\right)}{e^{\lambda_m}\ h_m^{\frac{2+\beta}{\beta}}\ R_m^2\ \beta\ u_m!\ \Gamma(\kappa_{\xi_m})}. \tag{A.4}$$

Consequently, using the property $\Gamma_l(\cdot) + \Gamma_u(\cdot) = \Gamma(\cdot)$, and [24, Eq.(06.06.21.0002.01)] and after some algebraic manipulations, the CDF of h_m, i.e., $F_{h_m}(h_m) = \int_0^{h_m} f_{h_m}(u)du$ can be derived as follows:

$$F_{h_m}(h_m) = \sum_{u_m=0}^{\infty} \frac{\lambda_m^{u_m} e^{-\lambda_m}\ \left(\frac{P_m\Theta_{\xi_m}}{1+u_m}\right)^{\frac{2}{\beta}}}{h_m^{\frac{2}{\beta}}\ R_m^2\ u_m!\Gamma(\kappa_{\xi_m})} \times \left(\frac{R_m^2\ \Gamma_l\left(\kappa_{\xi_m}, \frac{h_m R_m^{\beta}(1+u_m)}{P_m\Theta_{\xi_m}}\right)}{(P_m\Theta_{\xi_m})^{\frac{2}{\beta}}(h_m(1+u_m))^{-\frac{2}{\beta}}} - \Gamma_l\left(\kappa_{\xi_m} + \frac{2}{\beta}, \frac{h_m\ (1+u_m)}{R_m^{-\beta} P_m\Theta_{\xi_m}}\right)\right). \tag{A.5}$$

A.2 PDF and CDF of h_s

The PDF of $h_{(s)}$ can then be derived by conditioning on the distribution of U_s and $r_{(s)}$ in (3.3), doing transformation of RV, i.e., $f_{h_{(s)}}(h_{(s)}|U_s, r_{(s)}) = \frac{r_{(s)}^{\beta}(U_s+1)}{P_s} f_{\xi_s}\left(h_{(s)}\frac{r_{(s)}^{\beta}(U_s+1)}{P_s}\right)$, and averaging over the distributions of U_s and truncated

$r_{(s)}$, respectively, as follows:

$$f_{h_{(s)}}(h_{(s)}) = \sum_{u_s=0}^{\infty} \frac{\lambda_s^{u_s} e^{-\lambda_s} (\frac{u_s+1}{P_s \Theta_{\xi_s}})^{\kappa_{\xi_s}} h_{(s)}^{\kappa_{\xi_s}-1}}{u_s! \Gamma(\kappa_{\xi_s})} \int_0^T r_{(s)}^{\beta\kappa_{\xi_s}} f_{\xi_s} \left(h_{(s)} \frac{r_{(s)}^{\beta}(u_s+1)}{P_s \Theta_{\xi_s}} \right) \tilde{f}_{r_{(s)}}(r_{(s)}) dr_{(s)}, \tag{A.6}$$

where $\xi_s \sim \text{Gamma}(\kappa_{\xi_s}, \Theta_{\xi_s})$. By substituting $\tilde{f}_{r_{(s)}}(r_{(s)})$, solving the integral and doing some algebraic manipulations, I can rewrite (A.6) as:

$$f_{h_{(s)}}(h_{(s)}) = \sum_{n=0}^{S-s} \sum_{u_s=0}^{\infty} \frac{K_n \lambda_s^{u_s} \Gamma_l \left(\frac{\beta\kappa_{\xi_s}-2n+2S}{\beta}, \frac{h_{(s)} T^{\beta}(1+u_s)}{p_s \Theta_{\xi_s}} \right)}{u_s! \Gamma(\kappa_{\xi_s}) \beta \; e^{\lambda_s} h_{(s)} (\frac{h_{(s)}(1+u_s)}{p_s \Theta_{\xi_s}})^{\frac{2S-2n}{\beta}}}, \tag{A.7}$$

where

$$K_n = \frac{2 \; S! \; (-1)^{S-s-n} \left(R_m + D_l\right)^{2n-2S}}{\left(\int_0^T f_{r_{(s)}}(r_{(s)}) dr_{(s)} \right) (s-1)! \; (S-s-n)! n!}. \tag{A.8}$$

Consequently, using the property $\Gamma_l(\cdot) + \Gamma_u(\cdot) = \Gamma(\cdot)$ as well as [24, 3.381/1] and after doing some algebraic manipulations, the CDF of $h_{(s)}$, i.e., $F_{h_{(s)}}(h_{(s)}) = \int_0^{h_{(s)}} f_{h_{(s)}}(u) du$, can be derived as follows:

$$F_{h_{(s)}}(h_{(s)}) = \sum_{n=0}^{S-s} \sum_{u_s=0}^{\infty} \frac{K_n \lambda_s^{u_s}}{2 e^{\lambda_s} u_s! (n-S) \Gamma(\kappa_{\xi_s})} \times \left(\frac{\Gamma_l \left(\frac{\beta\kappa_{\xi_s}-2n+2S}{\beta}, \frac{h_{(s)} \; T^{\beta}(1+u_s)}{p_s \Theta_{\xi_s}} \right)}{\left(\frac{h_{(s)}(1+u_s)}{p_s \Theta_{\xi_s}} \right)^{\frac{2S-2n}{\beta}}} - \frac{\Gamma_l \left(\kappa_{\xi_s}, \frac{h_{(s)} T^{\beta}(1+u_s)}{P_s \Theta_{\xi_s}} \right)}{T^{2n-2S}} \right), \tag{A.9}$$

where K_n is given in (A.8).

A.3 Proof of (2.28)

The PDF of $\gamma_{(s)}$ can be derived by conditioning on the distribution of $r_{(s)}$ in (2.27), doing transformation of RV, i.e., $f_{\gamma_{(s)}}(\gamma_{(s)}|r_{(s)}) = \frac{r_{(s)}^{\beta}}{P_s} f_{\zeta}\left(\frac{\gamma_{(s)} r_{(s)}^{\beta}}{P_s}\right)$ and averaging over the truncated PDF of $r_{(s)}$ as follows:

$$f_{\gamma_{(s)}}(\gamma_{(s)}) = \int_0^T \frac{r_{(s)}^{\beta}}{P_s} f_{\zeta}\left(\frac{\gamma_{(s)} r_{(s)}^{\beta}}{P_s}\right) \tilde{f}_{r_{(s)}}(r_{(s)}) dr_{(s)}. \tag{A.10}$$

Given that $\zeta \sim \text{Gamma}(\kappa_{\zeta}, \Theta_{\zeta})$, substituting (2.18) and solving the integral using [24, 3.381/8], the closed-form PDF of $\gamma_{(s)}$ can be derived as follows:

$$f_{\gamma_{(s)}}(\gamma_{(s)}) = \sum_{n=0}^{S-s} K_n \frac{\Gamma_l\left(\frac{\beta\kappa_{\zeta} - 2n + 2S}{\beta}, \frac{T^{\beta}\gamma_{(s)}}{P_s\Theta_{\zeta}}\right)}{\left(\frac{\gamma_{(s)}}{P_s\Theta_{\zeta}}\right)^{\frac{2(S-n)}{\beta}} \beta\ \gamma_{(s)}\Gamma(\kappa_{\zeta})}. \tag{A.11}$$

Using the definition of MGF and substituting (A.11), the closed form MGF of $\gamma_{(s)}$ can be derived as given in (2.28).